MICROSTRUCTURAL CONTROLS ON THE GEOMECHANICS OF COARSE GRAINED SOFT ROCKS; WAITEMATA GROUP, AUCKLAND.

A thesis
submitted in partial fulfilment
of the requirments for the Degree
of
Master of Science in Earth Sciences
at the
University of Waikato

by

GRAHAM NORMAN DE LA MARE

University of Waikato
1992

ACKNOWLEDGEMENTS

I am indebted to my Supervisor, Dr. Vicki Moon, for suggesting the topic and for the many constructive criticisms throughout the compilation of the final manuscript.

Thanks must also go to Steve Bergin, the Geomechanics Technician, for his help in field work and in all aspects of laboratory work, and some more. He did everything really!

I also thank Wilma Blom for her assistance with the operation of the Scanning Electron Microscope, and with preparation of thin sections. Many technicians in the Earth Science Department have given of their time in helping me over these last two years. I thank them all for their help.

Thankyou to Mr. Dennis Bell, the Marine Inspector for the Takapuna City Council, for his kind permission to allow me to remove rocks from the East Coast Bays shoreline. Graeme Campbell from the Department of Conservation is thanked for his permission to allow me to sample rocks at Cape Rodney, from within the Marine Reserve.

Special thanks go to Nigel (you should have taken Physics) Harper, for being a great inspiration, even though you do like cricket!

Without the support of my wife Sandy I would not have completed this Thesis. Thankyou very much!

This thesis is dedicated to my parents for presenting me with the opportunity to attend University and for supporting me through the years.

ABSTRACT

The geomechanical behaviour of a variety of soft rocks from the Waitemata Group, Auckland, is characterised, and the influence of microstructure in determining the geomechanics examined. Field geotechnical measurements of joint spacing and Schmidt Hammer rebound are related to geomechanical properties to determine controls on joint development and applicability of field index tests for soft materials. Samples studied are dominantly sandstones, with one conglomerate; all of which have a significant component of swelling clay minerals.

Low bulk densities, high porosities and large void ratios are characteristic of the samples. They vary from extremely weak, very low durability rocks to moderately strong and durable materials. Extremely weak sandstones are highly deformable and undergo plastic deformation when loaded in compression. The stronger samples undergo strain softening and respond elastically to applied stresses prior to brittle failure. High softening factors indicate that compressive and tensile strengths are greatly reduced upon saturation.

All the study rocks have high proportions of sand and silt size material ($\leq$ 95 %), and up to 10 % of < 2 μm proportions; significant gravel size material only occurs in the conglomerate. Volcanic and detrital rock fragments are the dominant constituents in all samples, with abundant quartz, minor calcic plagioclase, and a variety of accessory minerals. The dominant clay is smectite with lesser amounts of illite, kaolinite, and mixed-layer clays.

Individual sand and silt grains are dominantly subrounded to subangular quartz, regular bricks of feldspar, and rods of rutile, and are often clay coated. Microaggregates and grains are combined into aggregates and assemblages, and in some cases macroassemblages, to form granular arrangements, which produce a network of interconnecting pores. The fabric of the rocks is characterised by discontinuous matrices. Fabric types range from skeletal to turbostratic, and arrangements range from tightly interlocking grains to loose granular structures. Clay microaggregates are either flocculated or form welded FF honeycomb arrangements.

Strength and durability are not influenced by quantity, size, or type of clasts or minerals present; rather, it is the arrangement of individual components (and associated pore spaces) in the rock fabric which directly determines the geomechanical behaviour. Strong, durable samples have an abundance of clean grain to grain contacts, and few

large clay aggregates. Clay microaggregates are arranged in welded FF arrangements, and pore space is restricted to micropores which resist water infiltration. Progressively weaker rocks are characterised by an increase in clay coated grains, clay aggregates, and clay connectors (which form weak links for stress transmission), and interconnecting pores at all levels in the fabric. In the weakest rock macroassemblages of clay coated grains, and open flocculated smectitic aggregates connected by point contacts, produce a network of macropores, allowing easy access of water which flocculates clays into weaker states by reducing bonding and cohesion.

Schmidt rebound values in the field do not provide a useful indication of either compressive or tensile strength of these rocks. The rebound values do, however, correlate well with laboratory determined dynamic elasticity values, suggesting that the instrument should be used in the field to predict rock elasticity and not strength.

Joint spacing within the rock units is related to elasticity with units capable of storing stress through plastic deformation having reasonably wide, uniformly spaced joints. Units which release stress through brittle fracture have closely spaced, and more complex joint systems.

TABLE OF CONTENTS

CHAPTER 9 CONCLUSIONS

LIST OF TABLES

LIST OF FIGURES

LIST OF PLATES

CHAPTER 1

INTRODUCTION

CHAPTER 1

INTRODUCTION

1.1 AIMS OF THE STUDY

Recent investigations have highlighted the importance of microstructure in determining the geomechanical behaviour of rock materials (Huppert, 1986, 1988; Moon, 1989; Beattie, 1990; Bannock, 1991). This has been shown to be particularly true for 'soft' sedimentary rocks which contain a high proportion of swelling clay minerals; such soft rocks are of considerable significance in engineering terms as their behaviour is little studied and hence poorly understood (Read *et al.*, 1981). Unfortunately, such materials have proven very difficult to work with, both in terms of obtaining reliable geomechanical data, and in terms of unravelling and understanding the complex microstructure resulting from a dominance of clay minerals.

In order to contribute to the understanding of the microstructural control on soft rock behaviour, this study aims to take a set of rocks which contain a predominance of larger clasts (mainly sand size) with a small, but significant, clay mineral component. In this way, the situation is simplified, and the means by which the microstructure influences geomechanical behaviour can be investigated.

To address this aim, two principle stages of investigation are recognised:

1] to characterise the geomechanical and petrographic properties of a variety of intact sandstones (and one conglomerate) using standardised field and laboratory techniques, and

2] to relate the geomechanical and petrographic properties both quantitatively and descriptively in order to investigate the means by which texture and fabric influence the geomechanical behaviour.

Two secondary aims are also defined:

1] to use the data collected above to determine any useful field properties which may be used as predictors of geomechanical behaviour, and

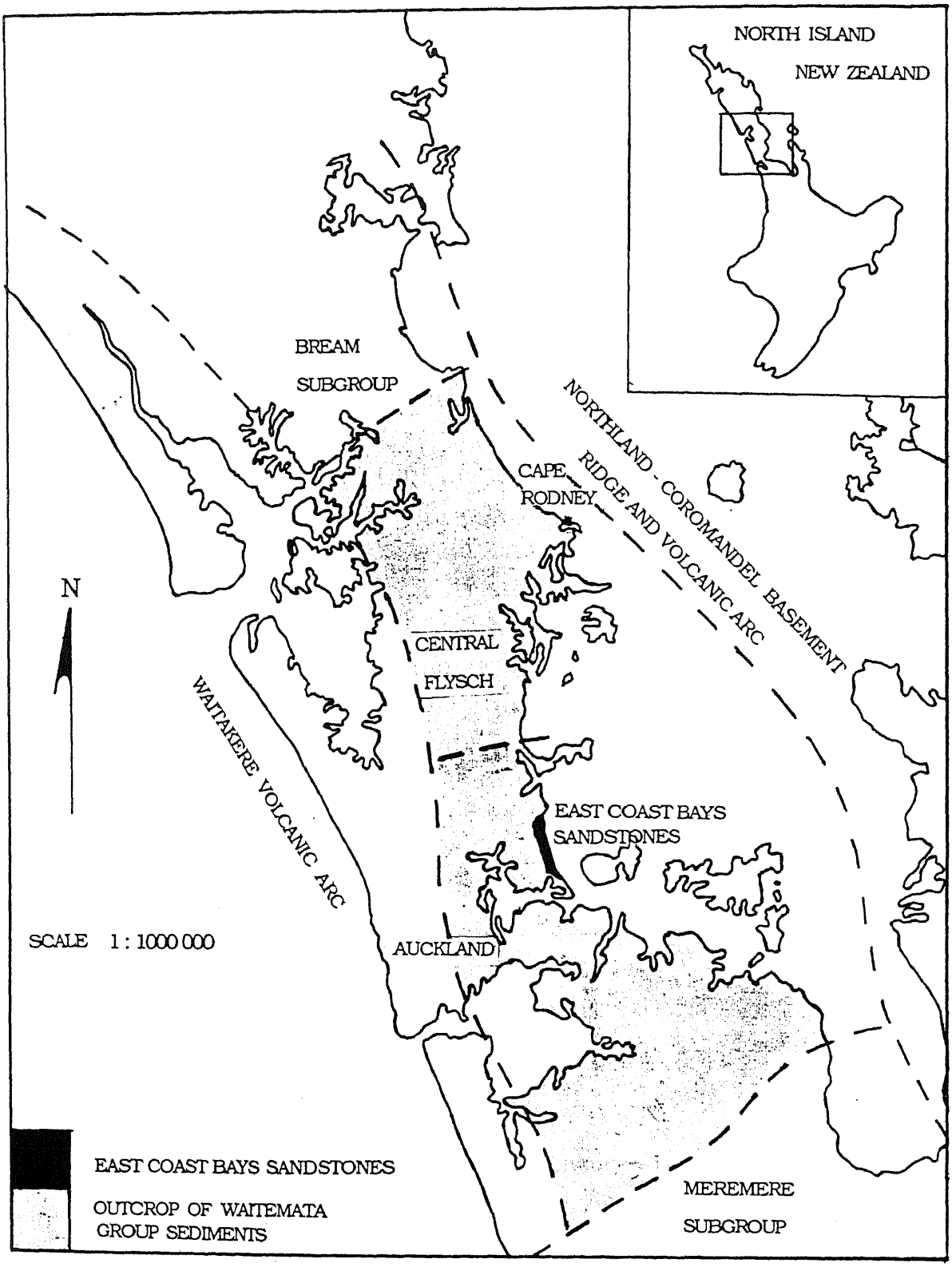

FIGURE 1.1 Outcrop of the Waitemata Group Sediments and locality of the East Coast Bays (ECB) Sandstones. (After Ballance, 1974)

2] to examine the relationships between jointing in the materials and the laboratory determined geomechanical properties in order to investigate the mechanisms of joint development.

1.2 STUDY AREA

The rocks used in this investigation are sandstones and a conglomerate from the Waitemata Group sediments of the Auckland region. These rocks characteristically contain up to 10 % of clay minerals, with varying proportions of silt, sand, and gravel sized clasts (Simpson, 1988). In general, they fulfill the requirements of 'soft' rocks (sedimentary rocks having compressive strengths of less than 10 MPa) and are non-calcareous.

Due to ready accessibility and availability of samples, sampling sites occur mainly along the 8 km of coastal cliffs bounding the East Coast Bays of Auckland, from Campbells Bay Beach in the south to Toroa Point in the north. One other site occurs further north at Cape Rodney. This site was chosen as literature review and field studies revealed a particularly coarse-grained, poorly sorted sandstone; a valuable contrast with most of the materials exposed in the East Coast Bays cliffs. Figure 1.1 defines the study area.

1.3 PREVIOUS WORK

Previous works on the Waitemata Group rocks have largely concentrated on the stratigraphy, paleontology, and geological history of the beds. Detailed accounts of the geological history and setting of the group are given by Ballance (1974, 1976, 1979), Ballance and Williams (1982), and Searle (1981), whilst a summary is given by Simpson (1988). Ballance (1976) provides an account of the stratigraphy and bibliography of the Waitemata Group. Other New Zealand works concentrating on the paleontology and stratigraphy of selected lithological units of the group include; Gregory (1966), Codling (1970), Geelen (1973), Weigel (1976), and Alldred (1980). Codling (1970) provides a useful account of the mineralogy and structure of the Parnell Grit.

Some work has been done on the geomechanical properties of the Waitemata Group sandstones concentrating on slope stability and slope

processes. Works on engineering geological aspects of the sediments at selected sites include those of Manning (1983), Shakes (1983), and Glading (1987). A recent study by Simpson (1988) determined the mineralogy, petrography, and physical properties (water content, density, porosity and durability) of the siltstone, sandstone and volcaniclastic units making up the East Coast Bays cliffs. A study was made of the jointing and structure of the cliffs and slope processes were related to the petrographic and physical properties of the units.

This study is not an attempt to duplicate the findings of Simpson (1988) but rather builds on his work by examining in detail the relationships between the geomechanical behaviour and petrography of a range of sandstones, representing his 'thick sandstones'.

The geomechanical properties of New Zealand soft rocks have been previously reported by Read *et al.* (1981) but classification to predict performance has had little success due to the difficulty of working with such soft materials. As a result, limited data exist to describe their geomechanical behaviour and even fewer attempts have been made to describe the microfabric of such materials. This has led to a poor understanding of soft rocks in general and to the factors controlling their strength.

The significance of microstructural control on the strength of soft rocks in New Zealand have been addressed recently. Soft tertiary sedimentary rocks have been investigated by Huppert (1986, 1988), strength of ignimbrites have been related to their fabric by Moon (1989), while Beattie (1990) concluded that strength was closely related to fabric for soft coal measure rocks.

1.4 MIOCENE WAITEMATA GROUP SEDIMENTS

The Waitemata Group, so named after the Waitemata Harbour, is a large body of flysch, composed of interbedded sandstone and mudstone/siltstone units, and associated rock types of Upper Oligocene to Lower Miocene age (Ballance, 1976). Within this group, four subgroups are recognised: the Warkworth Subgroup containing the central flysch deposits, the Northern Bream Subgroup of shelf facies, the Western Kaipara Subgroup of deep marine shelf facies, and the Southern Meremere Subgroup of shelf facies (Ballance, 1976; Simpson, 1988). The East Coast Bays Formation and Cape

Rodney Formations occur as members of the Warkworth Subgroup (figure 1.1).

The rocks sampled in this study are units within the East Coast Bays and Cape Rodney Formations. The former embraces the poor-volcanic facies of the central flysch as opposed to the latter, which make up the rich-volcanic basal facies of the Warkworth Subgroup.

1.5 RESEARCH METHODOLOGY

Four stages of investigation were carried out to address the aims of the study: field exposures were examined to obtain rock mass data, standard geomechanical tests were performed on rock cores obtained from intact blocks, detailed petrographic analyses were undertaken on material from the same blocks, and data from the above were related qualitatively and, where appropriate, statistically to determine the petrographic controls on strength.

1.5.1 Sampling

Five sampling sites were chosen which exhibited a range of grain sizes and hardness. Sites were described following the scheme of the New Zealand Geomechanics Society (1988). Hardness rebound values were recorded on the rock units using an L-Type Schmidt Hammer. Representative block samples were collected from each site for laboratory investigation.

1.5.2 Laboratory Investigation

Bulk rock properties (density, porosity, void ratio, particle size analysis) were determined prior to geomechanical testing. Rock strength was determined in both compression (uniaxial compressive strength) and tension (Brazilian Test). An attempt was made to determine Youngs Modulus and Poissons Ratio using the ultrasonic pulse method. Rock durabilty was determined using the slake durabilty test.

1.5.3 Petrography

Quantitative mineralogical data was obtained by X-Ray Diffraction (X.R.D.). Bulk rock mineralogy was determined from unorientated, back

filled powder mounts, whilst clay mineralogy was identified from orientated slide mounts. Texture was described from thin sections (optical microscopy) while fabric was determined using a scanning electron microscope (S.E.M.) on fractured rock surfaces. Crack propagation in rocks after compression was determined from use of a binocular microscope on broken rock cores.

1.5.4 Relationships

Linear regression analysis was used to correlate geomechanical, petrographical, and bulk rock properties. Rock properties were compared with geomechanical behavior to determine those properties which could easily be measured to predict the strength of the rock. The geomechanical properties were related statistically to microstructural components to derive a model for microstructural control on strength.

CHAPTER 2

FIELD INVESTIGATION AND SITE SELECTION

CHAPTER 2

FIELD INVESTIGATION AND SITE SELECTION

2.1 INTRODUCTION

In order to select suitable sampling sites a general survey of the coastal cliffs of the East Coast Bays was undertaken. The cliffs from Toroa Point in the north to Campbells Bay Beach in the south were surveyed, as well as the cliffs at Cape Rodney. These areas have been shown in figure 1.1.

This chapter initially records the methods used in the field to select sampling sites and discusses the use of the Schmidt Hammer. A brief description of the general lithology of the East Coast Bays is given prior to more detailed descriptions of the chosen sampling sites.

2.2 FIELD METHODOLOGY

It is commonly recognised that rock descriptions should include descriptions of both the rock material and discontinuities through the rock, as it is the discontinuities which greatly influence and control the mechanical behaviour of the rock mass (N.Z. Geomechanics Society, 1988). In this field investigation, a single sandstone bed from which block samples were collected is described as the rock mass. This is done to meet the primary aims of the study, which are not to provide a stability analysis of the cliff face at each site (which would include all the units and discontinuities present) but to characterise the field properties and geomechanics of an individual sandstone unit and relate these to the microstructure of the material.

2.2.1 Site Selection

An initial survey of the East Coast Bays and Cape Rodney coastal cliffs was undertaken to select suitable sampling sites. This survey involved noting the thickness, extent, grain size, sorting and jointing characteristics of all accessible sandstone beds, together with obtaining representative hardness measurements using a Schmidt Hammer (see section 2.2.2). Any notable characteristics of sandstone units were also

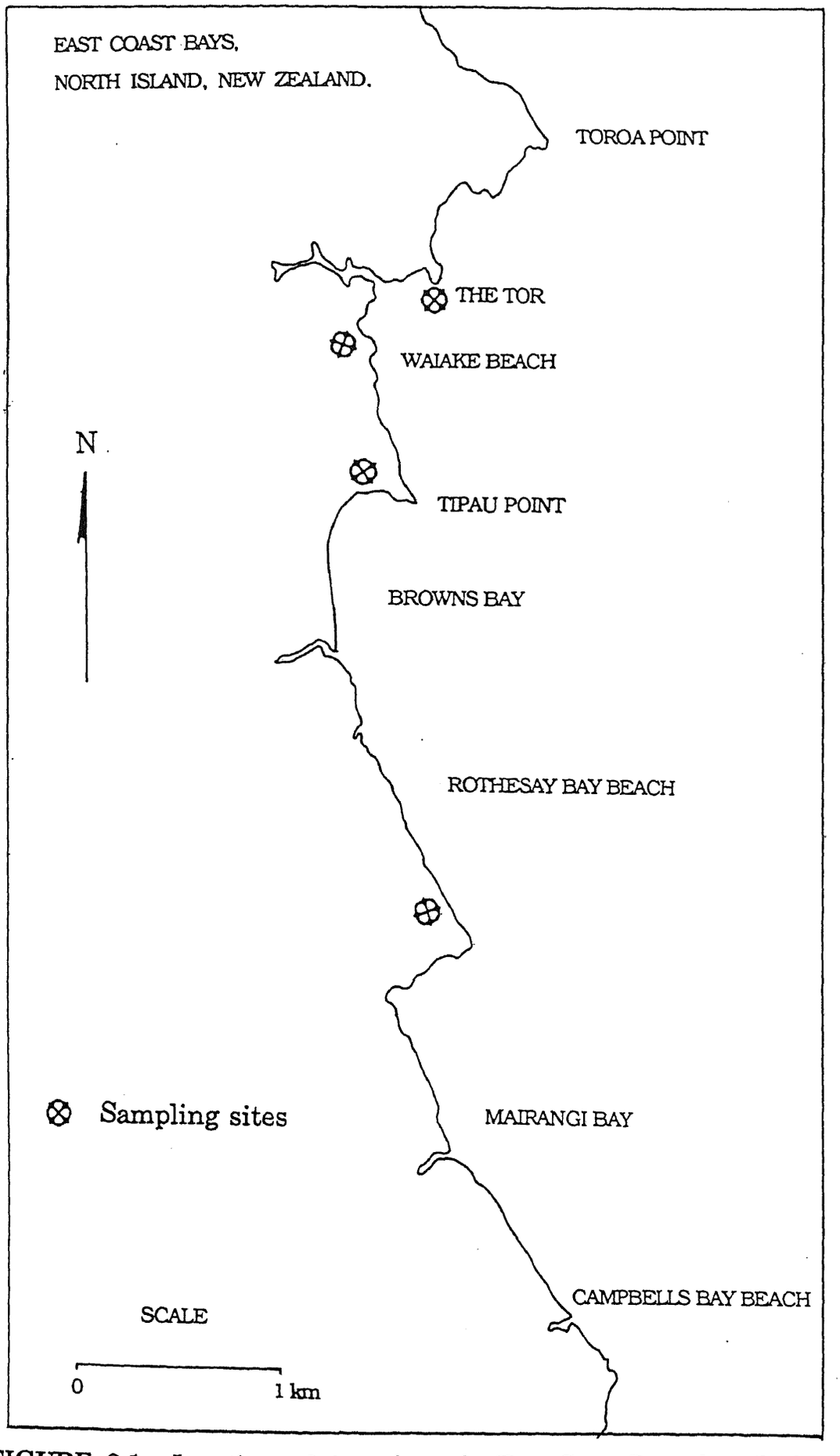

FIGURE 2.1 Locations of sites along the East Coast Bays described in the text. The map is an enlargement of the ECB area depicted in figure 1.1.

described, especially obvious structural features such as ripples and laminations.

Based on these descriptions and data, five sites were selected for sampling, with the aim of the sampling being to obtain material representing the greatest possible variety in terms of grain size, hardness, and joint spacing. These sites are noted below along with informal names which have been assigned to the selected sandstones:

Cape Rodney	(Cape Rodney {CR} Sandstone),
The Tor, Waiake Beach	(Parnell Grit),
Tipau Point	(Tipau Sandstone),
Waiake Beach	(Waiake Sandstone),
Rothesay Bay Beach	(Rothesay Sandstone).

The names are based on the field sampling locations, and will be used for the remainder of this investigation. They have no stratigraphic significance and are applicable only to this study. The sampling sites represent the greatest variation observed in grain size and sorting, and rebound hardness. The ECB locations are displayed in figure 2.1. The CR sandstone sampling site is shown in figure 1.1. Detailed descriptions of the sites are given in section 2.4.

It is notable that the Parnell Grit is not a sandstone, but a volcaniclastic conglomerate. This rock was included in the investigation to determine what effect larger clasts (in an otherwise muddy matrix) would have on its geomechanical behaviour.

2.2.2 Schmidt Hammer Testing

A field assessment of rock impact strength was determined by using the L and P-Type Schmidt Hammers.

The Schmidt Hammer, or Impact Hammer, was designed for carrying out non-destructive, *in situ* tests on concrete (Day and Goudie, 1977). It is employed extensively in the field as an indicator of the relative hardness of a rock *in situ*. This is due to its ease of use, portability, and robustness, as well as its use in predicting the compressive strength of rock (Sachpazis,

1990). For *in situ* testing it requires no sample preparation and is a rapid test which provides an indication of the hardness of a material. Suggested methods for its use in the field, as well as correlation with compressive strength, are reported by Deere and Miller (1966), Day and Goudie (1977), Brown (1981), Selby (1982), and Sachpazis (1990), while Poole and Farmer (1980) and Sheorey *et al.* (1984) examine the repeatability of the hammer results.

The Schmidt Hammer measures the distance of rebound of a spring controlled plunger impacting on a rock surface (Day and Goudie, 1977). The distance of rebound (read off a scale on the instrument) gives a relative measure of surface hardness. The L and N-Type Hammers are spring loaded as opposed to the P-Type which measures the rebound of a pendulum released from a vertical position. The L and P-Type Hammers are recommended for use on softer rocks (Day and Goudie, 1977), whilst the N-Type is recommended for rocks having a compressive strength of 20 MPa or greater (Sheorey *et al.*, 1984).

2.2.2.1 Field Use of the Schmidt Hammer

For use of the Schmidt Hammer in the field it is recommended that surfaces be essentially flat and free from flakes or dirt (Day and Goudie, 1977; Brown, 1981). It is also noted that tests carried out toward the edge of specimens or near discontinuities may show markedly lower rebound 'R' values. Day and Goudie (1977) recommend 10 to 15 impact readings at each site with a greater number for variable materials. Also, repeated tests on the same spot will result in increased values owing to partial crushing of the rock. Poole and Farmer (1980) have noted that 'R' values rise and show considerable variation over the first 3 to 4 impacts before levelling off. They suggest the peak value from at least five impacts at one point should be selected as a representative rebound value.

An extensive survey along the cliffs in the study area was undertaken using the L and P-Type Schmidt Hammers. Wherever sandstone units changed in physical appearance or new units appeared, impact readings were recorded. It was felt the rocks in this study were too soft for use of the N-Type Hammer. Although the Cape Rodney sandstone is far stronger

than the sandstones of the East Coast Bays, the L and P-Type hammers were still used for consistency.

The Schmidt Hammers were used, in this study, in accordance with the methods outlined by Brown (1981). Twenty rebound values were recorded at each site. Impacts were separated by at least a plunger diameter and the lower 50 % of values were ignored. Care was taken to avoid cracks or discontinuities and to place the hammer toward the centre of the sandstone beds. Surfaces were essentially flat, except for the Parnell Grit where large crystals and lithics created a variable, irregular surface.

2.2.3 Site Descriptions

It is recognised by the Geological Society Engineering Group Working Party (1977) that to facilitate communication of facts between various groups, standardisation should be achieved in the description and assessment of rock masses. To this end, many classification and description schemes have been proposed. Some of these include: Matula (1981), Williamson and Kuhn (1988), New Zealand Geomechanics Society (1988), and Kirkaldie (1988). Rock mass strength classifications have been produced which provide ratings for specific parameters in order to classify the rock strength (Waldvogel and Selby, 1980; Bieniawski, 1988). Brown (1981) has described methods for quantitative descriptions of discontinuities within a rock mass, whilst the Geological Society Engineering Group Working Party (1988) reported on methods used in geophysical surveys.

The site descriptions given in this investigation follow the guidelines proposed by the New Zealand Geomechanics Society (1988). This scheme follows closely those proposed by the Geological Society Engineering Group Working Party (1977) and Matula (1981). Features described at each site include:

- colour,
- degree of weathering,
- fabric (orientation of grains),
- strength,
- Schmidt Hammer rebound hardness,
- rock name.

The description of joints through individual beds include:

- spacing,
- continuity,
- width (aperture),
- orientation,
- roughness,
- presence of infill,
- number of joint sets.

Additional information includes the bed thickness and depth of the bed in the profile. It is important to note that the grain size and sorting in these descriptions are based on observations made by eye. More complete textural analyses are determined by Particle Size Analysis (chapter 3) and the study of thin sections (chapter 6).

2.3 GENERAL LITHOLOGY AND SCHMIDT HAMMER RESULTS

Along the East Coast Bays cliffs, two lithologies occur; flysch, which is dominant, and tuffaceous Parnell Grit. These two lithologies are briefly described next. Individual sampling sites selected are described in section 2.4.

2.3.1 Flysch Deposits (East Coast Bays)

Almost the entire length of the East Coast Bays cliffs surveyed consist of flysch. Commonly, thick sandstone beds are interlain with thin, frittery, mudstone/siltstone beds (plates 2.1 A + B). The average thickness of the sandstone units lies between 0.3 and 0.6 m. Rarely do they occur thinner than 0.2m, and only one 1.5 m bed was observed. These sandstone beds tend to stand proud of the cliff, overhanging thinner siltstone layers. Average thicknesses of the mudstone/siltstone layers vary between 0.1 m and 0.15 m although 0.5 m units do frequently occur. Often the layers are composed of crushed, frittery siltstone which grades into the lower sandstone unit. Upper bed contacts are sharp, representing successive turbidite deposits.

A Thicker sandstone units are separated by thin, frittery mudstone / siltstone layers. The orange sandstone unit is 90 cm thick. (Rothesay Bay Beach).

B Typical cliff face along the East Coast Bays. Flysch deposits are essentially horizontal and individual sandstone units can be traced for hundreds of metres. (Tipau Point).

PLATE 2.1 Flysch deposits along the East Coast Bays (ECB) shoreline.

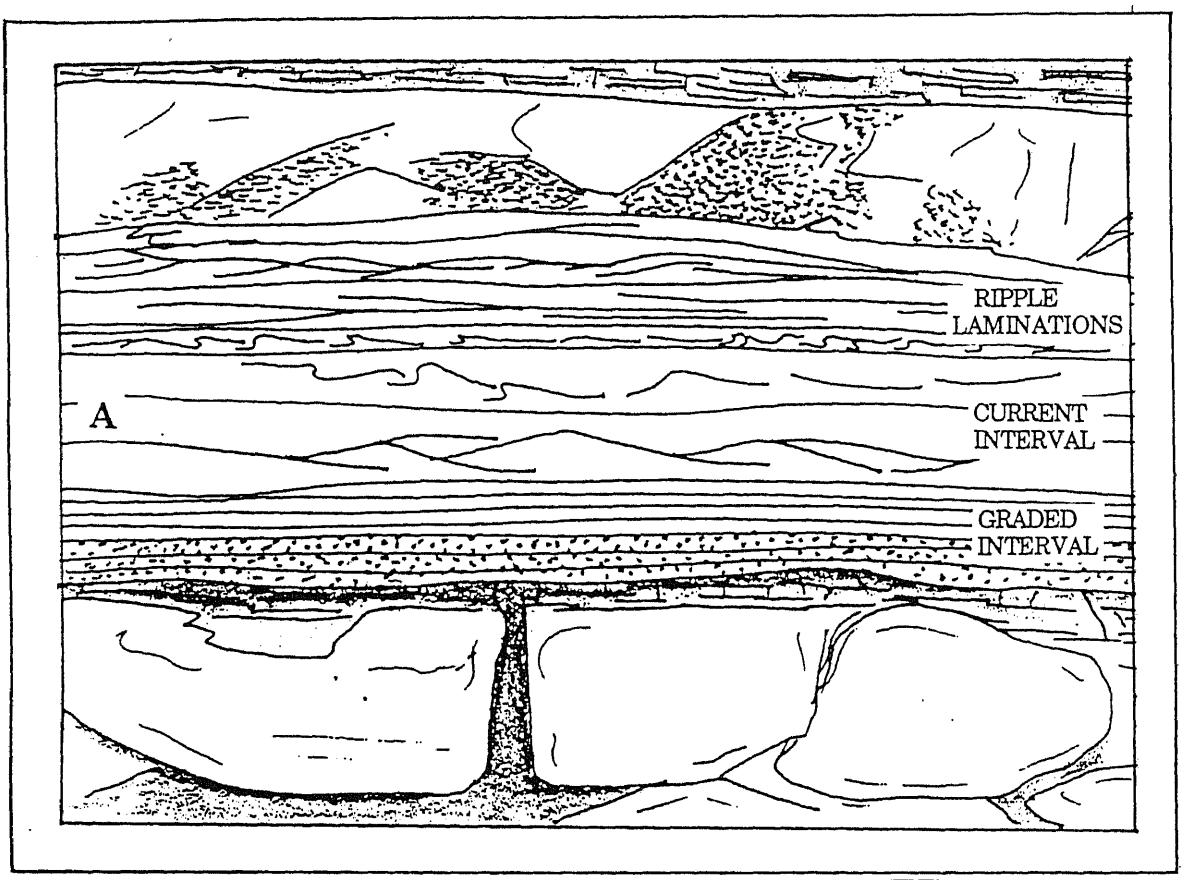

FIGURE 2.2 Bedding in Tipau Sandstone (A). Graded interval occurs at the base and is overlain by parallel laminations. Current ripple laminations occur at the top of the unit. Upper layers of parallel laminations in Bouma's (1962) sequence are absent. (Not to scale)

Joint spacing in the sandstone is generally large, averaging between > 0.3 m and 1.5 m. Average joint widths vary from 1 mm to 50 mm. Typically, vertical, limonite-stained joints occur through the entire thickness of individual sandstone beds, and are evenly spaced. In some sandstone units these joints form hard zones with the spaces in between slightly indented through weathering. The siltstone layers are commonly highly jointed and shattered with many discoloured (limonite-stained) surfaces.

Sandstone grain sizes vary from fine sand to medium sand. Generally, all sandstone beds are very well sorted with the finer grained rocks extremely well sorted. Within the coarser grained beds, sedimentary structures are apparent, obviously produced during deposition of the sediments. Coarse to fine grading (coarse at the base) is observed within the thicker beds. The same beds also exhibit bands of parallel laminations (figure 2.2). The sedimentary structures are gradational and are examples of structures formed through changes in the depositional flow regimes, described by Bouma (1962). Commonly, they represent incomplete Bouma sequences, where finer grained units lack the upper band of parallel laminations and in most cases have no size grading.

Trace fossils (ichnofacies) commonly occur within the strata. They occur as infilled trails left by 'sea bed' dwelling organisms. Evidence of modern rock boring bivalves occurs in mudstone units in the intertidal zone. They produce many circular burrows which form a network of small passages.

Most of the length of coastal cliffs is composed of near horizontal beds which dip marginally (approximately 5°) to the south east. Strata may be folded where tuffaceous grit outcrops, presumably a result of the grit emplacement. Steeply dipping faults occur regularly along the study area with displacements from a few centimetres to many metres.

2.3.2 Parnell Grit

Parnell Grit outcrops at Waiake Beach and Campbells Bay Beach (figure 2.1). It consists of mixed volcanic, sedimentary, and fossil detritus (Ballance, 1976) and is described as "... a heterolithologic mixture of clasts of widely variable size contained within a muddy matrix" (Ballance, 1974).

TABLE 2.1 Summary of Field Characteristics

	CAPE RODNEY SST	PARNELL GRIT	TIPAU SST	WAIAKE SST	ROTHESAY SST
COLOUR	LIGHT BROWN	LIGHT YELLOWISH BROWN	LIGHT GREYISH BROWN TO YELLOWISH BROWN	LIGHT YELLOWISH BROWN	LIGHT REDDISH BROWN
WEATHERING	MODERATE	MODERATE	MODERATE	MODERATE	MODERATE TO STRONG
FABRIC	HOMOGENEOUS	NORMAL GRADING	INCOMPLETE BOUMA SEQUENCE	MASSIVE (FAINT BEDDING)	PARALLEL THIN GREY LENSES
STRENGTH	STRONG	MODERATE	WEAK TO V.WEAK	WEAK	VERY WEAK
SCHMIDT 'R' VALUE	26.9 ± 2.5	17.5 ± 1.1	22.2 ± 1.5	18.5 ± 1.6	19.6 ± 2.3
ROCK NAME	ARENACEOUS SST	RUDACEOUS CONGLOMERATE	ARENACEOUS SST	ARENACEOUS SST	ARENACEOUS SST
GRAIN SIZE	COARSE	VERY COARSE	VERY FINE	FINE TO MEDIUM	MEDIUM TO COARSE
SORTING	WELL TO VERY WELL SORTED	MODERATELY SORTED	EXTREMELY WELL SORTED	VERY WELL SORTED	MODERATE TO WELL SORTED
BED THICKNESS	2.5 m	> 4 m	0.83 m	1 m	0.90 m
OVERBURDEN	1.5 m	12 m	20 m	10 m	7 m
DISCONTINUITIES.					
ORIENTATION	DOMINANTLY VERTICAL	015 / 52° (NEAR VERTICAL)	038 / 65° 160 / 79°	VERTICAL	VERTICAL
SPACING	EXTREMELY CLOSE TO WIDE	MOD. TO WIDE	MOD. TO WIDE	MOD. TO WIDE	MOD. TO WIDE
	< 100mm - 1.3m	0.4m - 1m	0.25m - 0.87m	0.4m - 1m	0.41m - 0.85m
PERSISTENCE	EXTENDS THROUGH UNIT	CONTINUOUS	CONTINUOUS	CONTINUOUS	DISCONTINUOUS
ROUGHNESS	ROUGH UNDULATING	ROUGH PLANAR	SMOOTH UNDULATING	SMOOTH UNDULATING	SMOOTH PLANAR
APERTURE	2.5mm - (1-10cm) OPEN (GAPPED FEATURES) - V. WIDE (OPEN FEATURES)	0.25 - 0.05mm PARTLY OPEN (CLOSED FEATURES)	2.5 - 10mm MOD. WIDE (GAPPED FEATURES)	2.5 - 10mm MOD. WIDE (GAPPED FEATURES)	0.5 - 2mm PARTLY OPEN (CLOSED FEATURES)
FILLING	NONE	LIMONITE INFILLED	NONE	LIMONITE STAINED	LIMONITE INFILLED
NO. SETS	2	2	2	1	1
SEEPAGE	NONE	NONE	NONE	NONE	NONE

Outcrop thicknesses reach 20 m, the main body of which contains primary volcanic clasts ranging from 5 to 12 mm. Normal grading is common, with repeated sequences of grading, representing several flow deposits, occurring at The Tor, Waiake Beach (plate 2.2). The volcanic clasts and intraclasts (surrounding rock incorporated into the flow deposit) are set in a pale yellow to grey/brown muddy matrix. Imbricated mudstone lenses occur at some sites toward the top of the outcrop. Sections surveyed had limonite infilled, continuous joints, spaced more than 0.5 m apart with joint widths of less than 5 mm.

2.3.3 Schmidt Hammer Results

Rebound values for the P-Type Hammer, along the length of the East Coast Bays and Cape Rodney, range from 7 to 63 (mean = 45 ± 13). L-Type 'R' values for the same locations range from 18 to 27 (mean = 21 ± 3). It can be seen the P-Type Hammer recorded extremely variable results (up to 35 % error) which have been attributed to the larger diameter of the plunger being affected more by surface irregularities in the rock. Conversely, the L-Type Hammer has a much smaller plunger diameter and recorded very consistent results. Thus, only the L-Type Hammer results are reported in this study.

Rock impact strengths for the sandstone units remain largely consistent throughout the study area. The site at Cape Rodney recorded the highest 'R' value of 27 ± 3. Along the East Coast Bays, sandstones show little variation with 'R' values ranging from 17 to 23. The Parnell Grit recorded a rebound value of 18 ± 1.

2.4 FIELD DESCRIPTIONS

Summary data for individual sampling sites are presented in table 2.1. Each site is discussed in turn in the following sections.

2.4.1 Cape Rodney Sandstone

A light brown, moderately weathered, homogeneous, strong, arenaceous sandstone. Average Schmidt Hammer 'R' value is 27 ± 3. The rock is coarse grained and varies from well sorted to very well sorted. Freshly

Crude flow banding in Parnell Grit outcrop. Moderately sorted volcanic clasts, and intraclasts are set in a pale yellowish brown matrix. (The Tor, Waiake Beach).

PLATE 2.2 Field Appearance of Parnell Grit

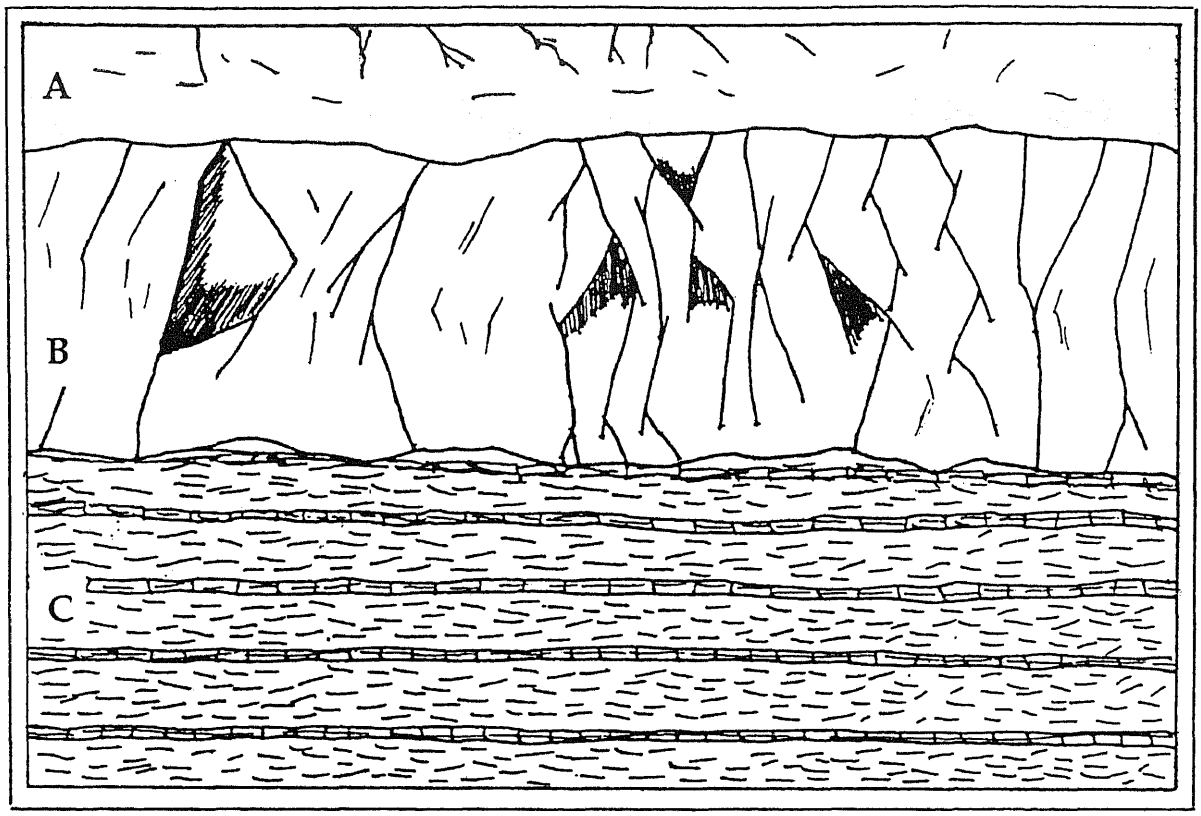

FIGURE 2.3 CR Sandstone unit (B) is overlain by soil (A) and underlain by interbedded, frittery mudstone/siltstone layers (C). (Not to scale)

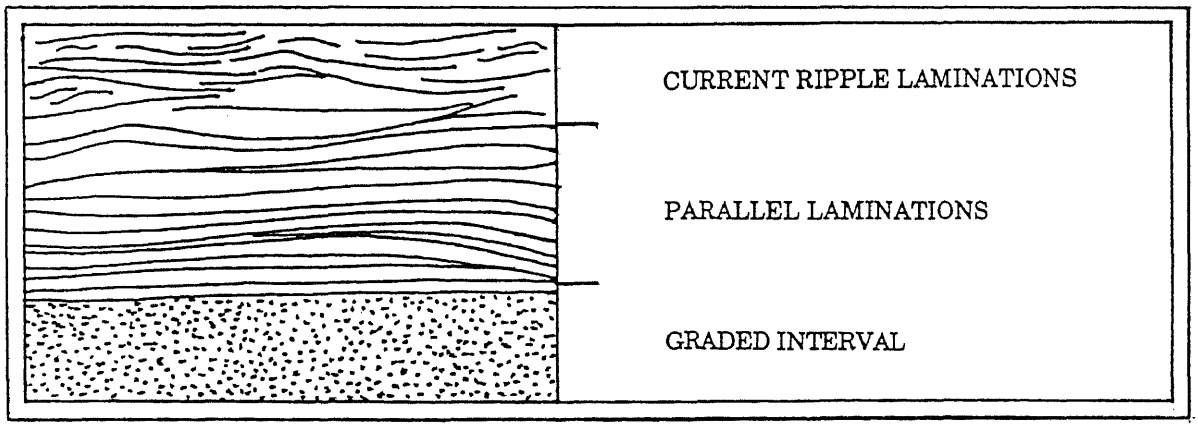

FIGURE 2.4 Sequence of grading commonly observed in Waiake Sandstone units. Graded interval at the base, overlain by parallel laminations and then current ripple laminations. (Not to scale)

exposed rocks are dark bluish/green in colour. The Cape Rodney beds are loosely referred to as the basal facies of the Waitemata Group (Ballance, 1976) and make up the rich volcanic facies of the Warkworth Subgroup.

Three sets of joints were observed. The dominant set is vertical and widely spaced with wide apertures. They are continuous through the sandstone unit, which is approximately 2.5m thick. Two minor joint sets occur to a limited extent. They cut diagonally at angles of 60° to 70° forming wedge shape blocks. Loose blocks or dislodged blocks give an appearance of very wide to extremely wide apertures to produce 'open' features. The unit lies at a depth of 1.5 m and is underlain by greater than 8 m of numerous thin (< 0.05 m), highly jointed, frittery, mudstone layers (figure 2.3).

2.4.2 Parnell Grit

The Parnell Grit sampled in this study occurs at 'the Tor', Waiake Beach. It is a light yellowish brown, moderately weathered, graded, moderately strong, rudaceous conglomerate. Normal grading occurs, with two flow units identified (plate 2.2). Equigranular volcanic clasts, and intraclasts, make up a moderately sorted, very coarse grained rock. Grains are sub-rounded to angular. Mudstone lenses reach up to 100 mm in length. Freshly exposed rock has a dark grey matrix. Average Schmidt Hammer rebound is 18 ± 1.

One vertical joint set was observed. This is continuous through the unit and extends across the intertidal platform composed of Parnell Grit. The joints are very closely spaced (< 0.3 m), smooth undulating joints, having tight apertures. All joints are totally infilled by dark orange limonite (plate 2.3A). The outcrop is greater than 4 m thick (lower boundary not determined).

2.4.3 Waiake Beach

A light yellowish brown, moderately weathered, faintly bedded, weak, arenaceous sandstone (plate 2.3B). The unit is usually massive at the base grading into faint laminations (figure 2.4). It is dominantly fine to medium grained and very well sorted. Vertical, discontinuous zones of

A Thin, limonite infilled joints, through Parnell Grit. Note dominant vertical joint set with discontinous, near horizontal, cross-cutting joints. (The Tor, Waiake Beach).

B Loose block of Waiake sandstone. Parallel laminations are obvious throughout the block. Limonite 'crusts' occur in patches across the rock surface. The block is approximately 1 m high.

PLATE 2.3 Parnell Grit and Waiake Sandstone

dark orange-stained, leached limonite occur regularly across the bed. The unit has an 'R' value of 19 ± 2.

This unit contains very regular, evenly spaced, vertical joints (plate 2.4). These are closely spaced, smooth and undulating, and limonite stained with partly open apertures. The bed is approximately 1 m thick and very uniform for hundreds of metres in length.

2.4.4 Tipau Point

A light greyish brown to yellowish brown, moderately weathered, very thinly bedded, weak to very weak, arenaceous sandstone. The bed displays most of the structures described by Bouma (1962). Massive sandstone at the base grades into parallel laminations and then ripple laminations (plate 2.5A and figure 2.2). Dominantly very fine grained and extremely well sorted, 83 cm thick unit. It has a rebound hardness of 22 ± 2.

Two sets of joints are evident. The major set cuts the unit diagonally at 70° to 85° and is continuous through the bed. They are very closely spaced joints with moderately wide apertures, lacking infill. A second set of discontinuous joints cut diagonally across the major set, extending from the centre of the unit to its base, producing wedge shaped blocks. Some blocks have fallen out of the bed producing wedge shape indentations (plate 2.5B).

2.4.5 Rothesay Bay Beach

A light reddish brown, moderately to strongly weathered, faintly bedded, very weak, arenaceous sandstone. This unit is distinctive for its reddish colour and unconsolidated nature. It is medium to coarse grained and moderate to well sorted. Distinctive bedding occurs in the form of parallel, thin (< 2 mm) light grey lenses. These are not continuous across the length of the unit but are most easily viewed on large, loose blocks on the intertidal platform (plate 2.6). Coarse normal grading occurs through the bed. Schmidt hardness is 20 ± 2.

One set of joints occurs. These are closely spaced, vertical, discontinuous, hairline fractures, darkly stained orange from leached limonite.

Waiake sandstone unit (W) forms one of the thickest beds in this profile. Note the regular spaced, vertical joints.

PLATE 2.4 Waiake sandstone unit in the cliff profile

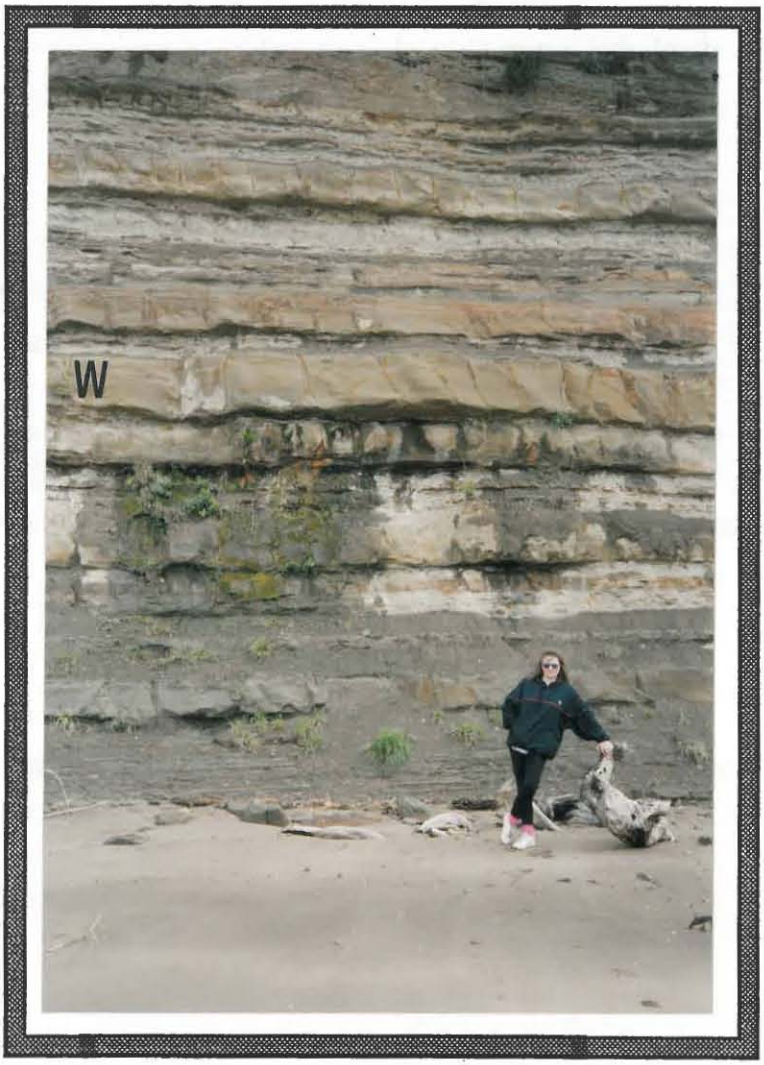
W

A Sandstone bed at Tipau Point, massive at the base, grading into thick parallel laminations. Much thinner, wavy laminations occur in line with the hammer tip. This section of the unit has slipped from its original position just off the top of this photograph.

B Wedge shape indentation produced through cross jointing. Note the 'open' joint in the centre. This feature is typical of this unit. (Tipau Point).

PLATE 2.5 Field appearance of Tipau Sandstone

Loose block of faintly laminated, Rothesay sandstone (1m thick). Bands of coarse grains occur toward the top of the sample. Mudstone lenses are apparent at the base. Note the very regular jointing pattern on the platform in the background. (Rothesay Bay Beach).

PLATE 2.6 Rothesay sandstone

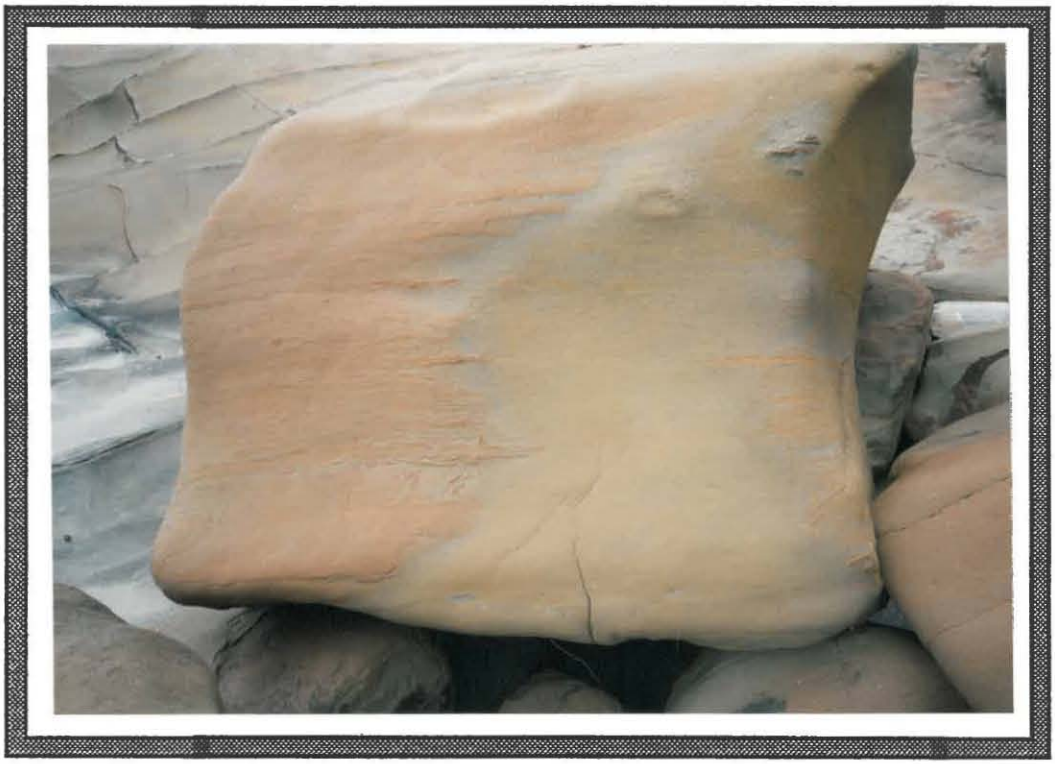

2.5 SUMMARY

Two lithologies make up the East Coast Bays cliffs; flysch, which is dominant, and localised outcrops of volcaniclastic units (Parnell Grit). Grain sizes and Schmidt hardness values remain largely consistent through the study area.

East Coast Bays samples (ECB) have similar low Schmidt Hammer 'R' values while the Cape Rodney sandstone (CR) has a much higher rebound value. The ECB samples are characterised by moderate to extremely well sorted units and are coarse to very fine grained. The CR sandstone is coarse grained and only moderately sorted. Based on the greatest variations observed in grain sizes and sorting, and Schmidt Hammer results, five sites were selected for sampling. Blocks were collected from each site for laboratory investigation.

CHAPTER 3

BULK ROCK PROPERTIES AND PARTICLE SIZE ANALYSIS

CHAPTER 3

BULK ROCK PROPERTIES AND PARTICLE SIZE ANALYSIS

3.1 INTRODUCTION

Bulk rock properties such as porosity and bulk density are useful index properties which characterise a rock and aid in determining its mechanical behaviour (Goodman, 1980; Farmer, 1983). They exert a significant control over the strength of the material (Attewell and Farmer, 1976).

To examine the relationship between these bulk rock properties, particle size analysis, and strength, and to evaluate these properties as strength indices for the sandstones, effective porosity (η_{eff}), dry bulk density (ρ_{dry}), and saturated bulk density (ρ_{sat}) were measured. From these, grain density (ρ_s) and void ratios (e) were derived. Particle size distributions were measured as these are fundamental to the classification of sedimentary rocks (Lewis, 1984). This chapter presents the results of these measurements.

3.2 DEFINITIONS

The porosity (η) of a rock expresses the percentage of void space to total volume in a material (Goodman, 1980). It is defined as the ratio of the volume of internal open spaces (pores) to the bulk volume of the rock (Lama and Vutukuri, 1978). Effective porosity (η_{eff}) measured here, refers to the volume of rock occupied by interconnected pores which become filled with water on saturation. The density (ρ) is the mass per unit volume of the material. Dry bulk density (ρ_{dry}) is the density obtained when the pore spaces are filled with air as opposed to saturated bulk density (ρ_{sat}), where the pores are filled with water. Grain density (ρ_s) is the mass of a unit volume of the grains (solid phase) of the rock material. The void ratio (e) is simply the ratio of the volume of the voids or pores to the volume of the solid phase of the material. The void ratio determines the average, statistical grain spacing in a material (Derski, 1989).

TABLE 3.1 Bulk Rock Properties

SAMPLE	ρ_{dry}	ρ_{sat}	ρ_s	η_{eff}	e
CAPE RODNEY	2310 ± 40	2410 ± 30	2570 ± 10	10 ± 2	0.11 ± 0.03
PARNELL GRIT	2010 ± 30	2180 ± 10	2430 ± 70	18 ± 4	0.22 ± 0.06
TIPAU SST	1800 ± 20	2050 ± 3	2390 ± 50	25 ± 2	0.33 ± 0.04
WAIAKE SST	1760 ± 10	2020 ± 10	2380 ± 20	26 ± 1	0.35 ± 0.02
ROTHESAY SST	1740 ± 4	2060 ± 20	2560 ± 100	32 ± 3	0.47 ± 0.06

ρ_{dry}	dry bulk density	($kg.m^{-3}$)
ρ_{sat}	saturated bulk density	($kg.m^{-3}$)
ρ_s	grain density	($kg.m^{-3}$)
η_{eff}	effective porosity	(%)
e	void ratio	

TABLE 3.2 Dry Bulk Densities and Porosities for some common rock types

ROCK TYPE	DRY BULK DENSITY ($kg.m^{-3}$)	POROSITY (%)
GRANITE	2500 - 2900	0.5 - 5.0
GABBRO	2800 - 3150	0.1 - 3.6
BASALT	2800 - 2900	0.1 - 22
GNEISS	2600 - 3100	0.5 - 1.5
SLATE	2700 - 2850	0.1 - 0.5
SANDSTONE	2100 - 2700	0.7 - 34
LIMESTONE	2300 - 2750	0.2 - 43
SHALE	2000 - 2800	1.6 - 34
CHALK	1850 - 2250	25 - 29
GRANULAR SAND	1200 - 2200	29 - 50
GRANULAR SILT	1260 - 1850	29 - 52

Data from Attewell and Farmer (1976), Goodman (1980), Farmer (1983), and Jumikis (1983).

3.3 METHODS

Effective porosity and bulk densities were determined following the methods outlined by Brown (1981) using saturation and caliper measurements on regular, long (137mm) core specimens prepared for geomechanical testing. Five cores for each sample were measured. From these properties, grain density and void ratios were determined using the formulas proposed by Brown (1981). The bulk rock properties for each of the samples are presented in table 3.1. The values are means of five measurements. Errors are 95 % confidence limits.

Problems were encountered, during the saturation process, with the Tipau sandstone. After one hour submerged in water, all five of the cores cracked diametrally and axially. While it is assumed that the cores underwent a minimal change in volume and weight, it is accepted that calculated values of porosity will be higher, and bulk density lower, than 'true' values. This has been accepted as a limitation on measuring bulk rock properties for this sample. Calculated values have errors compatible with those found for other samples, and this lends some justification to the above assumptions.

3.4 BULK DENSITY AND POROSITY

Dry bulk densities of the sandstones are relatively low for sedimentary rocks, ranging from 1740 to 2310 $kg.m^{-3}$. Table 3.2 summarises dry bulk densities and porosities for a number of common rock types. The Cape Rodney sandstone is the densest in this study at 2310 $kg.m^{-3}$ and is comparable to other porous sedimentary rocks such as shales and limestones. Saturated bulk densities are higher than dry densities for all the samples, and span a narrower range from 2060 to 2410 $kg.m^{-3}$.

Porosities cover a wide range from 10 to 32 %. The Cape Rodney sandstone is the least porous. All other samples are very porous with values comparable to granular soils. Following the scheme reported by Derski (1989), and presented in table 3.3, the Cape Rodney sandstone is porous, the Parnell Grit, Tipau and Waiake sandstones are very porous, while the Rothesay sandstone is pervious. As expected, the most porous sample is the least dense while the least porous sandstone is the densest.

TABLE 3.3 Classification of Porosity (Derski *et al.*, 1989)

POROSITY (%)	DESCRIPTION
$\eta < 0.5$	Fully impervious rock
$0.5 \leq \eta < 1.5$	Impervious rock
$1.5 \leq \eta < 2.5$	Sufficiently impervious
$2.5 \leq \eta < 5$	Low-porous rocks
$5 \leq \eta < 10$	Porous rocks
$10 \leq \eta < 30$	Very porous rocks
$\eta \geq 30$	Pervious rock

TABLE 3.4 Results of Particle Size Analysis

SAMPLE	GRAVEL (%)	SAND (%)	SILT (%)	<2 μm (%)
CAPE RODNEY	—	66.3	25.8	7.9
PARNELL GRIT	48.0	24.0	20.0	6.0
TIPAU SST	—	49.9	43.5	6.6
WAIAKE SST	—	76.5	17.8	5.7
ROTHESAY SST	—	70.1	20.5	9.4

Both the dry bulk densities and porosities compare closely to sandstones investigated by Bell (1978), Caruso *et al.* (1985), Wilkens *et al.* (1986), Dobereiner and De Freitas (1986), and Dyke and Dobereiner (1991).

3.5 GRAIN DENSITY AND VOID RATIOS

The grain densities are very similar for all samples and range from 2380 to 2570 $kg.m^{-3}$. These values are in keeping with a felsic composition of mainly quartz and feldspar with lighter volcanic glass components. They are similar to those values reported by Bell (1978) and Wilkens *et al.* (1986) for sandstones having similar bulk densities and porosities.

Most noticeable is the least dense, most porous Rothesay sandstone having a grain density comparable to the dense Cape Rodney sandstone. This would indicate that the samples are composed of similar mineral constituents having similar grain densities. It also appears that the higher volcanic component of the CR sandstone has little influence on grain density.

Void ratios range from 0.11 to 0.47. These values are quite high for sandstones and, again, are very similar to those of granular soils or porous sedimentary rocks. The high void ratios suggest a wide spacing of grains in the material and indicate that the material may be quite weak (Derski, 1989). By definition, the void ratios are closely related to porosity.

3.6 PARTICLE SIZE ANALYSIS

Particle size distribution was determined by the pipette method described by Folk (1968) and more recently by Lewis (1984). Percentages of gravel, sand, silt, and clay for each sample are presented in table 3.4. Samples were prepared following the disaggregation techniques adopted by Beattie (1990).

Beattie (1991) notes a discrepancy in the definition of the clay/silt boundary used by Sedimentologists and Engineering Geologists. The former use 4 μm as the boundary as opposed to the latter who use 2 μm as the clay/silt boundary. In this study the 2 μm size boundary is used to distinguish

between clay and silt size particles. The use of the word 'clay' is restricted, for the remainder of this study, to refer to the actual clay minerals of the study rocks. The clay size particles in the particle size analysis are described as the <2 μm group.

Results are very similar for most of the rocks. Each sandstone is dominated by sand size grains, ranging from 49.9 to 76.5 %, while the Parnell Grit is dominated by 48 % gravel component. All the samples have low < 2 μm percentages ranging from 5.7 to 9.4 %. The finest grained Tipau sandstone is dominated by sand (49.9 %) but has the highest proportion of silt size grains (43.5 %) of all the samples. This rock would classify as a sandy silt in the classification of Folk *et al.* (1970). All the other samples classify as silty sands except the Parnell Grit, which is a silty sandy conglomerate. The classification terms have been correctly applied using 2 μm as the silt/clay boundary rather than 4 μm, as used by Folk *et al.* (1970).

3.7 SUMMARY

The rocks in this study have high porosities and range from porous to pervious rocks. Bulk densities are low for sedimentary rocks and have values characteristic of granular soils. Grain densities are similar irrespective of porosity or bulk density and indicate that all samples are composed of similar mineral constituents. Void ratios relate closely to porosities. Ratios are high for sedimentary rocks and indicate an open spacing of grains in the rock material.

All the sandstones are dominated by sand size grains, while Parnell Grit is dominated by gravel size material. All samples have low quantities of <2 μm size particles. The Tipau sandstone is characterised by having the largest proportion of silt size grains and is described as a sandy silt. The other samples are described as silty sands. Parnell Grit is described as a silty sandy conglomerate.

CHAPTER 4

GEOMECHANICAL PROPERTIES

CHAPTER 4

GEOMECHANICAL PROPERTIES

4.1 INTRODUCTION

The strength of intact rocks is commonly used to characterise the mechanical reactions of the rock material, and to classify the material by providing an index which can be used to compare the rock with others. To further characterise the mechanical behaviour of the rock material, and to determine the elastic moduli, velocities of compression (P) waves and shear (S) waves through rocks may be measured.

This chapter reports the methods and results of measurements of rock strength in compression (σ_c) and tension (σ_t), records the velocities of primary and shear waves through rock specimens under stress in an attempt to measure dynamic elastic constants, and finally, records the results of rock hardness and durability tests. This is done in order to:

1] characterise the geomechanical properties of the intact sandstone samples,
2] classify the strength of the sandstones,
3] provide index data which may be correlated with textural and microfabric properties in chapters 6 and 7, and
4] correlate the bulk rock properties reported in chapter 3 with the geomechanical properties in order to determine strength indices for the prediction of geomechanical behaviour.

4.2 UNIAXIAL COMPRESSIVE STRENGTH

Uniaxial compressive strength is the simplest index used to describe the mechanical properties of a rock (Attewell and Farmer, 1976), and is the most quoted index (Farmer, 1983). The uniaxial compressive strength (UCS) test is a convenient, direct test, whereby a regular rock specimen is loaded axially (compressed) in one direction (Hawkes and Mellor, 1970).

4.2.1 METHOD

4.2.1.1 Sample Preparation

Regular cylindrical rock cores were used to determine uniaxial compressive strength (σ_c) and were prepared following the method of Brown (1981). Right circular cylinders of NX- core size were drilled, each having a diameter not less than 54 mm and a length to diameter ratio of 2.5 (core length of 137 mm). Cores were cut perpendicular to bedding. For those samples not exhibiting any bedding (Cape Rodney sandstone) cores were cut vertically down into the block samples in terms of the original orientation of the block *in situ*.

Right circular cylinders were used as they minimise 'end effects' such as friction along the contact between the sample and platens of the testing machine, stress distributions are symmetrical in them about the axis, and they are easy to produce (Vutukuri *et al.*, 1974).

Cores were cut using a water cooled, modified drill press. The ends of the cores were cut parallel to each other using a diamond saw blade, and lapped (polished) to obtain flat surfaces. The Rothesay and Waiake sandstones could not be lapped because of their coarse, gritty textures, but were flat to within 0.025 mm after cutting.

4.2.1.2 Sample Measurements

Core lengths were measured at three positions using calipers accurate to within 0.025 mm. Diameters were measured at either end of the core and in the centre of the specimen. The means of these measurements were used to obtain core volumes and end surface areas.

4.2.1.3 Test Environment

It is widely accepted that compressive strength varies with moisture content (Vutukuri *et al.*, 1974; Attewell and Farmer, 1976). In this investigation cores were tested in oven dry and saturated conditions in order to investigate the extremes of strength. Five cores of each sample were oven dried at 105°C for 24 hours prior to testing. Five other cores for each sample were immersed in water under vacuum until all bubbles

ceased to be released. This required between 24 and 36 hours of immersion.

Saturation problems encountered with the Tipau sandstone have been noted in chapter 3. As a result of all five cores cracking upon immersion in water for one hour, no saturated tests could be carried out. Some of the Waiake and Rothesay sandstones began to disintegrate after 12 hours. These samples were removed from the water after a period of 6 to 8 hours; it is recognised that this time may not have allowed complete saturation, but it represents a practical compromise. Saturated specimens were wiped with a moist cloth and weighed to ± 0.05 g prior to testing.

4.2.1.4 Rate of Loading

Brown (1981) recommends that loads on specimens be applied continuously at a constant stress rate such that failure occurs within 5 to 10 minutes, or alternatively, the stress rate should be within the limits of 0.5 to 1.0 $MPa.s^{-1}$. The sandstones in this investigation generally failed within 3 to 4 minutes which corresponded to load rates of less than 0.1 $MPa.s^{-1}$. Samples were consistently loaded at rates of less than 0.01 $MPa.s^{-1}$ such that failure occurred at approximately five minutes. The stronger CR sandstone and Parnell Grit were loaded such that failure occurred within 5 to 10 minutes, which corresponded to rates of around 0.1 $MPa.s^{-1}$.

4.2.1.5 Testing Machine

Compressive testing was carried out using a 'Soiltest' Concrete testing machine (Model C.T.710, Soil Test Inc., U.S.A.) with plates conforming to the American Society of Testing and Materials C39 specifications. Compression was applied by means of a high pressure pump with flow control valves linked to a hydraulic ram via two gauges. These gauges measured the applied load; the first ranged from 0 to 9000 kg for weaker materials and the second ranged from 0 to 120 000 kg for weak to strong materials. For the remainder of this study the test is referred to as the 'UCS' test.

TABLE 4.1 Uniaxial Compressive and Tensile Strengths for the study rocks

	$\sigma_{c,dry}$	$\sigma_{c,sat}$	$\frac{\sigma_{c,dry}}{\sigma_{c,sat}}$	$\sigma_{t,dry}$	$\sigma_{t,sat}$	$\frac{\sigma_{t,dry}}{\sigma_{t,sat}}$
CAPE RODNEY	79 ± 7	62 ± 4	1.3	10 ± 1	7.1 ± 0.9	1.5
PARNELL GRIT	19 ± 2	12 ± 1	1.6	3.0 ± 0.3	2.3 ± 0.3	1.3
TIPAU SST	16 ± 1	—	—	2.6 ± 0.3	1.2 ± 0.2	2.2
WAIAKE SST	13 ± 1	2.8 ± 0.1	4.7	1.9 ± 0.2	0.8 ± 0.1	2.4
ROTHESAY SST	7.2 ± 0.7	1.9 ± 0.1	3.8	1.1 ± 0.1	0.9 ± 0.1	1.2

$\sigma_{c,dry}$ — oven dry compressive strength (MPa)
$\sigma_{c,sat}$ — saturated compressive strength (MPa)
$\sigma_{t,dry}$ — oven dry tensile strength (MPa)
$\sigma_{t,sat}$ — saturated tensile strength (MPa)

4.2.2 RESULTS

Compressive strength data are presented in table 4.1; this includes both dry ($\sigma_{c,dry}$) and saturated ($\sigma_{c,sat}$) values, and softening factors ($\sigma_{c,dry}/\sigma_{c,sat}$). All values represent means and standard errors of five replicate measurements. Dry compressive strengths range from 7.2 to 79 MPa. Saturated compressive strengths are lower, ranging from 1.9 to 62 MPa.

Cape Rodney sandstone is the strongest sample in both dry and saturated conditions, and undergoes a 21 % strength reduction upon saturation. Parnell Grit is the strongest ECB sample with a dry compressive strength of 19 MPa. Rothesay sandstone is the weakest rock having a dry compressive strength of 7.2 MPa. Tipau and Waiake sandstones have dry compressive strengths of 16 and 13 MPa respectively. The weakest Rothesay and Waiake samples undergo 74 and 79 % strength reductions upon saturation and, consequently, have the highest softening factors of 3.8 and 4.7 respectively.

4.2.3 STRENGTH CLASSIFICATION

Compressive strength data are used widely in the strength classification of rocks. Dobereiner and De Freitas (1986) classify weak sandstones on the basis of saturated compressive strengths because of the variation in compressive strength with degree of sample saturation. They define weak sandstones as having saturated uniaxial compressive strengths ranging from 0.5 to 20 MPa. The boundary between soil and rock is taken as 0.5 MPa. This scheme is similar to that of the International Society of Rock Mechanics, reported by Brown (1981).

The Engineering classification for intact rock proposed by Deere and Miller (1966) class all the rocks in this study as having very low strengths (<28 MPa), except the CR sandstone which has a medium strength (55 to 110 MPa). Similarly, Attewell and Farmer (1976) would class the sandstones as very weak to medium strength.

For this investigation, the proposed scheme of Dobereiner and De Freitas (1986) for the classification of weak sandstones is adopted.

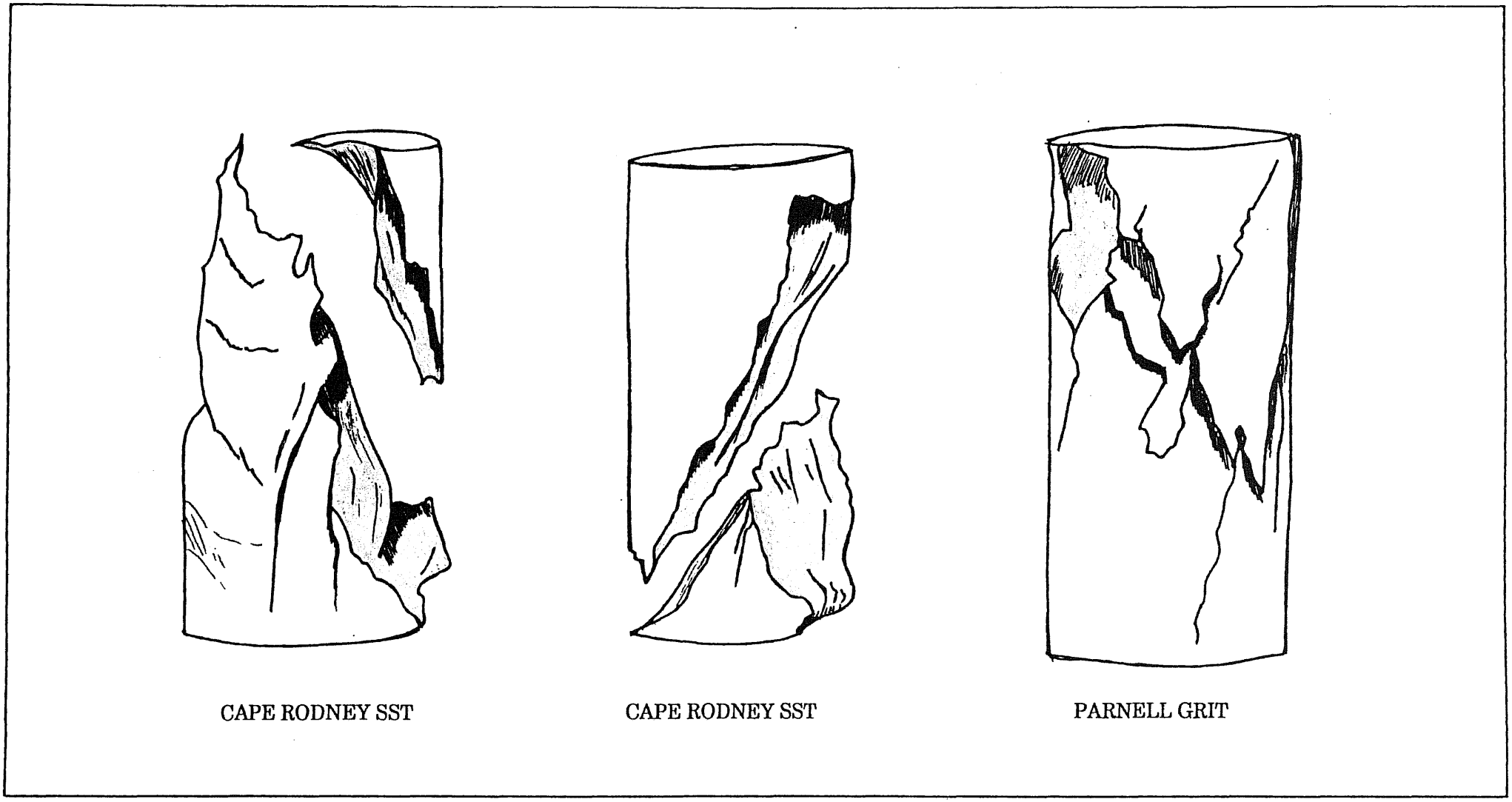

FIGURE 4.1 Sketches of cataclasis failure mechanisms in CR sandstone and Parnell Grit.

The samples classify as follows:

Cape Rodney Sst	- moderately strong rock	(20 - 80 MPa)
Parnell Grit	- weak rock	(7 - 20 MPa)
Tipau Sst	- very weak rock	(3 - 7 MPa)
Waiake Sst	- extremely weak rock	(0.5 - 3 MPa)
Rothesay Sst	- extremely weak rock	(0.5 - 3 MPa)

4.2.4 MODE OF FAILURE

The dominant mode of failure exhibited by the rocks in this study is the cataclasis mode of Hawkes and Mellor (1970). This mode of failure is best illustrated by the stronger CR sandstone (plate 4.1a and figure 4.1). Conical end fragments are usually all that remains on the platens once failure occurs. The saturated CR sandstone failed by a combination of cataclasis and axial cleavage. Vertical cracks appeared and audible cracking could be heard. Flakes peeled off the sides toward the core ends prior to catastrophic failure. Study of failed specimens indicates that individual grains were crushed as the rocks were compressed to failure.

The Parnell Grit failed primarily through a combination of cataclasis and axial cleavage (plate 4.1b and figure 4.1). Internal cracking and the formation of vertical cracks axially led to relatively quiet failures. No conical wedge shapes remained after failure but cracks in failed specimens revealed the early stages of their development. Shearing along an oblique plane occurred in three oven dry samples. These planes were bisected by vertical splitting. The shear mode of failure may be more characteristic of the loading system due to either platen rotation or lateral translation of the plates relative to each other (Hawkes and Mellor, 1970). Failure was quiet in both dry and saturated conditions. In these samples, cracks propagated through the muddy matrix with their direction and continuity controlled by individual clasts. Many samples revealed cracks around grains but not through them.

The weaker sandstones failed by a combination of cataclasis and shear. Vertical cracks appeared at low stresses and split the length of the core almost instantly (plates 4.2a, 4.2b, and figure 4.2). No audible cracking was heard for any of these weaker sandstones. It appears that as the samples were compressed individual grains were dislodged and rolled, similar to

A Remnants of failed specimens (in compression) of Cape Rodney sandstone

B Failed core specimens of Parnell Grit

PLATE 4.1 Failed core specimens of CR sandstone and Parnell Grit

A Remains of core specimens after compressive strength tests, Rothesay sandstone

B Failed ECB sandstones tested in compression. Tipau sandstone on the left, and Waiake sandstone on the right.

PLATE 4.2 Remains of ECB sandstones after compression tests

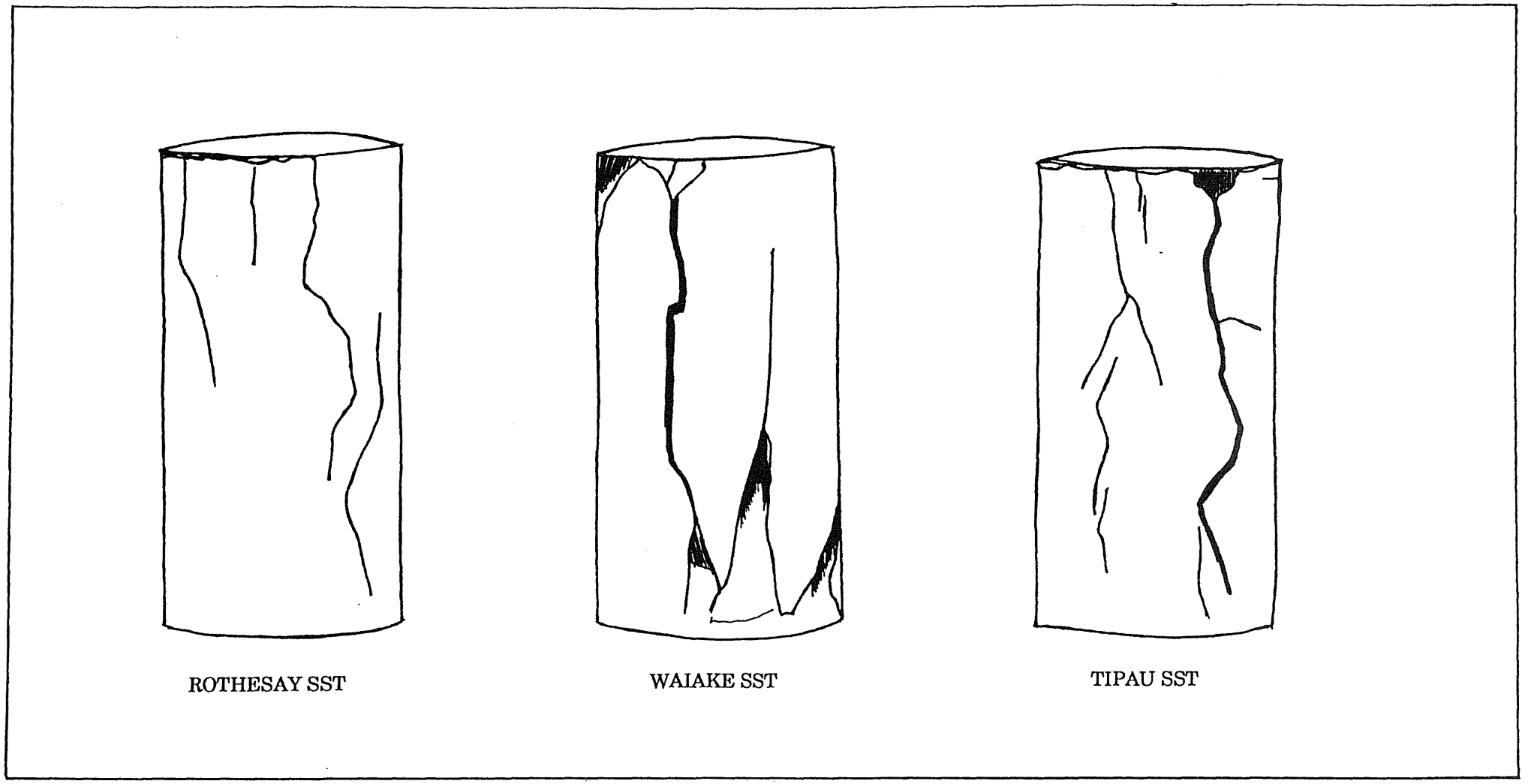

FIGURE 4.2 Sketches of cataclasis and axial cleavage failure mechanisms in ECB sandstones.

the failure of loose granular soils. This was also observed by Dobereiner and De Freitas (1986).

4.3 INDIRECT TENSILE STRENGTH

Determination of indirect tensile strength was carried out using the Brazilian test. This method is widely accepted as representing a good approximation of tensile strength (Hawkes and Mellor, 1970; Vutukuri *et al.*, 1974; Attewell and Farmer, 1976). The Brazilian test involves the diametral compression of solid disks but produces failure in a biaxial rather than a uniaxial stress field.

4.3.1 METHOD

4.3.1.1 Sample Preparation

Preparation of samples and test procedures were carried out following the method of Brown (1981). Long rock cores were prepared as outlined in section 4.2.1.1. Short disks were cut from these, having length to diameter ratios of 0.5 (length = 27 mm). Ten samples were oven dried at 105°C for 24 hours while ten others were immersed in water under a vacuum until no bubbles were released (24 - 36 hrs).

The Tipau sandstone samples were successfully saturated because the short core lengths enabled the pale grey portions found in longer cores (and observed cracking upon saturation) to be avoided. This may result in slightly biased data as it ignores the effect of swelling clays on tensile strengths. Consequently, the quoted results may suggest a somewhat higher tensile strength than the rock actually possesses. Dry tensile strength may, therefore, be a more accurate indicator of the true tensile strength.

4.3.1.2 Test Machine

The Soiltest Concrete testing machine used for determination of compressive strength was employed for this test. Disks were placed in two steel loading jaws positioned above and below the specimen, and joined by a guide pin. One layer of masking tape was wrapped around the circumference of the disks as suggested by Brown (1981). The jig and specimen were compressed as for the UCS test.

TABLE 4.2 Compressive and Tensile Strengths for some common rock types

ROCK TYPE	σ_c (MPa)	σ_t (MPa)
GRANITE	100 - 250	7 - 25
BASALT	100 - 350	10 - 30
DOLERITE	100 - 350	15 - 35
SANDSTONE	20 - 200	1 - 25
SHALE	5 - 200	0.2 - 20
LIMESTONE	30 - 250	2 - 25
COAL	5 - 50	2 - 5

σ_c — unconfined uniaxial compressive strength
σ_t — tensile strength

Data compiled from; Attewell and Farmer, 1976; Goodman, 1980; Selby, 1982; and Jumikis, 1983.

4.3.1.3 Rate of Loading

Load on the specimens was applied at a constant rate such that failure in the weakest samples occurred within 15 to 30 seconds as proposed by Brown (1981). This corresponded closely to the recommended rate of 200 $N.s^{-1}$ (0.1 $MPa.s^{-1}$). Load rate was kept constant for all specimens.

4.3.2 RESULTS

Results are presented in table 4.1. Tensile strengths range from 1.1 to 10 MPa (oven dry) and 0.9 to 7.1 MPa (saturated); CR sandstone is the strongest rock at both moisture extremes. Parnell Grit is the strongest ECB sample in tension, with a dry tensile strength of 3.0 MPa, whereas the Rothesay sandstone is the weakest rock with a dry tensile strength of 1.1 MPa, an order of magnitude less than that of the CR sandstone. These results follow the trends observed for compressive strengths in section 4.2.2 with CR sandstone being the strongest sample and Rothesay sandstone the weakest.

The Tipau and Waiake sandstones have the highest softening factors (2.2 and 2.4 respectively) which correspond to strength reductions upon saturation of 54 and 58 %. The softening factor of 1.2 for the Rothesay sandstone is believed to be inaccurate due to the inability of the test machine to record accurate load values at very low stresses. This means that saturated tensile strength values for Rothesay sandstone may be marginally overestimated. However, oven dry tensile strengths for the sandstones are, on average, 85% lower than UCS strengths. This is remarkably consistent for all samples with percentages ranging from 84 to 87 %. Saturated tensile strengths average 74 % lower than saturated compressive strengths. These results indicate that the reported saturated tensile strengths are most probably reliable.

4.4. COMPARISON OF STRENGTH DATA

Typical compressive and tensile strengths for a variety of rocks are presented in table 4.2. The rocks in this study have extremely low compressive strengths, with only the CR sample within the 'normal' range of sandstone strengths. The ECB samples have strengths comparable to weak shales or coal. Table 4.2 shows tensile strengths for sandstones to

range from 1 to 25 MPa. While the results in this investigation fall within this range, they are all less than 10 MPa and are more characteristic of shales, limestones or coal.

Similar results were reported by Dobereiner and De Freitas (1986). Some of their samples behaved as low strength (< 20 MPa) rock whilst others (Coina Sand) behaved as a dense sand (σ_c < 0.5 MPa). They observed that a 10 % change in moisture content resulted in a drop of 20 MPa in strength and quote an example of Kidderminster sandstone where compressive strength dropped from 2.3 to 0.45 MPa upon saturation, representing an 80 % drop in strength.

Bell (1978) reports strength reductions of 30 % upon saturation for Northumberland sandstones. Tensile strengths were, on average, 90 % lower than compressive strengths and ranged from 2.1 to 9.5 MPa. Compressive strengths ranged from 33 to 112 MPa.

4.5 DETERMINATION OF DYNAMIC ELASTIC CONSTANTS

Measurement of the propagation of ultrasonic and seismic waves is common practice in the characterisation of rock masses. King (1983) provides examples where this technique is employed in mineral exploration, mining operations and site investigations. Measurement of seismic waves through the rocks in this study was undertaken to determine the deformability of the samples in compression. The laboratory ultrasonic pulse method was employed to determine the dynamic elastic constants of Youngs Modulus (E) and Poissons ratio (υ). Velocities of compression (P) and shear (S) waves are denoted by Vps and Vss respectively in this study.

Youngs Modulus (or deformation modulus) is simply the ratio of normal (axial) stress to axial strain at a specified stress level, while Poissons Ratio is the ratio between transverse and longitudinal strain (Farmer, 1983).

4.5.1 TEST PROCEDURE

The procedure of King reported in Anon (1983) is used in this investigation. A PUNDIT (Portable Ultrasonic Non-destructive Digital Indicating Tester) manufactured by CNS Electronics Ltd, London, was used to measure elastic wave pulse arrival times. Elastic waves were produced using piezoelectric transducers placed at either end of short (54 mm long) rock

cores (length to diameter ratios of 1:1). Short cores were used due to the limiting distance between platens in the testing machine.

Acoustic coupling was provided by placing thin aluminium foil plates between the rock core and transducers. To allow for the additional delay in pulse signal arrival times caused by the foil plates, the calibration procedure described by Major (1986) was followed. The foil was bedded between the transducers by placing a small load on them initially. Transit times for P and S waves were recorded at each stress level as loads were applied.

In the actual test, the rock core specimens were inserted between the foil discs and placed in the UCS machine. At increments of stress, pulse arrival times for the calibrated foil plates were subtracted from those recorded from the core plus the foil. For each stress level, elastic wave velocities (Vps and Vss) were recorded for the final calculated pulse times. Loads were removed just prior to failure.

4.5.2 DYNAMIC ELASTIC MODULI EQUATIONS

Dynamic Elastic Modulus (Youngs Modulus, E) is determined from the following relationship:

$$E = \frac{\rho\, Vss^2\,(3Vps^2 - 4Vss^2)}{Vps^2 - Vss^2} \qquad [4.1]$$

ρ	= rock bulk density	$(kg.m^{-3})$
Vps	= velocity of compression waves	$(m.s^{-1})$
Vss	= velocity of shear waves	$(m.s^{-1})$

This relationship assumes an isotropic material (King, 1983) and shows E to be dependant on the wave velocity, and density of the rock material.

4.5.3 WAVE ATTENUATION

The shear wave velocity could not be determined in dry or water saturated cores at any stress level. In the most porous sandstones Vps could not be determined from saturated specimens. It appears that in these porous rocks wave attenuation is great, resulting in a signal too weak to be detected. The effects of wave attenuation and energy dispersion have been addressed by O'Connell and Budiansky (1970), Johnston and Toksov (1980), and Winkler (1983, 1985). In particular, Johnston and Toksov (1980) provide a list of authors who have measured attenuation using varying techniques.

As attenuation occurs in both dry and saturated specimens, the mechanisms operating here are most likely to be scattering and friction. These mechanisms are referred to as 'material deformation' by Attewell and Farmer (1976). Winkler (1983, 1985) reports on scattering theory for waves in solids containing spherical inclusions. He concludes that in dry samples of sandstones, wave propagation is dominated by scattering effects, although a scattering model does not yet exist that can be usefully applied to rocklike materials. Johnston and Toksov (1980) observed the primary mechanism for wave attenuation in Berea and Navajo sandstones at low stresses was friction at crack and grain boundary contacts. They observe that in saturated rock 'the effect of friction is enhanced owing to wetting and lubrication of the sliding contacts by the pore fluid.'

In the saturated samples attenuation may also be caused by fluid flow. O'Connell and Budiansky (1974, 1977) have accounted for attenuation of seismic waves in water saturated rocks by this mechanism. It involves the flow of fluids out of regions of compression and is essentially that of consolidation. Internal flow of fluids within pore spaces results in energy dissipation (Johnston and Toksov, 1977). Wave attenuation in this investigation is attributed to a combination of these three processes: friction, scattering, and fluid flow.

In this study, Vss could not be determined at any stress level for all samples, therefore Poissons ratio (υ) was estimated (for each sample) from values reported by Attewell and Farmer (1976), Lama and Vutukuri (1978), Goodman (1980), Farmer (1983), and Jumikis (1983) for other porous sedimentary rocks (predominantly sandstones) having similar bulk densities, porosities, and tensile strengths to the rocks of this study.

TABLE 4.3 Seismic velocities and Dynamic Youngs Modulus

SAMPLE	V_{ps} (dry) (low stress)	V_{ps} (sat) (low stress)	V_{ps} (dry) (peak stress)	V_{ps} (sat) (peak stress)	E_i (dry)	E_i (sat)	E_p (dry)	E_p (sat)
CAPE RODNEY	340 ± 20	280 ± 80	1770 ± 130	2550 ± 1070	0.24 ± 0.02	0.2 ± 0.1	6.4 ± 1.0	6.0 ± 1.2
PARNELL GRIT	150 ± 60	450 ± 90	1060 ± 80	1110 ± 140	0.04 ± 0.03	0.3 ± 0.1	1.8 ± 0.3	1.9 ± 0.5
TIPAU SST	230 ± 40	—	890 ± 50	—	0.06 ± 0.02	—	1.0 ± 0.1	—
WAIAKE SST	370 ± 50	—	1070 ± 60	—	0.16 ± 0.04	—	1.3 ± 0.2	—
ROTHESAY SST	290 ± 70	—	1190 ± 60	—	0.08 ± 0.04	—	1.2 ± 0.1	—

V_{ps} (dry) — P wave seismic velocity (oven dry core) ($m.s.^{-1}$)
V_{ps} (sat) — P wave seismic velocity (saturated core) ($m.s.^{-1}$)
E_i (dry) — Youngs Modulus at low stress (oven dry) (GPa)
E_i (sat) — Youngs Modulus at low stress (saturated) (GPa)
E_p (dry) — Youngs Modulus at peak stress (oven dry) (GPa)
E_p (sat) — Youngs Modulus at peak stress (saturated) (GPa)

Youngs Modulus was then determined from:

$$E = \frac{(1 - 2\upsilon)(1 + \upsilon)\,\rho\, Vps^2}{(1 - \upsilon)} \qquad [4.2]$$

υ	= Estimated Poissons Ratio	
Vps	= velocity of compression waves	$(m.s^{-1})$
ρ	= rock density	$(kg.m^{-3})$

Equation 4.2 is reported by Lama and Vutukuri (1978).

4.5.4 RESULTS

Velocity of compression waves (Vps), and values of Youngs Modulus (E) are presented in table 4.3. Vps and E are reported at peak and low stresses. Low stress corresponds to the stress level at which the first pulse arrival time was displayed on the PUNDIT and commonly occurred at approximately 2 MPa. Estimated Poissons ratios appear in table 4.4. Poisson Ratio values are not recorded for ECB sandstones (saturated conditions) because neither Vps nor Vss were recorded from saturated cores, due to the effects of wave attenuation.

4.5.4.1 Velocity of Compression Waves (Vps)

The primary wave velocity values range from 150 to 370 $m.s^{-1}$ at low stresses and 890 to 1770 $m.s^{-1}$ at peak stresses. These values are low for sandstones. Bell (1978) records velocities in the order of 2000 to 3000 $m.s^{-1}$ for Fell sandstones. However, Dyke and Dobereiner (1991) record a saturated velocity of 400 $m.s^{-1}$ for Constanheira Sand with 35 % porosity. Typical values for wave velocities are provided by Attewell and Farmer (1976) and range from 1500 to 3500 $m.s^{-1}$. Sand has typical values of 300 to 1200 $m.s^{-1}$. The ECB sandstones and Parnell Grit have values characteristic of sands whilst CR sandstone is the only sample with velocities typical of sandstones.

Velocities of primary waves increase as stress increases for all samples. Likewise, for CR sandstone and Parnell Grit, Vps increases with sample saturation. At a low stress this is not the case for CR sandstone but given the large error of $\pm$ 80 $m.s^{-1}$ it could be assumed to follow a similar trend as the others. These observations have been reported by O'Connell and

TABLE 4.4 Estimated Poisson Ratios

SAMPLE	υ (dry)	υ (sat)
CAPE RODNEY	0.22	0.25
PARNELL GRIT	0.28	0.30
TIPAU SST	0.33	—
WAIAKE SST	0.35	—
ROTHESAY SST	0.40	—

Budiansky (1974), King (1983, 1984), and Yang and King (1986). This increase in Vps with saturation is due to the fact that Vp is greater in water than air. King (1984) concludes that small moisture content increases in dry rocks having appreciable crack porosity results in large increases in Vp and Vs. Similarly, O'Connell and Budiansky (1974) have shown that Vp and Vs increase as pressure (or stress) increases due primarily to the closing of cracks reducing the pore space, until they no longer have an appreciable effect on the elastic properties of the rock.

4.5.4.2 Deformation Modulus (E)

Deformation modulus values presented in table 4.3 were calculated using equation 4.2. They follow similar trends to Vps because E is dependant upon Vps, rock density and Poissons ratio. The values of E (0.04 to 6.4 GPa) indicate that the samples are all highly deformable. Typical E values for sandstones range from 2 to 70 GPa (Selby, 1985). At peak stress levels, only the CR sandstone (6.4 GPa oven dry core) falls within this range and occurs at the lower end of the range. All other values are less than 2 GPa and have deformation characteristics more akin to sands.

4.5.4.3 Deformation modulus (E) versus Axial Stress

The deformation modulus increases as stress increases. Plots of E against axial stress appear in figures 4.3, 4.4 and 4.5. Typical curves for ECB sandstones are presented in figure 4.3. These sandstones are typified by extremely low deformation moduli even at peak stresses. In each case, the curves follow similar trends with E starting at very low stresses and rapidly reaching a maximum before levelling off.

In general, Youngs Modulus increases rapidly and continuously for small increments of stress in Tipau and Rothesay sandstones. The steep curves show E increases as loads are applied and indicate that there is a decreased strain with every increment of load (non-elastic response). This is termed strain hardening and is typical behaviour for sandstones loaded perpendicular to their bedding planes (Lama and Vutukuri, 1978).

The curves for Waiake sandstone reveal an initial flatter segment prior to rising steeply and levelling off at peak stresses. This initial flat segment is less pronounced, but still present, in some samples of Rothesay sandstone (R2,R3,R5 in figure 4.3) and Tipau sandstone (T2,T5 in figure 4.3). It

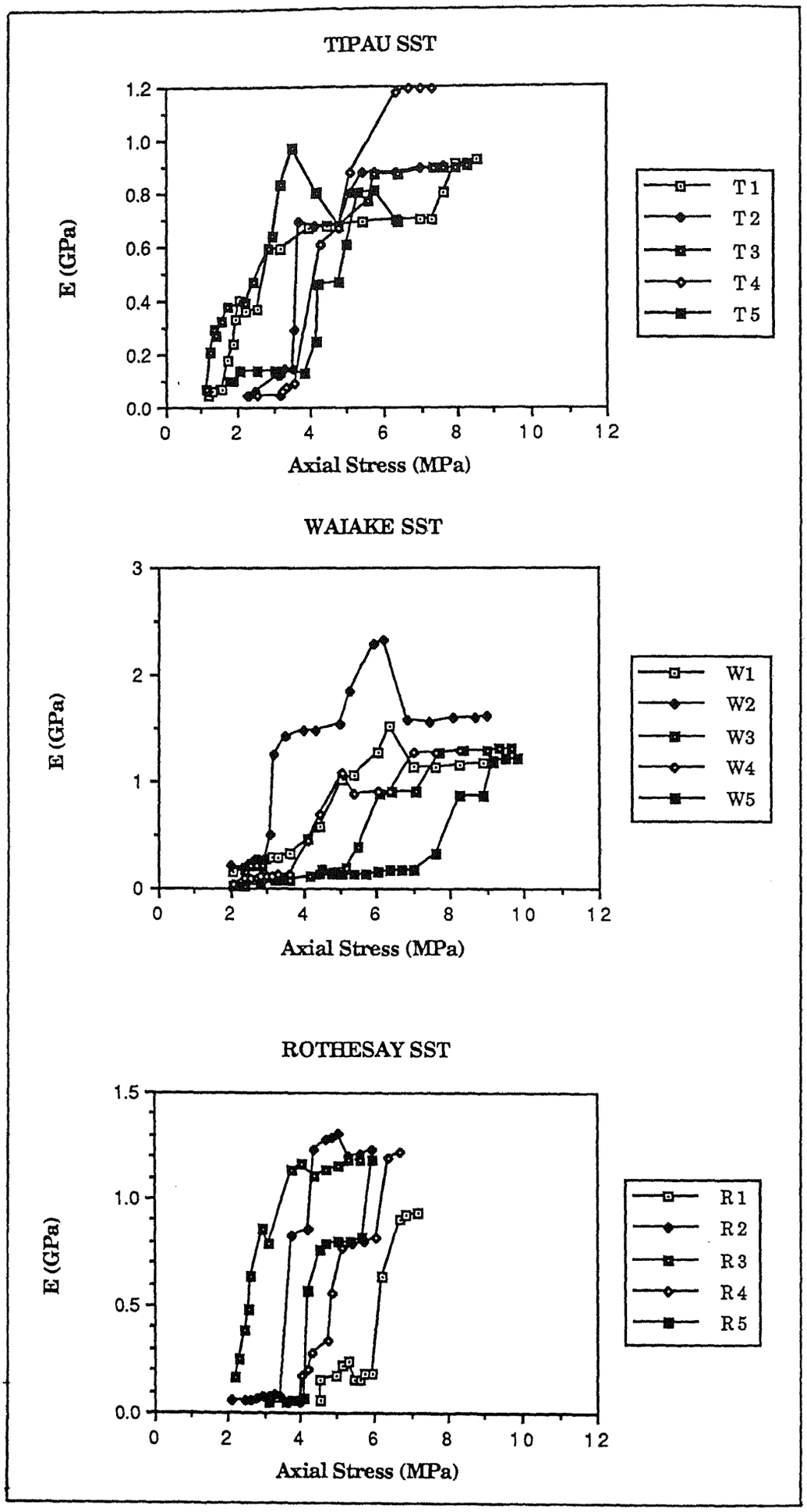

FIGURE 4.3 Plots of E versus axial stress for oven dry ECB sandstones.

indicates that Youngs Modulus remains constant as loads are initially applied, resulting in an increase in strain. As further axial stresses are applied, Youngs Modulus rapidly increases, representing a non-elastic response to applied load. Approaching peak stresses E remains constant.

Plots for oven dry Parnell Grit and CR sandstone are flatter than those of ECB samples (figure 4.4). In particular, CR sandstone has remarkably similar curves for each sample. Youngs Modulus increases initially as loads are applied but then remains constant over a wide stress range. This represents an elastic behaviour typical of strong igneous rocks and strong sandstones (Lama and Vutukuri, 1978). At high stresses of around 20 MPa, E again increases with stress before remaining constant to failure.

Youngs Modulus increases continuously with applied stress for Parnell Grit. The curves are flatter than those of ECB sandstones and indicate the increase in E is at a slower rate. Between 6 to 11 MPa the curves are nearly flat (E remains fairly constant as stress increases) and the rocks exhibit an elastic response to load.

Plots of E against axial stress for saturated CR sandstone and Parnell Grit are characterised by much greater increases in E at low stresses (figure 4.5). After this initial rapid and continuous increase the curves level off and E remains largely constant to failure.

4.5.4.4 Discussion

The observed trends of Youngs Modulus against axial stress are similar to results reported by Bell (1978) and Dyke and Dobereiner (1991).

The steep curves of E against axial stress for ECB sandstones indicate a non-elastic response to load. Dyke and Dobereiner (1991) note that for weak sandstones, the region of elastic behaviour is not always clearly defined. The rocks undergo an initial 'plastic deformation' associated with closure of pre-existing microcracks and pores at low stress levels. The onset of dilatancy in these weak sandstones occurs at low stress levels. East Coast Bay samples are characterised by rapid pore and microcrack closure. At intermediate stress levels the rocks exhibit a strain hardening behaviour as cracking of grain contacts results in a closure of the fabric, with an associated increase in grain contact areas, prior to microcrack development and propagation. No interval of elastic behaviour is observed.

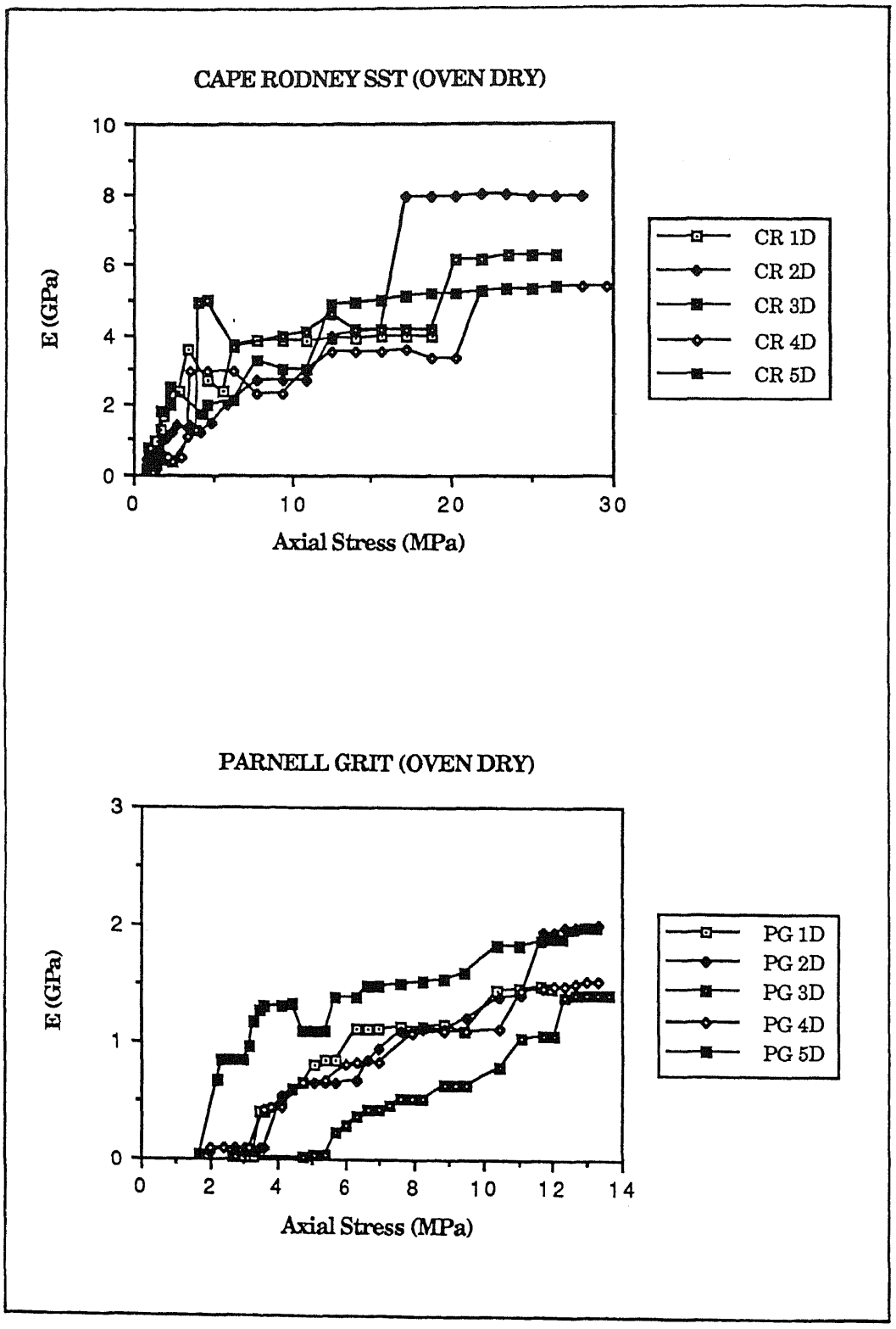

FIGURE 4.4 Plots of E versus axial stress for oven dry CR sandstone and Parnell Grit.

Pore closure is less rapid in Parnell Grit and even less so in CR sandstone. These rocks undergo similar deformation mechanisms to Fell sandstones described by Bell (1978). Their behaviour is described as plastic-elastic-plastic. Initial plastic pore and crack closure is followed by the rock compressing elastically as further loads are applied. The samples become elastically stiffer prior to microcrack development at a controlled rate. As stresses increase microcracks coalesce, resulting in rapid macrocracking described as strain softening deformation by Farmer (1983).

A large component of non-elastic behaviour occurs in the initial stages of deformation for saturated samples of Parnell Grit and CR sandstone. Dyke and Dobereiner (1991) observe that an increase in moisture content tends to reduce the range of elastic behaviour by promoting stress corrosion-aided microcracking at low levels of stress. The presence of water increases the velocity of crack propagation because strong silica - oxygen bonds are replaced by weaker hydrogen bonds within the silicate lattice. When this occurs at the tip of a microcrack propagating under tension, the stress required for failure at the tip is reduced by weakening the strength of the crystal lattice that lies in the path of failure. This mechanism is most likely producing the trends observed in saturated specimens in this investigation.

4.5.4.5 Usefulness of Data

The method of measuring seismic wave velocities through short rock cores under stress was only partially successful in determining dynamic elastic constants. Wave attenuation was significant in most samples so Vss could not be determined and Poissons ratio had to be estimated and assumed to be constant for each sample. This is probably not true in practice.

Dyke and Dobereiner (1991) observe 'the elastic range of material behaviour for sandstone is often below 20 % of peak strength. Consequently, elastic properties should be measured at low stress levels rather than at 50 % of peak strength'. They strongly recommend that volumetric strain be observed as normal practice when testing sandstones in order to ascertain when non-elastic strain has initiated. This was not physically possible in this investigation and must be accepted as a limitation on this method of measuring E.

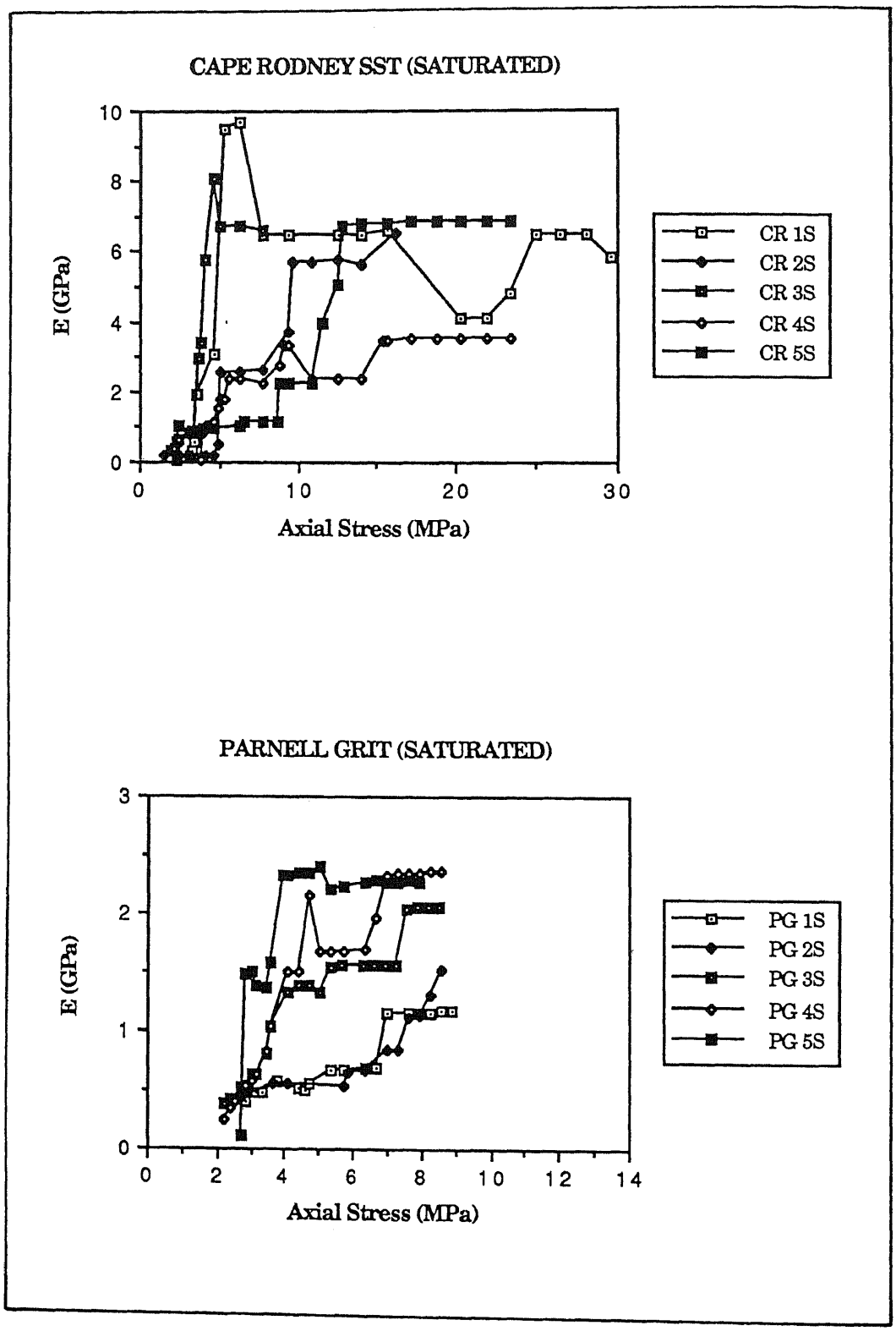

FIGURE 4.5 Plots of E versus axial stress for saturated CR sandstone and Parnell Grit.

The values for E_i and E_p do provide an indication of the behaviour of the samples. These high porosity, inhomogeneous rocks with low strengths are likely to undergo a large amount of deformation under stress. Although upto 50 % error is recorded in the results, they are used in correlations with other mechanical index properties in chapter 5. It is, however, recommended that this method of measuring E for porous sandstones not be adopted as common practice, primarily due to the extreme wave attenuation observed but also because volumetric strain cannot be observed by this method.

4.6 HARDNESS AND DURABILITY

The index parameters of hardness and durability were measured primarily to determine their usefulness as predictors of geomechanical strength. Hardness was measured using both the L-Type Schmidt Hammer and the Shore Scleroscope. The Schmidt Hammer was used on intact rock blocks collected for coring so as to eliminate the deleterious effects of joints and cracks *in situ*. Shore Scleroscope hardness was determined on short cores (length to diameter ratios of 1:1) of 54 mm length. The slake durability index was used to measure the durability of the rocks.

4.6.1 HARDNESS

The complexity of defining hardness requires that all measures of hardness be made on a relative scale. Hardness measurements have been made for many years to assess the general mechanical properties of metals (Deere and Miller, 1966). In geomechanics, hardness of a mineral and rock is sometimes the resistance to abrasion (Jumikis, 1983). It is noted by Deere and Miller (1966) that in all types of hardness, the properties of resilience, strength, and elasticity are involved to some degree. Hardness is dependant on the strength of grain-to-grain and grain-to-cement contacts, the strength of cementing material, and the strength of individual grains. In this study, dynamic (rebound) hardness (Deere and Miller, 1966) is determined, where the elastic properties may be as important as the plastic properties.

TABLE 4.5 Schmidt Hardness 'R' and Shore Hardness results

SAMPLE	R_{field}	R_{block}	S.H
CAPE RODNEY	27 ± 3	35 ± 2	45 ±7
PARNELL GRIT	18 ± 1	20 ± 1	26 ± 5
TIPAU SST	22 ± 2	17 ± 1	19 ± 3
WAIAKE SST	19 ± 2	18 ± 1	11 ± 1
ROTHESAY SST	20 ± 2	14 ± 2	11 ± 1

R_{field} — Schmidt Hardness *in situ*

R_{block} — Schmidt Hardness on rock blocks

S.H — Shore Hardness on short cores

4.6.1.1 Test Procedures

Schmidt Hammer

The L-Type Schmidt Hammer was used on intact rock blocks collected for laboratory mechanical testing. It was used in accordance with the method suggested by Brown (1981) and follows the same procedure as used in the field, and described in chapter 2. The instrument was used in the horizontal position so direct comparisons could be made with field measurements. The same L-Type hammer was used in both field and laboratory tests.

Shore Scleroscope

A model C-2 Shore Scleroscope was used to determine dynamic hardness on short air dry cores. Rock cores were stored in the same environment (laboratory) as the intact block samples (for a minimum of two weeks) so that Schmidt Hammer values (R_{block}) could be directly compared with Shore Hardness values at similar moisture conditions. With the Shore Scleroscope, the distance of rebound of a small diamond tipped hammer falling under the influence of gravity, is measured on a relative scale from 0 to 140. The machine was calibrated using calibration bars supplied with the machine and having nominal rebound values of 23 to 25 and 90 to 92 units.

The procedure of Brown (1981) was adhered to. At least 20 rebound readings were recorded on the flat core ends and each indentation was recorded at a new position. Both ends of sample cores were tested and the average readings taken as representing the Shore hardness of the specimen.

4.6.1.2 Hardness Results

Schmidt hammer rebound values for *in situ* and laboratory conditions as well as Shore hardness are reported in table 4.5.

It is apparent from the table that there is a much greater range in R_{block} values (14 to 35) than for R_{field} results (20 to 27). Also apparent are the smaller errors associated with R values recorded from the intact block samples. These findings indicate that the field conditions reduce hardness

variability between sites, but increase variability within sites; these are very undesirable features for an index (predictive) test.

The CR sandstone has a higher 'R' value for the intact block (35) compared with its *in situ* reading (27). The lower field value is attributed to the effects of cracks and discontinuities absorbing some of the impact energy, and hence lowering the rebound values. No plausible explanation can be given to explain the low rebound value for the laboratory R values of the Rothesay and Tipau sandstones when compared with their field values. The effect of cracks within intact block samples must be minimal because cores drilled from the same blocks were complete and free of visible cracks.

The Shore hardness values follow similar trends to the 'R' values in that the least porous CR sandstone has the highest rebound values (45) and the pervious Rothesay sandstone has, on average, the lowest rebound value (11). The ECB sandstones are characterised by generally low rebound values.

4.6.2 SLAKE DURABILITY

The durability of a rock is a measure of its resistance to weakening and disintegration when exposed to short term weathering processes such as wetting and drying (Brown, 1981). Durability of a rock is a relative term (Jumikis, 1983). The slake durability test is an index test initially devised for measuring the durability of clastic sedimentary rocks for classification purposes (Beavis, 1985). In this study, the test is used not only to classify the durability of the sandstones, but to assess any relationships which may exist between strength and durability of the rocks.

4.6.2.1 Method

The method of Brown (1981) was adhered to. Samples underwent 10 minutes of slow rotation in water filled drums and were then dried at 105°C for 24 hours. Three cycles were run and the weight of material lost after each cycle used to determine the slake durability index. For classification purposes, the second cycle was used as the slake durability index (Id_2).

TABLE 4.6 Durability Results (Id_2)

SAMPLE	Id_2	CLASSIFICATION
CAPE RODNEY	98 ± 1	V. HIGH DURABILITY
PARNELL GRIT	83 ± 4	MEDIUM
TIPAU SST	50 ± 8	LOW
WAIAKE SST	41 ± 2	LOW
ROTHESAY SST	49 ± 7	LOW

Id_2 — Slake durability index (%)

Classification after Gamble (1971).

4.6.2.2 Results

Slake durability index values appear in table 4.6. They are classified according to Gamble's (1971) durability scheme reported by Goodman (1980). Loss of material for each sample is plotted in figures 4.6 and 4.7.

The strong CR sandstone has a very high durability, the Parnell Grit a medium durability, and the ECB sandstones all have low durabilties. Beavis (1985) notes that the slake durability test has components of both simple slaking (wetting and drying) and mechanical abrasion. To assess which process dominates, rock fragments from each sample were subjected to simple wetting and drying by repeatably placing the sample from an oven dry state into a beaker of water. The Waiake sandstone underwent disintegration within a few hours. Both Tipau and Rothesay sandstones cracked with minor flaking and spalling of outer grains. In contrast, Parnell Grit and CR sandstone underwent no visible change.

It is obvious from these results that the mechanical abrasion mechanism is more responsible for the loss of material from CR sandstone and Parnell Grit. Direct evidence was observed for Parnell Grit where, after each cycle, individual grains had been physically plucked from the rock matrix. Rock fragments were also quite rounded after the final slaking cycle.

Simple wetting and drying is sufficient to almost totally disintegrate Waiake sandstone. This, coupled with the process of mechanical abrasion accounts for its low durability. A combination of mechanical abrasion and simple slaking is most likely the cause of the low durability of Tipau and Rothesay sandstones. Both these samples were extremely rounded after the final cycle providing direct evidence for mechanical abrasion. The cracking of these samples upon immersion in water provides evidence for a simple wetting and drying process.

The direct effect of the < 2 μm size fraction on durability is not immediately apparent. All the samples have similar proportions of < 2 μm material, but exhibit a wide range of durabilities. These observations suggest that it is the type of material, and the arrangement of mineralogical components in the fabric, which accounts for variable durabilities of the sandstones. This is discussed in chapter 8.

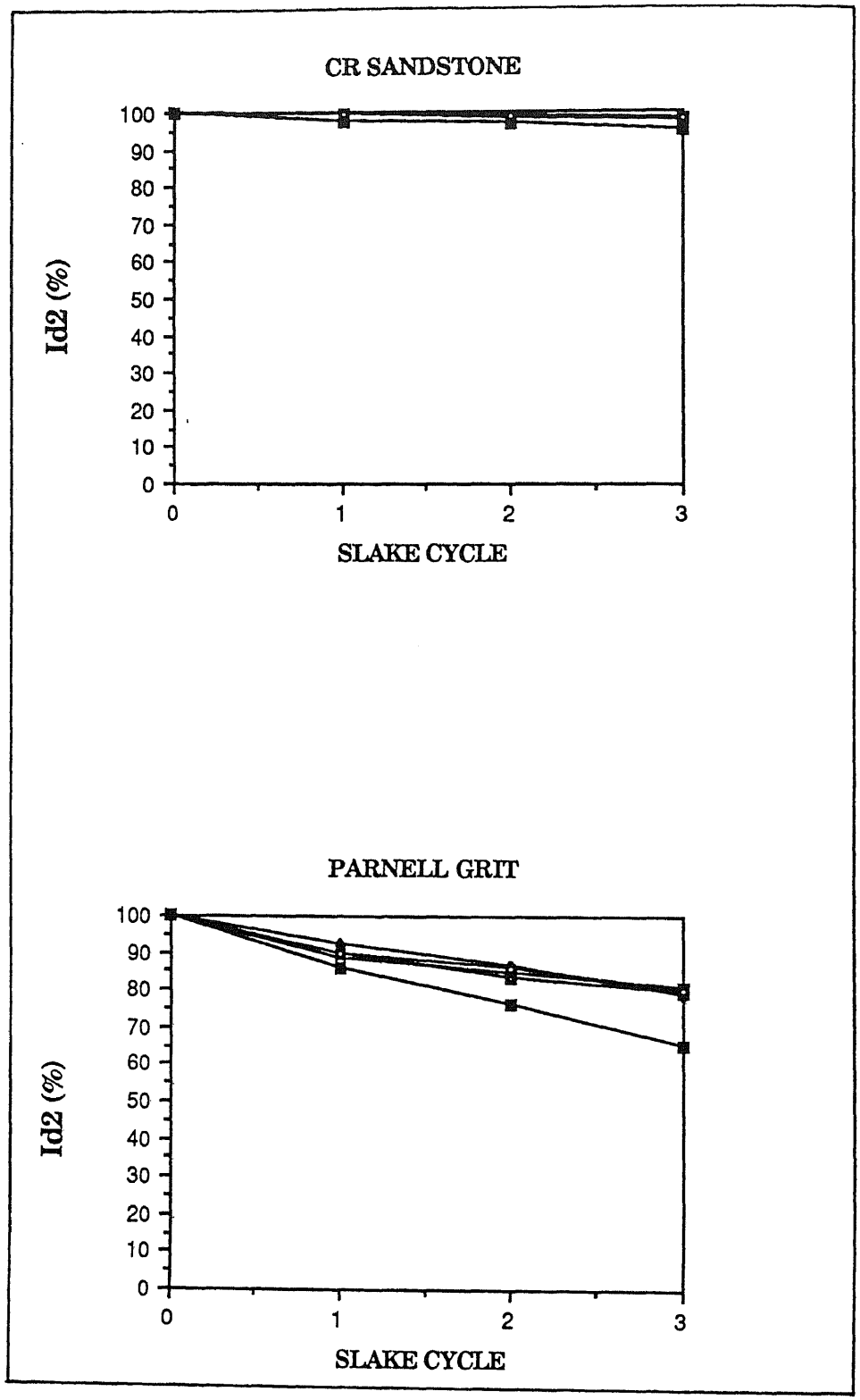

FIGURE 4.6 Plots of slake index (I_{d2}) versus slake cycle for CR sandstone and Parnell Grit.

4.7 SUMMARY

The rocks in this study have dry compressive strengths ranging from 7.2 to 79 MPa. Saturated compressive strengths range from 1.9 to 62 MPa. Cape Rodney sandstone is the strongest of the samples in both dry and saturated conditions and is classed as a strong rock. Parnell Grit is the strongest ECB sample with a dry compressive strength of 19 MPa. It is classified as a weak rock. Rothesay sandstone is the weakest sample with a compressive strength of 7.2 MPa. Waiake sandstone is slightly stronger in compression (13 MPa). These two samples are classified as extremely weak rocks. Tipau sandstone is a very weak rock with a dry compressive strength of 16 MPa.

Softening factors for compressive stresses are greatest for the extremely weak Waiake and Rothesay sandstones (4.7 and 3.8 respectively). They undergo up to 79 % strength reduction upon saturation. Cape Rodney sandstone has the lowest softening factor for compressive stresses of 1.3 and undergoes a 21% strength reduction upon saturation.

The dominant mode of failure for the rocks in compression is the cataclasis mechanism. This process was best exibited by the strong CR sandstone where the specimen crumbled through the propagation of cracks in the direction of the applied stress. Catastrophic failures resulted in disintegration of the cores with conical end fragments remaining on the platens. The weaker sandstones failed by a combination of cataclasis and shear. The shear mode of failure may be more characteristic of the loading system due to platen rotation or lateral translation of the platens relative to each other. Failure in the ECB sandstones and Parnell Grit was quiet, characterised by crumbling of the specimens rather than by explosive collapse.

Tensile strengths range from 1.1 to 10 MPa (oven dry conditions) and 0.9 to 7.1 MPa (saturated). Cape Rodney sandstone is the strongest rock in tension at both moisture extremes. Parnell Grit is the strongest ECB sample with the Rothesay sandstone the weakest. Tipau and Waiake sandstones have dry tensile strengths intermediate between those of Parnell Grit and Rothesay sandstone.

Softening factors for tensile stresses are greatest for the ECB sandstones which undergo up to 58 % strength reductions upon saturation. The CR sandstone and Parnell Grit have the lowest softening factors for tensile

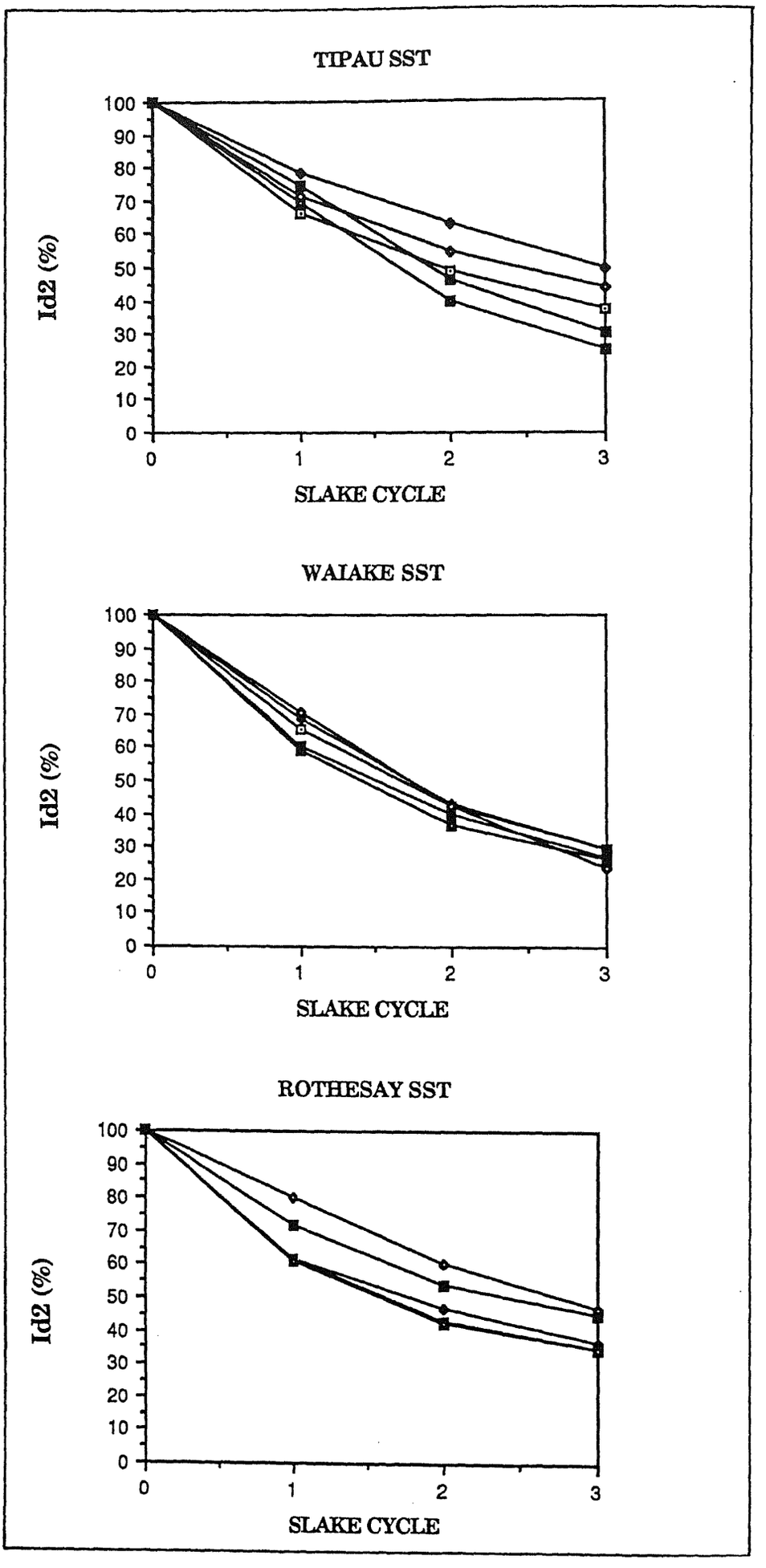

FIGURE 4.7 Plots of slake index (I_{d2}) versus slake cycle for ECB sandstones.

stresses.

Dynamic elastic constants, Youngs Modulus and Poissons ratio, were measured with limited success, to determine the deformation of the samples under compression. The measurement of elastic wave velocity through cores under stress provided the essential data. Poissons ratio had to be estimated for each specimen due to the high wave attenuation experienced in the porous sandstones. Youngs Moduli at initial stresses range from 0.08 to 0.24 GPa (oven dry), while those at peak stresses range from 1.2 to 6.4 GPa (oven dry). The samples are all highly deformable and have values more akin to sands. Only CR sandstone falls within the 'normal range' for sandstones, with its peak Youngs Modulus value of 6.4 GPa.

East Coast Bays sandstones are characterised by initial plastic pore and crack closure. At intermediate stress levels the rocks undergo strain hardening as grain contacts increase, prior to rapid microcrack development and propagation. The CR sandstone and Parnell Grit behave elastically when axial stresses are increased. Their deformation mechanisms are described as plastic-elastic-plastic. Initial plastic closure of pores and microcracks is followed by compression of the rocks and they become elastically stiffer. Microcrack development and coalescence results in rapid macrocracking described as strain softening deformation.

Hardness values determined from the L-Type Schmidt Hammer and Shore Scleroscope reveal the CR sandstone to be the hardest sample. Its hardness values range from 27 to 45 which are typical values for moderately strong rock. Parnell Grit is the hardest of the ECB samples with values ranging from 18 to 26, consistent with a weak rock. The low hardness values of ECB samples are typical of very weak, weathered and compacted sedimentary rocks.

Slake durability tests classify the sandstones from very high durability (CR sandstone) to low durability (ECB samples). The loss of material for both CR sandstone and Parnell Grit have been attributed largely to mechanical abrasion. Simple wetting and drying is sufficient to disintegrate the Waiake sandstone. A combination of wetting and drying, and mechanical abrasion causes the loss of material from Tipau and Rothesay sandstones.

CHAPTER 5

RELATIONSHIPS BETWEEN GEOMECHANICAL STRENGTH AND INDEX PROPERTIES

CHAPTER 5

RELATIONSHIPS BETWEEN GEOMECHANICAL STRENGTH AND FIELD AND INDEX PROPERTIES

5.1 INTRODUCTION

Simple linear regression was used to examine relationships between measured geomechanical strength properties (compressive and tensile) determined in chapter 4, and index properties determined in chapters 3 and 4 (bulk rock properties, dynamic Youngs Modulus, hardness and durability). Field parameters were also related to strength and index properties. This analysis was undertaken to:

1] determine significant relationships between index properties and strength in order to investigate the causes of the sample's strength, and

2] determine the relationship between field properties (such as joint spacing and bed thickness) and laboratory measured properties, in order to investigate field parameters which could be used to describe the geomechanical behaviour of the rocks, and to investigate the controls on joint development.

5.2 METHOD

Possible general relationships between index, geomechanical, and field properties were sought using simple linear regression between two variables. The geomechanical property was used as the dependant variable in all cases. Index properties were only used as dependant variables when plotted against field properties. A regression coefficient of $r^2 \geq 0.5$ was used as a cut-off point for the purposes of presenting the data. Regression coefficient values of less than 0.5 were considered insignificant.

In some cases very high correlations were recorded. These were due to having a cluster of data points at one end of the plot with one outlier (CR sandstone) at the other end. Simply plotting a line joining the points produced correlations of ~ 0.98. In such cases, a further regression analysis was carried out ignoring the outlier, to determine if the correlation

TABLE 5.1 Regression Coefficients between Strength and Bulk Rock Properties

	$\sigma_{c,dry}$	$\sigma_{c,sat}$	$\sigma_{c,tot}$	$\frac{\sigma_{c,dry}}{\sigma_{c,sat}}$
ρ_{dry}	0.88	0.90	—	0.79
ρ_{sat}	0.90	0.94	—	0.76
ρ_{tot}	—	—	0.51	—
ρ_s	—	—	—	—
η_{eff}	0.79	0.78	—	0.72
e	0.72	0.71	—	0.69
<2 μm	—	—	—	—

	$\sigma_{t,dry}$	$\sigma_{t,sat}$	$\sigma_{t,tot}$	$\frac{\sigma_{t,dry}}{\sigma_{t,sat}}$
ρ_{dry}	0.90	0.94	—	—
ρ_{sat}	0.91	0.97	—	—
ρ_{tot}	—	—	—	—
ρ_s	—	—	—	—
η_{eff}	0.82	0.82	—	—
e	0.75	0.74	—	—
<2 μm	—	—	—	—

ρ_{dry}	— dry bulk density	($kg.m^{-1}$)
ρ_{sat}	— saturated bulk density	($kg.m^{-1}$)
ρ_{tot}	— total bulk density data set	($kg.m^{-1}$)
ρ_s	— grain density	($kg.m^{-1}$)
η_{eff}	— effective porosity	($kg.m^{-1}$)
e	— void ratio	($kg.m^{-1}$)
<2 μm	— proportion <2 μm size material	(%)

was real. If r^2 was greater than 0.5 then the correlation was considered real, otherwise the relationship was considered insignificant.

5.3 BULK ROCK PROPERTIES

Table 5.1 summarises regression coefficients for all measured bulk rock properties (dry and saturated bulk densities, grain density, effective porosity, void ratio, and particle size) against strength. Total compressive and tensile strength data sets (include both dry and saturated data) are denoted by $\sigma_{c,tot}$ and $\sigma_{t,tot}$ respectively. Similarly, total bulk density is denoted by ρ_{tot}.

5.3.1 Compressive Strength versus Bulk Density

It is obvious from Table 5.1 that a significant relationship exists between bulk density and compressive strength. Total compressive strength is generally related to total bulk density, having a regression coefficient of 0.51. However, bulk densities at the two moisture extremes (oven dry and saturated) are far more significantly related to compressive strength. Saturated compressive strength is slightly better correlated with both dry and saturated bulk densities than is dry compressive strength.

The softening factor for compressive strength is related equally well to dry and saturated bulk densities (0.79 and 0.76 respectively). These, and the high correlations between strength and bulk density at the moisture extremes, support measured σ_c values, that compressive strengths are moisture dependant.

Linear regression equations describing these relationships are:

$$\sigma_{c,dry} = 0.11\rho_{dry} - 192.4 \quad [5.1]$$

$$\sigma_{c,sat} = 0.10\rho_{dry} - 180.7 \quad [5.2]$$

$$\sigma_{c,dry} = 0.17\rho_{sat} - 347.5 \quad [5.3]$$

$$\sigma_{c,sat} = 0.16\rho_{sat} - 328.6 \quad [5.4]$$

Using measured bulk densities, dry or saturated compressive strengths (for Waitemata Group sediments) may be estimated from the above equations. It is surprising that equations 5.1 and 5.2 are so similar. This suggests that bulk density may be used to predict either dry or saturated compressive strength. The same is true for equations 5.3 and 5.4, where saturated bulk

density may be used to determine both dry and saturated strengths. The similarities between the equations are due to the CR sandstone outlier forcing the lines to similar slopes.

The observed relationship between compressive strength and bulk density is similar to the findings of Deere and Miller (1966) who observed a linear relationship between these properties, with rocks of greater density having higher compressive strengths. Lama and Vutukuri (1978) suggest bulk density is related to mechanical strength.

Cape Rodney sandstone is a dense rock and is the strongest of the samples whereas the least dense Rothesay sandstone is the weakest. Bell (1978) observed density to be related to compressive strength for Fell sandstones, with more compact rocks having higher strengths than less compact samples. Similar findings (for sandstones) were observed by Caruso *et al.* (1985) and Dyke and Dobereiner (1991).

No significant relationship was found between grain density and compressive strength. This may indicate that the type of mineral grains composing the sandstones has no influence on the strength. Rather, it is the closeness of packing of solid grains which controls sandstone strength. These relationships are discussed further in chapter 8.

5.3.2 Tensile Strength versus Bulk Density

Tensile strength is closely correlated with saturated and dry bulk densities; indeed the correlations are stronger than those for compressive strength. Saturated tensile strengths are more strongly related to bulk densities (both dry and saturated) than are dry tensile strengths. The lack of any significant correlation between the softening factor for tensile strengths and bulk density suggests that these relationships are moisture dependant. No correlation exists between total tensile strengths and total bulk density, strengthening this observation. The regression equations describing the major relationships are:

$$\sigma_{t,dry} = 0.01\rho_{dry} - 24.4 \quad [5.5]$$

$$\sigma_{t,sat} = 0.01\rho_{dry} - 18.2 \quad [5.6]$$

$$\sigma_{t,dry} = 0.02\rho_{sat} - 44.0 \quad [5.7]$$

$$\sigma_{t,sat} = 0.02\rho_{sat} - 32.9 \quad [5.8]$$

The similarity between equations 5.5 and 5.6, and again between 5.7 and 5.8, are due to the CR sandstone outlier forcing the lines to similar slopes, as discussed in the previous section.

As found for compressive strengths, no relationship occurs between tensile strength and grain density.

5.3.3 Compressive Strength versus Effective Porosity

Effective porosity is strongly correlated with compressive strength. Regression coefficients in table 5.1 are very similar for both dry and saturated compressive strengths. A strong relationship also exists between effective porosity and the softening factor. Compressive strengths are inversely related to effective porosity by the following equations:

$$\sigma_{c,dry} = -3.04\eta_{eff} + 93.8 \qquad [5.9]$$

$$\sigma_{c,sat} = -2.62\eta_{eff} + 75.6 \qquad [5.10]$$

Effective porosity is generally related to compressive strength but not quite as significantly as bulk densities. Porosity provides an indication of both dry and saturated compressive strengths equally well, strengthening the conclusion that the sample's strength is controlled by closeness of packing of solid grains and the pore space between these grains, rather than the type of mineral grains present. This claim is further supported when it is noted that the weakest Rothesay sandstone and strongest CR sandstone have very similar grain densities but very different porosities, as reported in chapter 3.

The very porous Rothesay sandstone is the weakest in this study. Dyke and Dobereiner (1991) note that pores are zones of weakness along which cracks may propagate under stress. Crack propagation may increase in saturated rock through the phenomenon of stress corrosion discussed in chapter 4.

5.3.4 Tensile Strength versus Effective Porosity

Tensile strength is very closely related to effective porosity, more so than is compressive strength. However, this correlation is not as great as that with bulk density. Both dry and saturated tensile strengths are equally well related to effective porosity, as revealed by r^2 values in table 5.1.

The regression equations are:

$$\sigma_{t,dry} = - 0.39\eta_{eff} + 12.4 \qquad [5.11]$$

$$\sigma_{t,sat} = - 0.28\eta_{eff} + 8.7 \qquad [5.12]$$

The strong relationship between tensile strength and effective porosity (and bulk density) is significant, indicating that the development and propagation of cracks under tension are controlled by these properties. Cracks propagate through weak pore spaces, in tension, through the concentration of stress at these weak points.

The lack of any relationship between the softening factor for tensile stresses and effective porosity indicates that no one equation will adequately describe the change in tensile strength with porosity, at all moisture conditions. Equations 5.11 and 5.12 apply for tensile strengths at the two moisture extremes, oven dry and saturated.

5.3.5 Compressive Strength versus Void Ratio

Compressive strength is related to void ratio. This is expected as the void ratio is simply the average statistical grain spacing in a material (as defined in chapter 3) and is closely related to porosity. Regression coefficients in table 5.1 indicate that void ratio is less significantly related to compressive strengths than are bulk density and effective porosity. The good correlation between the softening factor for compressive strengths and void ratio suggests a general relationship between these variables at all moisture conditions.

Although void ratio is related to compressive strength, porosity provides a better indication of strength.

5.3.6 Tensile Strength versus Void Ratio

A significant relationship occurs between tensile strength and void ratio for both oven dry and saturated conditions. These correlations are slightly better than those for compressive strengths. The lack of any relationship between the softening factor for tensile strength and void ratio suggests no general relationship exists between these two variables for intermediate moisture conditions.

TABLE 5.2 Regression coefficients between Strength and Durabilty and Hardness

	$\sigma_{c,dry}$	$\sigma_{c,sat}$	$\sigma_{c,tot}$	$\frac{\sigma_{c,dry}}{\sigma_{c,sat}}$
I_{d2}	0.66	0.69	—	0.97
R_{block}	0.97	0.95	—	—
R_{field}	—	—	—	—
SH	0.89	0.91	—	—
	$\sigma_{t,dry}$	$\sigma_{t,sat}$	$\sigma_{t,tot}$	$\frac{\sigma_{t,dry}}{\sigma_{t,sat}}$
I_{d2}	0.69	0.78	—	—
R_{block}	0.97	0.94	—	—
R_{field}	—	—	—	—
SH	0.92	0.94	—	—

Porosity is again seen as a more significant physical parameter in relation to strength and thus little emphasis is placed upon void ratio as an indicator of tensile strength.

5.3.7 Strength versus Particle Size

No significant relationship was found between strength and sand size proportion or silt size proportion of grains (or proportion of gravel size material in the case of Parnell Grit).

Also, no relationship was found between strength (both compressive and tensile) and the proportion of less than 2 μm material. This is a surprising result as the clay component of the rocks may be expected to exert a significant control over the geomechanical behaviour. Despite the samples in this investigation having considerably variable strengths, the proportion of < 2 μm material is similar for all samples. This implies that it is either the mineralogy or the distribution of mineralogical components in the samples, or a combination of both, and not simply the proportion of grain sizes in the material, that determine the strength of the rocks.

5.4 DURABILITY AND HARDNESS

Regression coefficients between strength and slake durability (I_{d2}), Schmidt hammer rebound *in situ* (R_{field}) and on intact blocks (R_{block}), and shore hardness (SH), are presented in table 5.2.

5.4.1 Compressive Strength versus Durability

Slake durability is related to compressive strength, although not as closely as other index properties. The more durable sandstones are characterised by having high compressive strengths. A very high correlation of 0.97 exists between the softening factor for compressive strengths and the slake durability index. This relationship is an inverse one, and indicates that samples having high durabilities are characterised by having low softening factors. Clearly, this shows that the change in strength that the sandstones undergo from the dry to the saturated state, is directly related to their durability. The weak Waiake and Rothesay sandstones, for example, undergo the greatest change in compressive strength when saturated (they have high softening factors) and have the lowest durabilities.

5.4.2 Tensile Strength versus Durability

Tensile strength is more closely related to durability than is compressive strength. Again, this relationship is not as strong as those found between tensile strength and the other index properties. No correlation occurs between the softening factor for tensile strength and the slake durability index.

These relationships are related to the physical plucking and tensile breakage of grains from the samples as they are mechanically broken down. The stronger correlation between saturated tensile strength and durability represents the effect of saturation which loosens the bonds holding the grains in the clay matrix. Tensile breakage and plucking of grains is more characteristic of the slake test than are compressive stresses.

5.4.3 Compressive Strength versus Hardness

The use of the Schmidt Hammer as a field indicator of compressive strength for rocks, due to its quick and easy use, has been discussed in chapter 2. Ideally, a relationship between this simple field test and compressive or tensile strength would be invaluable in rapidly assessing sandstone strength in the field.

In this study no correlation was found between compressive strength and Schmidt Hammer rebound in the field. Conversely, a very strong relationship exists between saturated and dry compressive strengths and Schmidt Hammer rebound carried out on intact blocks of rock prior to coring. Similarly high correlations are found between compressive strength and shore hardness (table 5.2).

These results reflect higher degrees of control in the test conditions. Strength parameters were determined from cores drilled from the same blocks as those tested with the Schmidt Hammer. Thus compressive strengths for those blocks are closely related to rebound hardness carried out on those same intact blocks. Similarly, shore hardness was determined from oven dry and saturated cores.

The lack of any relationship between compressive strength and Schmidt Hammer rebound *in situ* suggests that the hammer cannot be used as a

predictor of compressive strength for the Waitemata Group rocks, from field data, due to the poor field readings caused by discontinuities, the little variation of field data between sites and, in some cases (Tipau sandstone and Parnell Grit) as a result of variable readings within one unit. For these lithologies a descriptive terminology of rock strength, such as that given by the New Zealand Geomechanics Society (1988), is a more useful predictor of rock strength.

5.4.4 Tensile Strength versus Hardness

Good correlations exist between saturated and dry tensile strengths and Schmidt Hammer rebound on intact blocks. Shore hardness is strongly related to tensile strength. Significantly, Schmidt Hammer rebound carried out *in situ* is not related to tensile strength. Similar conclusions as to those made in section 5.4.3 may be drawn. Tensile strengths cannot adequately be predicted for Waitemata sandstones from the use of the Schmidt Hammer in the field.

5.4.5 Strength versus Dynamic Youngs Modulus and Field Properties

No relationship was found between either compressive or tensile strengths and dynamic Youngs Modulus. A correlation coefficient of 0.66 was obtained for tensile strength and Youngs Modulus at peak stress (Ep) but this value is more the result of a circular argument than having any real physical significance. Youngs Modulus was determined from estimated Poissons Ratios obtained from the literature; this estimation was based largely upon tensile strengths previously obtained. Thus the correlation reflects the method used in calculating Ep.

No relationships were found between strength and field properties. A correlation coefficient of 0.72 between the softening factor for compressive strengths and bed thickness is more likely the result of mathematical coincidence rather than any real physical significance.

TABLE 5.3 Regression Coefficients between Dynamic Youngs Modulus and Field Properties

	E_i	E_p
R_{block}	0.64	0.94
R_{field}	0.53	0.73
Jsp	—	0.71
Overburden	0.54	0.54

Jsp average joint spacing
Overburden overburden thickness

5.5 RELATIONSHIP BETWEEN DYNAMIC YOUNGS MODULUS AND FIELD PROPERTIES

Table 5.3 summarises regression coefficients between dynamic Youngs Modulus at initial (Ei) and peak (Ep) stresses, and field properties.

5.5.1 Youngs Modulus versus Hardness

Schmidt rebound hardness is closely related to Youngs Modulus at both initial and peak stresses. This is intuitively reasonable as the Schmidt Hammer is measuring a rebound distance of a hammer impacting upon the rock. The elasticity of the rock should be directly related.

Significantly, both Ei and Ep are related to rebound hardness obtained from the field. However, the greater correlation between Youngs Modulus and the Schmidt Hammer rebound carried out on intact blocks of rock again reflects the influence of greater control in the test procedure. Dynamic Youngs Modulus determined from cores drilled from the same block tested with the hammer should reflect a closer relationship than that obtained from *in situ* measurements of hardness.

The fact that Youngs Modulus correlates well with the Schmidt Hammer readings *in situ* suggests that the instrument can be used, in the field, to provide reliable estimates of rock elasticity.

In both cases Schmidt rebound hardness is more closely correlated to Ep than E_i, which reflects the greater variability in initial stress measurements used to detemine E_i, as discussed in chapter 4.

5.5.2 Youngs Modulus versus Overburden Thickness

Table 5.3 indicates that a general relationship exists between E_i, E_p and the overburden thickness above each sampling unit. The importance of this correlation is not seen as very great as the close proximity between the majority of sampling sites implies the overburden thickness should be reasonably uniform. Also, removal of overburden, such as has occurred at the Rothesay Bay site, implies that there may be large errors associated with the measured thicknesses.

5.5.3 Youngs Modulus versus Joint Spacing

There is a significant correlation between Ep and joint spacing (Jsp). The relationship is described by the following regression equation:

$$Ep = -0.15Jsp + 6.77 \qquad [5.13] \qquad r^2 = 0.71$$

No correlation occurs between Ei and joint spacing, probably reflecting the variable initial stresses used to determine Ei as mentioned earlier. The relationship between Jsp and E, and the lack of any relationship between Jsp and compressive or tensile strengths, indicates that joint spacing provides a good indication of the amount of stress that the rock units are capable of accepting and storing (through plastic deformation).

The relationship between Ep and joint spacing is an inverse one. Highly deformable ECB sandstones are characterised by reasonably wide joint spacings of approximately 0.6m. The CR sandstone is characterised by two joint sets. Vertical continuous joints spaced 1.3m occur across the unit but more predominant are closely spaced (0.1m) cross cutting joints resulting in wedge type failures. These dominant joints in this sandstone are reflected by the blocks which have fallen out of the cliff face being appreciably smaller than those found along the ECB coastline.

In this study, the joints are primarily tension (or extension) joints where total displacement is directed normal to the fracture surfaces and the shear component is zero (Price, 1966; Hobbs *et al.*, 1976). The relationship between Ep and the spacing of these joints suggests that the highly deformable ECB sandstones are capable of storing applied stress through plastic deformation.

Gabrielson (1990) has shown that a homogeneous rock body exposed to a simple and uniform stress field (such as gradual loading through burial) should develop a homogeneous fracture pattern. The vertical joints observed in ECB sandstone units are simple planar structures related to a vertical and constant stress produced through gradual burial of sandstone units by subsequent turbidity current deposits. The joints are consistently orientated vertically in the planes of maximum shear indicative of a uniform stress field developed through gradual loading of the units through burial.

The near horizontal beds, uniform bed thicknesses, and similar depth of units in the cliff profile indicate the beds have undergone minor tectonic disturbances. The reasonably wide and regular spacing of these joints in ECB sandstones is directly related to their ability to store stress as they deform plastically under these uniform stress fields.

The close association, and similar jointing pattern, of Parnell Grit, with the neighbouring flysch deposits, suggest that it has experienced similar uniform stress fields as the ECB sandstones. The slightly closer joint spacing in the conglomerate (compared with that of the sandstones) indicates its slightly more restricted ability to deform plastically under stress. Parnell Grit has been shown to fail predominantly by plastic deformation in chapter 4.

The CR sandstone, with its variable joint spacing and concentration of joints in zones, reflects a more variable stress history. The extension of continuous vertical joints through the unit is a result of overburden stresses produced through burial of the unit. Increasing stress fields result in the development of conjugate sets of fractures, followed by increased consolidation and the development of deformation bands or joint zones. Cross-cutting splay fractures are produced due to slight inhomogeneities in the sandstone unit and minor changes in the stress field. Close joint spacing is attributed to the inability of the less deformable CR sandstone to store stress, with the subsequent release of stress through brittle fracture.

5.6 SUMMARY

Both compressive and tensile strengths are related to bulk rock properties, with slightly stronger correlations with tensile strength. Bulk densities and porosities are very closely related to strength, as is void ratio. The strength of the sandstones is controlled primarily by the closeness of packing of individual grains and the associated pore spaces. Sandstone strengths do not seem to be controlled by grain density or size.

A lesser correlation is found between strength and durability but the strong relationship between the softening factor for compressive strengths and durability suggests that saturation effects greatly reduce the durability of ECB sandstones.

Schmidt Hammer rebound *in situ* is not related to strength for Waitemata sandstones. Hardness tests on blocks and shore hardness measurements on cores result in high correlations with strength, reflecting a greater degree of control in the test conditions. The Schmidt Hammer is not seen as a good field predictor of compressive or tensile strength for the sandstones of this study.

Youngs Modulus is closely related to both *in situ* and laboratory determined Schmidt hardness. This relationship is due to the hammer measuring a dynamic rebound and associated rock deformation due to the hammer impact. These results suggest that the Schmidt Hammer can be used in the field as a reliable predictor of rock elasticity.

No correlations were found between field properties and strength, but dynamic Youngs Modulus is inversely related to joint spacing. The joint spacing is directly related to the ability of the rocks to store stress. Weak ECB sandstones have reasonably wide joint spacing as they deform plastically, but the close jointing observed in the CR sandstone may be attributed to brittle fracture. The regularity of jointing within the ECB samples reflect a very uniform stress history as opposed to the CR sandstone which has probably undergone a more complex stress history as reflected in the development of joint zones.

CHAPTER 6

MINERALOGY

CHAPTER 6

MINERALOGY

6.1 INTRODUCTION

Microscopic characteristics (in particular, mineral components, texture, and clay mineralalogy) of the rocks of this study, were analysed to investigate the petrographic control over geomechanical behaviour of the samples. The aims of this chapter are, therefore, to:

1] determine the mineralogical composition of the study rocks,
2] quantify the texture of the rocks (size, shape and proportion of the individual components), and
3] determine the general clay mineralogy and semi-quantify clay mineral abundances within the samples.

This chapter initially describes the methods used in identifying mineralogical components, and in quantifying the texture of the samples. Major components making up the bulk mineralogy of the rocks are then described, prior to an analysis of the texture of the rocks. The mineralogy of each sample is discussed in turn, followed by a discussion of the major types of clay minerals identified.

The relationship between sample mineralogy and strength will be discussed in chapter 8.

6.2 METHODS

6.2.1 Thin Sections

Thin sections were analysed to determine the mineralogical composition of the samples. All specimens, except the CR sandstone, required resin impregnation due to their unconsolidated, porous nature. Prepared cubes were dried on a hotplate at 60 °C for 24 hours prior to impregnation with Araldite K142 applied as a 5:1 ratio in combination with a curing agent. Sections were cut parallel to bedding where applicable.

TABLE 6.1 Modal Proportions of Major Mineral Constituents

	ROCK FRAGMENTS	QUARTZ	TOTAL QUARTZ	PLAGIOCLASE FELDSPAR	MATRIX	CALCITE	AUGITE	LIMONITE
CR SANDSTONE	60.1 ± 0.9	11.6 ± 0.3	21 ± 10	1.3 ± 0.3	—	22.3 ± 0.3	1.9 ± .04	—
PARNELL GRIT	63.1 ± 2.2	3.6 ± 0.8	10 ± 10	9.3 ± 0.2	26.2 ± 0.4	T	0.9 ± 0.2	—
TIPAU SST	—	34.7 ± 0.1	59 ± 10	T	56.6 ± 0.7	T	4.2 ± 0.1	—
WAIAKE SST	58.1 ± 0.9	30.6 ± 1.9	50 ± 10	1.7 ± 0.3	4.8 ± 0.5	T	3.8 ± 0.9	T
ROTHESAY SST	45.6 ± 1.1	13.9 ± 0.2	63 ± 10	T	—	7.9 ± 0.2	T	31.2 ± 2.0

	GLAUCONITE	EPIDOTE	ZEOLITE	HORNBLENDE	CHLORITE	BIOTITE
CR SANDSTONE	T	T	1.2 ± 0.5	T	T	T
PARNELL GRIT	T	—	T	—	T	—
TIPAU SST	T	T	—	T	—	3.3 ± 0.2
WAIAKE SST	T	T	—	T	—	—
ROTHESAY SST	T	—	—	—	—	—

TOTAL QUARTZ = CALCULATED FROM XRD STANDARDS

T = TRACE

6.2.2 Optical Microscopy

Optical microscopy was used to determine the mineralogy and texture of the samples. Modal analysis of mineral proportions was carried out from point counting of thin sections using a James Swift Stage and Counter. Errors for modal proportions represent 95 % confidence limits.

The size of individual components was measured directly from the micrometer scale in the optical microscope. Component lengths and widths were determined in groups of ten. After each set of ten measurements, the mean length and width, and associated standard errors for the entire sample were determined. Measurements were continued until taking a further sample of ten measurements made no difference to these statistics.

6.2.3 X-Ray Diffraction

Unorientated backfill powder mounts were used to determine the bulk rock mineralogy following the method of Hume and Nelson (1982). This was done to identify, and verify the identification of, minerals determined under the optical microscope.

Clay minerals were identified from orientated clay mounts prepared by the dropper-on-glass slide (DOGS) method of Hume and Nelson (1982) using aliquots of <2 μm suspensions. Untreated slides were alternatively glycolated using ethylene glycol in a dessicator and then heated at 500 °C for one hour. These treatments were carried out to aid in the identification of clay mineral species. Semi-quantitative clay abundances were determined using the technique of Hume and Nelson (1982).

6.3 BULK MINERALOGY RESULTS

6.3.1 Modal Analysis

The proportions of major mineral species occurring in each sandstone are presented in table 6.1. It is important to note that the quartz abundance refers to actual quartz crystals observed in thin section and does not include mega and microquartz inclusions in volcanic rock fragments. Total quartz represents the total proportion of quartz occurring in any one sample. This value was obtained directly from XRD traces of bulk mineralogy using the

4.26 Å low quartz peak and directly reading off the proportion of quartz from intensity-concentration calibration curves of a prepared quartz standard.

Rock Fragments

All specimens are dominated by rock fragments. Although not obvious from table 6.1, Tipau sandstone is also dominated by rock fragments (largely detrital), but due to the fine grained nature of the sample, optical microscopy techniques were inadequate to accurately distinguish between matrix and rock fragments. Thus, all material which had no defineable grain boundary was included as matrix material. Lewis (1984) recognises this problem and notes that it is exacerbated by the creation of clayey matrix during the chemical diagenetic destruction of unstable accessory minerals.

Parnell Grit and CR sandstone are enriched in andesitic/dacitic volcanic rock fragments as opposed to detrital rock fragments. The large size and dominance of volcanic rock fragments in these samples suggest a close volcanic source.

Quartz

Quartz grains are abundant in all samples and range from 4 to 35 %. The greatest quartz crystal content occurs in the Tipau sandstone. XRD diffractograms reveal quartz to be the most abundant of all minerals present in each sample due largely to the fact that almost all volcanic rock fragments consist of micro or megaquartz. The crystals are not dominant over other minerals, suggesting only a short time period for preferential destruction of other minerals (Pettijohn, 1975).

Feldspar

Plagioclase feldspar crystals occur only in Parnell Grit in any appreciable amount, making up 9 % of the sample. They are believed to be calcic plagioclases which are easily destroyed by chemical weathering. Alteration of plagioclase cores to zeolite has occured in both CR sandstone and Parnell Grit. Feldspars and quartz commonly occur in the <2 μm size fraction.

TABLE 6.2 Major Mineral Component Sizes

	LENGTH (mm)			WIDTH (mm)		
	MIN	MAX	MEAN	MIN	MAX	MEAN
			CAPE RODNEY SST			
RF	0.25	1.70	0.65 ± 0.17	0.17	1.41	0.44 ± 0.11
QTZ	0.07	0.32	0.19 ± 0.07	0.05	0.19	0.11 ± 0.04
PLAG	0.05	0.36	0.19 ± 0.08	0.05	0.26	0.12 ± 0.02
AUG	0.04	0.45	0.14 ± 0.02	0.03	0.18	0.09 ± 0.02
			PARNELL GRIT			
RF	0.33	10.01	2.24 ± 0.23	0.17	8.49	1.42 ± 0.22
PLAG	0.13	1.75	0.57 ± 0.19	0.13	1.58	0.39 ± 0.06
QTZ	0.08	0.22	0.13 ± 0.04	0.06	0.17	0.10 ± 0.03
			TIPAU SST			
QTZ	0.07	0.26	0.14 ± 0.03	0.05	0.17	0.10 ± 0.03
			WAIAKE SST			
RF	0.23	0.93	0.47 ± 0.10	0.14	0.50	0.31 ± 0.09
QTZ	0.15	0.35	0.24 ± 0.05	0.09	0.26	0.17 ± 0.04
AUG	0.11	0.35	0.19 ± 0.04	0.05	0.30	0.12 ± 0.04
			ROTHESAY SST			
RF	0.32	0.66	0.49 ± 0.09	0.13	0.59	0.29 ± 0.08
QTZ	0.13	0.40	0.22 ± 0.06	0.10	0.25	0.16 ± 0.03

RF = ROCK FRAGMENTS
QTZ = QUARTZ
PLAG = PLAGIOCLASE FELDSPAR
AUG = AUGITE

Calcite

Calcite occurs only in CR sandstone in any great abundance, making up 22 % of the rock. Brenchley (1969) suggests that a calcite cement in sandstone forms a protective coat around grains and limits water circulation through a general reduction in porosity, which might promote diagenesis.

Calcite occurs in trace amounts in all other samples except the Rothesay sandstone in which it makes up 5 % of the rock.

Matrix

A fine grained argillaceous matrix darkened by clay minerals is common in ECB sandstones and makes up over 50 % of the Tipau sandstone. A muddy clay matrix occurs in Parnell Grit. Cape Rodney sandstone is characterised by a calcite cement as discussed previously.

Accessory Minerals

Minor detrital grains occurring in most samples include augite, glauconite, hornblende, chlorite, zeolite, epidote, and biotite. Augite ranges from trace to 4 %. Glauconite occurs in trace amounts in all samples. Zeolite (analcime and clinoptilolite) occurs in CR sandstone and Parnell Grit, and has preferentially altered plagioclase feldspar. Biotite makes up 3% of Tipau sandstone, yet is largely unobserved in other specimens. Hornblende, chlorite, and epidote are rare in all samples.

These petrographic observations are consistent with those made by Simpson (1988) on 'thick sandstones' along the ECB coastline.

6.3.2 Texture

The sizes (lengths and widths) of individual components making up the samples are presented in table 6.2. This table includes maximum and minimum measured lengths and widths as well as calculated mean lengths and widths. Minerals occurring in trace amounts were not measured. Also, it was physically impossible to determine 'dimensions' of matrix material. Thus, the data are measurements of the major

components in each sample and do not represent the total mineralogy of each rock.

Table 6.1 shows that volcanic rock fragments are the largest components in each sample. These may reach up to 10 mm in length in Parnell Grit, but are restricted to less than 2 mm in the sandstones. Parnell Grit is the coarsest sample, dominated by the volcanic rock fragments. It also has the largest crystals of plagioclase feldspars, but, conversely, quartz crystals are very small in this conglomerate.

Cape Rodney sandstone is the coarsest sandstone and this is primarily due to the volcanic rock fragments and large plagioclase crystals, the latter of which may reach up to 0.36 mm in length. Waiake and Rothesay sandstones have similar mineral sizes to each other. Rock fragments are, again, the largest components, followed by quartz crystals. It is noticeable that the quartz crystals in these sandstones are marginally larger than those in the CR sandstone. Augite crystals are also slightly larger in Waiake sandstone than in CR sandstone.

Although not shown in table 6.2 (due to the difficulty in determining grain boundaries as discussed previously), volcanic rock fragments in Tipau sandstone are the smallest of all samples. This sandstone also has the smallest quartz crystals of any of the samples.

The above discussion indicates that mineral grain sizes are largest in Parnell Grit. Cape Rodney sandstone is the coarsest sandstone. Waiake and Rothesay samples are similarly fine grained while Tipau sandstone is the finest grained sample. These observations agree with those made in the field.

6.3.2.1 Cape Rodney Sandstone

The CR sandstone is dominated by anhedral andesitic to dacitic volcanic rock fragments set in a calcite cement (plate 6.1A). Andesitic fragments are large, subrounded to rounded, and contain a combination of megaquartz and microquartz. Some rock fragments are composed of very uniform microcrystalline quartz (plate 6.1B), often with felted masses of very small lath-like plagioclase crystals in a fine crystalline matrix. Dacitic rock fragments are felsic, composed of variously devitrified volcanic glass which often show embayments around their edges due to replacement by calcite

A Photo of thin section of CR sandstone. Andesitic (A) and dacitic (D) rock fragments are set in a calcite cement. Augite occurs in the upper centre and upper right of the photo. Note volcanic quartz (Q) and calcite filled microcrack to the left. Crossed Nicols, x 10 mag.

B Andesitic volcanic rock fragments (A) in CR sandstone. These rock fragments are composed of micro and megaquartz. Dacitic rock fragments (D) occur to the right. Crossed Nicols, x10 mag.

PLATE 6.1 Photos of thin sections of CR sandstone.

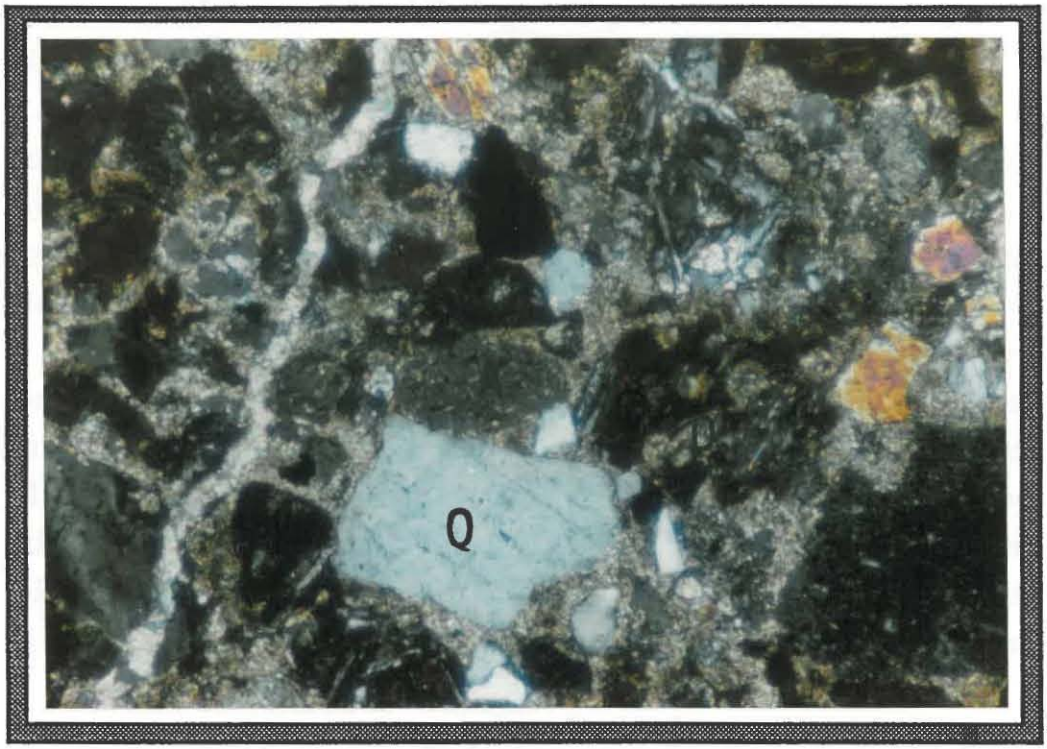
Q

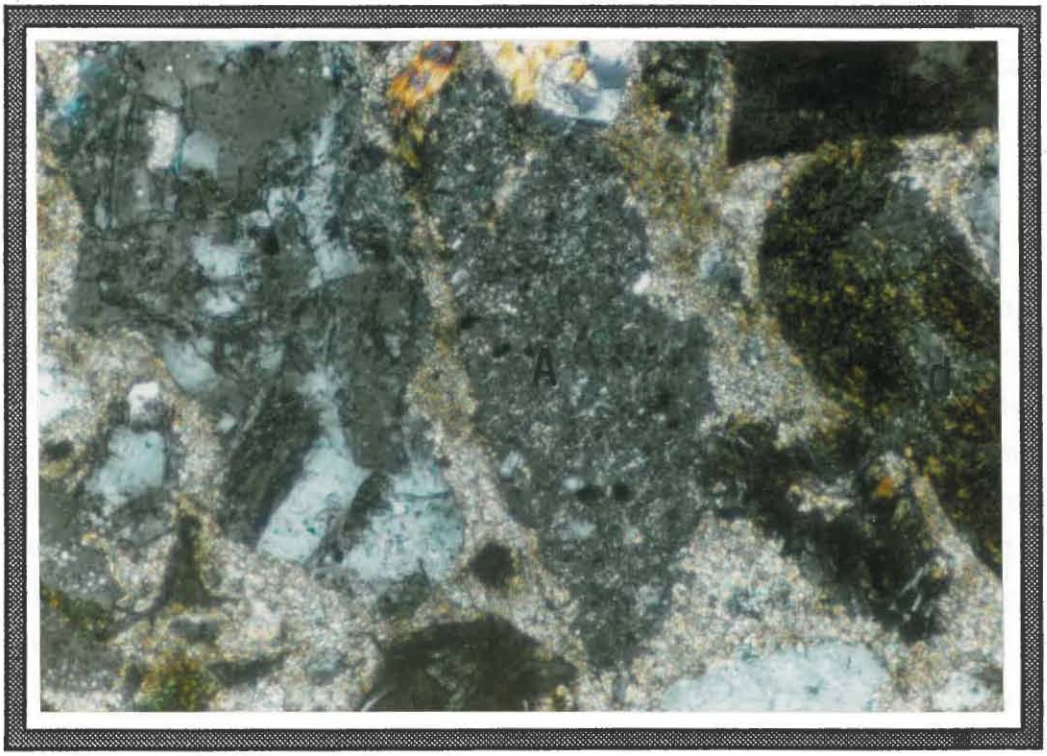
A

cement. These rock fragments are dominantly vitrophyric. The majority of volcanic rock fragments have undergone diagenetic modification through silicification and chemical weathering, recognisable from the abundance of lath-like feldspars, devitrified glass, and mineralised vesicles.

Detrital quartz crystals are small, subrounded to subangular, cloudy yellow to grey, and exhibit slightly undulose extinction. They are dominantly monocrystalline with some polycrystalline varieties. Often quartz contains inclusions of rutile.

Plagioclase feldspar occurs in minor amounts, generally as small (0.19 mm length), euhedral crystals displaying well defined crystal zoning and albite twinning. Rare plagioclase feldspar with multiple types of alteration occurs. Grains have fragmented ends and are partly replaced by clay minerals as well as calcite. Large etched voids are filled with a clayey matrix. Wavy, zeolitised (analcime and clinoptilolite) plagioclase occurs.

Calcite occurs as a pore filling, poikilotopic cement and has partially replaced volcanic rock fragments and feldspars, leaving ragged mineral grain edges.

Other detrital grains include rounded, authigenic, ellipsoidal glauconite with a granular texture, small anhedral magnetite with hematite alteration, and small, subhedral to anhedral, stubby, prismatic cystals of augite. Rare hornblende and epidote occur in some thin sections.

6.3.2.2 Parnell Grit

Parnell Grit is characterised by very large (upto 10 mm length), andesitic/dacitic volcanic rock fragments. Subrounded, irregular shaped andesitic rock fragments dominate and consist of phenocrysts of anhedral augite, tabular plagioclase, and subrounded megaquartz in a crystalline matrix. Plagioclase inclusions reach upto 1 mm in these rock fragments and are generally fractured with broken ends but still display polysynthetic twinning (plate 6.2A). Some andesitic rock fragments are composed entirely of small plagioclase laths, strongly aligned parallel to one another, and set in a fine crystalline matrix (plate 6.2B). Dacitic rock fragments contain an abundance of devitrified volcanic glass.

A Twinned plagioclase feldspar crystals (with fractured ends) in a dacitic rock fragment (Parnell Grit). Crossed Nicols, x 10 mag.

B Felted mass of parallel orientated, thin laths of plagioclase crystals in an andesitic rock fragment. Round black spots are air bubbles. Crossed Nicols, x 10 mag.

PLATE 6.2 Photos of thin sections of Parnell Grit.

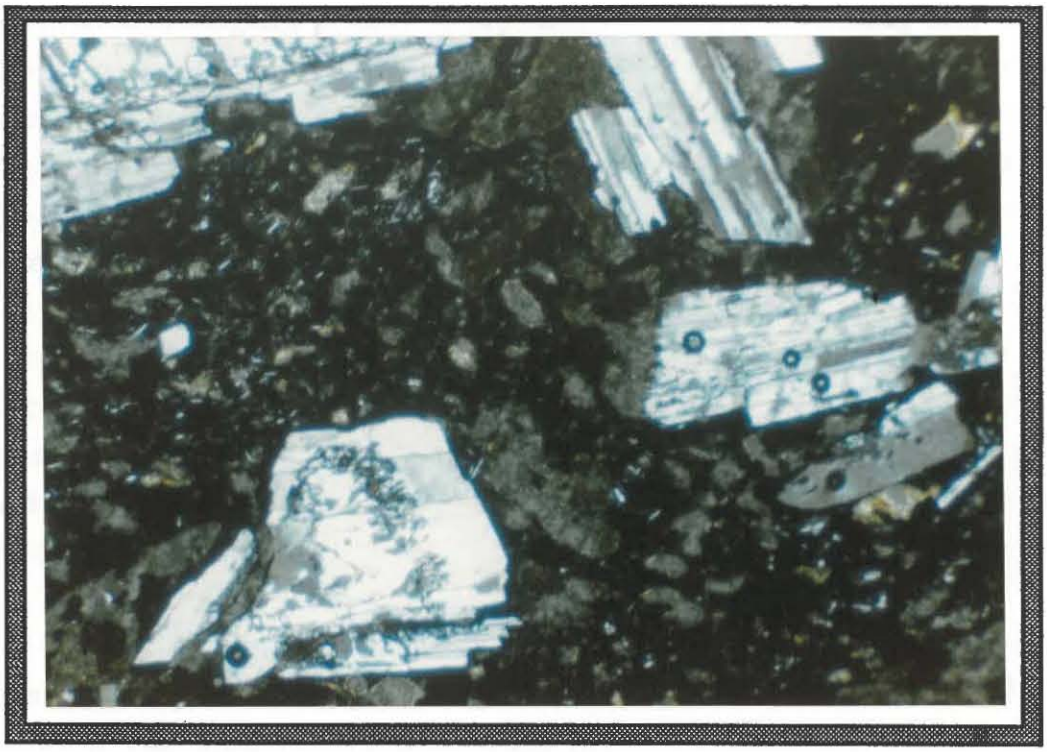

Large plagioclase phenocrysts are common in the green/brown muddy groundmass darkened by clay minerals (dominantly smectite). They are large (1.75 mm length), prismatic crystals with crude twinning and have a dirty and fractured appearance. Often dark holes in their centres represent 'chewed cores' replaced by isotropic analcime. Small, fractured plagioclase pieces occur commonly in the groundmass. Volcanic plagioclase is common with well defined crystal zoning and albite twinning. Microcline feldspar with spindle twinning occurs in minor quantities.

Sub-rounded quartz crystals are small (0.13 mm length) and monocrystalline, with slightly undulose extinction. Many are cracked or have small embayments around their perimeters. Rare polycrystalline quartz occurs. These composite quartz grains are polygonal and exhibit wavy extinction.

Other detrital grains occuring in trace amounts include ellipsoidal glauconite, subhedral augite, microcrystalline calcite, and hornblende, zeolite, and rare chlorite set in a muddy green/brown matrix.

6.3.2.3 ECB Sandstones

The ECB sandstones are characterised by a large proportion of detrital rock fragments as opposed to volcanic rock fragments. The latter are entirely andesitic containing microquartz or, more commonly, have a microcrystalline matrix. Small, euhedral augite crystals are common in some volcanic rock fragments. Detrital rock fragments are subrounded and generally elongated, composed of microcrystalline quartz. In the Rothesay sandstone a very crude alignment of rock fragments occurs associated with the crude bedding observed in the field (plate 6.3A).

Along with rock fragments, detrital quartz makes up a large proportion of these sandstones. It occurs as small (0.14 to 0.24 mm length), subrounded grains, almost all of which are characterised by having undulose extinction (plate 6.3B). Very few grains 'touch' one another and few have cracks or inclusions. Their subangular to subrounded shapes are indicative of mechanical abrasion with possible low intensity chemical weathering, associated with tectonic quiescence. Rothesay sandstone is characterised by a dark, orange/brown heamatite or limonite cement infilling pores and concentrated around the rims of grains, obscuring the matrix and imparting a dark reddish/brown colour to the rock (plate 6.3A). It makes up

A Very crude alignment of detrital rock fragments in Rothesay sandstone. Note the very dark orange-brown limonite cement surrounding grains. White grains are quartz crystals. x 5 mag.

B Rounded detrital quartz crystals dominate this photo, and are set in a fine grained argillaceous matrix. Crossed Nicols, x 2.5 mag.

PLATE 6.3 Photos of thin sections of Rothesay and Tipau sandstones.

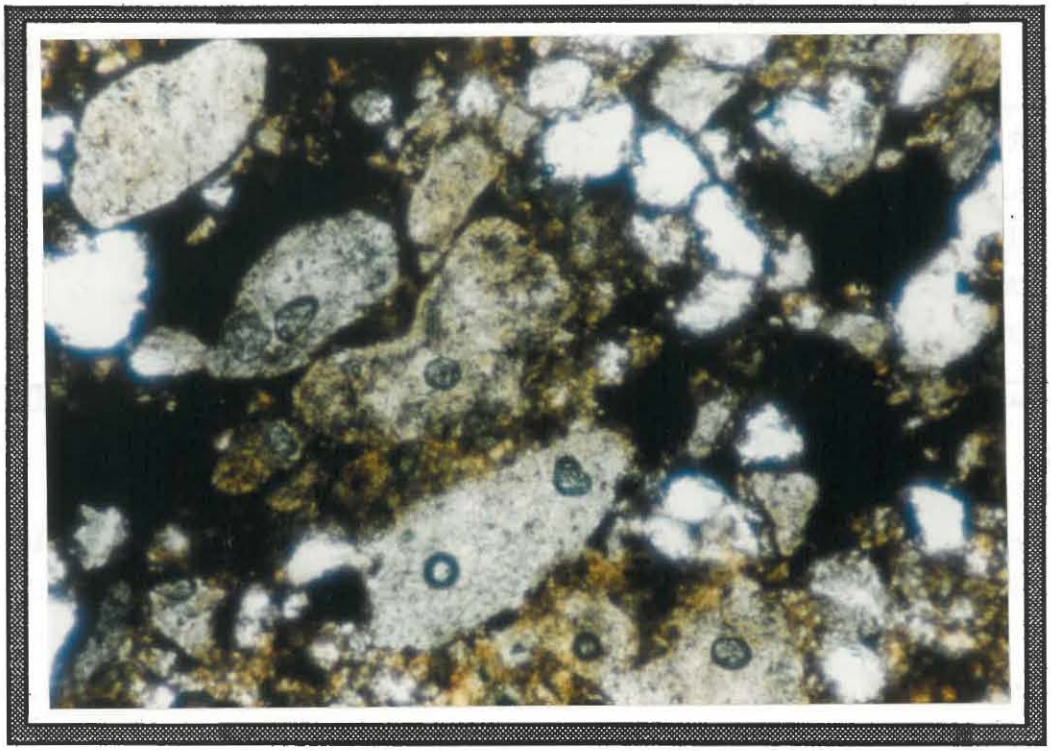

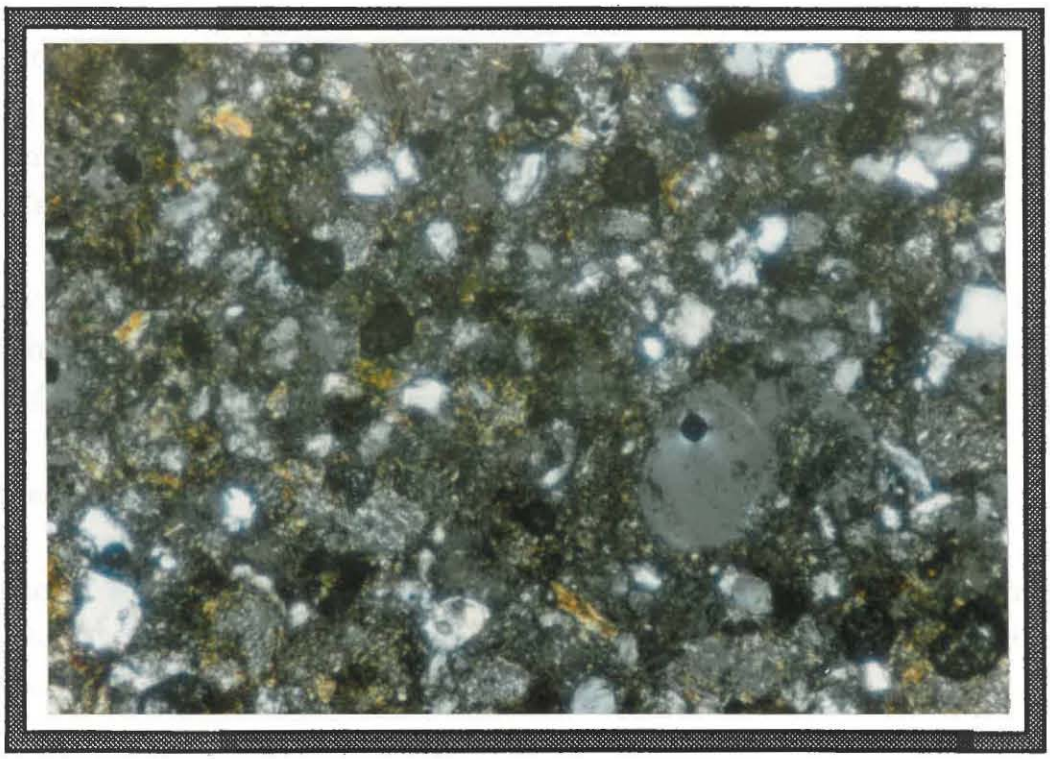

TABLE 6.3 Clay Mineral Percentages

	SMECTITE	ILLITE	KAOLINITE	SMECTITE-CHLORITE	MIXED LAYER
CR SANDSTONE	43	6	6	40	5
PARNELL GRIT	79	8	10	—	3
TIPAU SST	52	19	19	—	10
WAIAKE SST	47	21	18	—	14
ROTHESAY SST	48	17	14	—	21

31 % of the sample and is secondary in abundance to rock fragments, followed by quartz and calcite.

Plagioclase feldspar is a minor constituent in all ECB sandstones only occurring in trace amounts. It occurs as small, tabular phenocrysts displaying polysynthetic twinning (plate 6.4).

Euhedral augite occurs mainly in Tipau and Waiake sandstones as small, stubby phenocrysts with poor cleavage, and fractured ends.

All ECB sandstones are characterised by a fine grained, argillaceous matrix, darkened by clay minerals.

Detrital glauconite, epidote, and microcrystalline calcite occur in trace amounts, with very rare hornblende and chlorite (in Waiake and Tipau samples respectively) and occur as very small grains often obscured by the matrix. Fibrousy, elongated biotite makes up 3 % of the Tipau sandstone.

6.4 CLAY MINERALOGY

Table 6.3 summarises the abundance of the major clay minerals occurring in the <2 μm size range. The semi-quantitative method used is that of Hume and Nelson (1982) which assumes that the reported clay minerals comprise 100 % of the sample. However, quartz and feldspar occur in the <2 μm fraction in the Waitemata sandstones, and in the Rothesay sandstone iron oxide minerals (probably primarily lepidocrocite at 6.27Å) are reasonably abundant.

For the purpose of determining major clay abundances, it is assumed that clay minerals comprise 100 % of the samples. Values in table 6.3 have errors of ± 10 %.

Smectite

Smectite is the most common clay type in all specimens and ranges from 43 to 79 % in abundance. Almost all the muddy matrix in Parnell Grit is composed of smectite.

The clay is authigenic and its abundance is probably due to replacement of volcanic rock fragments (Wilson and Pittman, 1977). On XRD traces, the

Twinned plagioclase feldspar crystals in Waiake sandstone. Crossed Nicols, x 5 mag.

PLATE 6.4 Photo of thin section of Waiake sandstone.

smectite peak expands to 17.3 Å upon glycolation and is reduced to 9.8 Å upon heating at 500 °C, indicative of the highly expandable clay species montmorillonite. Presumably the clay is composed of two layers of water with Ca^{2+} and/or Mg^{2+} as the exchangeable cations.

The smectite is reasonably crystalline, and extremely weak higher order basal reflections are typical of layer silicates with random stacking parallel to a and b crystallographic axes (Hume and Nelson, 1982).

Illite

Illite is a group name for the clay size micaceous components in argillaceous sediments (Brindley and Brown, 1980). In the samples of this study, illite makes up 6 to 21 % of the clay proportion and is primarily fine grained, non-expansible 10 Å mica. It has a poorly defined, broad diffuse XRD peak at 10.05 Å which is unaffected by glycolation treatment. The low 002/001 peak ratio suggests that these micas are rich in iron and magnesium.

Illite is generally abundant in argillaceous sedimentary rocks, and is fine grained and poorly crystalline (Wilson, 1987). It forms as authigenic growths (which project short lath-like appendages) on sand grains (Wilson and Pittman, 1977).

Glauconite is defined by Wilson (1987) as a 'green, fine-grained dioctahedral, often hydrous, micaceous mineral, which contains more iron and less aluminium than do illites'. This mineral has been recognised in thin section (section 6.3.2) and also occurs within the <2 μm size fraction. It is usually identified by its strong 10 Å peak (Wilson, 1987) which in these sandstones has been attributed to illite. Glauconite was identified by its broad based peak at 5 Å, and well defined reflections at 3.63 and 3.09 Å which are characteristic of glauconite.

Kaolinite

Authigenic kaolinite ranges from 6 to 19 % in the samples and is as abundant as illite. It has formed primarily through the replacement of feldspars and calcic plagioclase, as observed by Shelton (1964) and Wilson and Pittman (1977). This clay is readily identified in the samples by its peak at 7.14 to 7.20 Å, and by its total collapse upon heating at 500 °C. The

generally poorly defined peaks suggest the presence of disordered kaolinites.

Smectite - Chlorite

Randomly interstratified smectite - chlorite is only recognised in CR sandstone where the XRD peak can clearly be distinguished from the glycolated 17 Å smectite peak. Chlorite is only recognised in the CR sandstone, under the scanning electron microscope.

Mixed Layer Clays

These clays make up 5 to 21% of total clay proportions but cannot clearly be identified due to their broad, diffuse XRD patterns which are commonly masked by smectite and illite.

More detailed descriptions of the mode of occurrence of clays in the sandstones are given in chapter 7 when the fabric of the rocks is discussed.

6.5 SUMMARY

Cape Rodney sandstone and Parnell Grit are dominated by andesitic/dacitic volcanic rock fragments. These are set in a calcite cement (CR sandstone) or a muddy argillaceous matrix (Parnell Grit). The ECB sandstones are dominated by volcanic and detrital rock fragments. Quartz is abundant in all samples as small, sub-rounded to sub-angular crystals often displaying undulose extinction. Calcic plagioclase is the dominant feldspar and is most abundant in Parnell Grit where it occurs as inclusions in volcanic rock fragments. Plagioclase cores may be chewed to form zeolites.

Clays in all samples are authigenic, and dominated by smectite with lesser amounts of illite and kaolinite. Randomly interstratified smectite - chlorite is only recognised in CR sandstone. Mixed layer clays occur in small quantities but are not readily identified.

The petrography of CR sandstone and Parnell Grit are in keeping with those of volcaniclastic sandstones and conglomerates respectively (Pettijohn, 1975). All the ECB sandstones have similar petrographies to those reported for other sandstones in general (Pettijohn, 1975; Bell, 1978;

Lewis, 1984; Caruso *et al.*, 1985). The observed mineralogy for the ECB sandstones are similar to the findings of Simpson (1988).

CHAPTER 7

MICROFABRIC

CHAPTER 7

MICROFABRIC

7.1 INTRODUCTION

This chapter qualitatively describes and classifies the microfabric of the rocks of this study. The fabric is defined here as the spatial arrangement and organisation of components and component groups, together with associated pore space, occurring within the rocks.

Microfabric has been shown to exert a direct influence on the geomechanical behaviour of soft tertiary rocks of the North Island, New Zealand (Huppert, 1986, 1988). Moon (1989) has shown ignimbrite strength to be related to fabric features. Similarly, Beattie (1990) and Bannock (1991) have shown microfabric to influence rock strength. To determine the influence of microfabric on the geomechanics of the samples of this study a scanning electron microscope (SEM) study was undertaken to characterise and define the fabric arrangements. The relationship between observed fabric features and geomechanical behaviour will be discussed in chapter 8.

7.2 PREVIOUS STUDIES

Scanning Electron Microscopy has been used extensively in the study of microfabrics. Past efforts have concentrated primarily on those of soils, sediments, or loess deposits (Barden *et al.*, 1973; Grabowska-Olszewska, 1975; Torresan and Schwab, 1987). The scanning electron microscope has also been used in determining the different types of microstructure of discontinuity fillings (Samalivkova, 1985), or for studying the configuration, texture and fabric of clay samples (Bohor and Hughes, 1971). Collins and McGown (1974) have shown how particular fabric features in natural soils can be associated with certain types of engineering behaviour.

More recently, the fabric of rocks has been studied to determine the influence it has on their geomechanical properties (Gillot, 1975; Huppert, 1986, 1988; Simpson, 1988; Moon, 1989; Beattie, 1990; Bannock, 1991). In

this study the terminology developed by Huppert (1986) for the description of microfabrics of soft tertiary sedimentary rocks has been adopted.

7.3 METHOD

Small, fractured 5 mm cubes of rock were prepared and air dried in a dessicator for one week prior to being gold coated. A Philips SM4100 Scanning Electron Microscope was used to observe the fabric. The machine was not equipped with an analytical facility, thus the description of fabric features is largely qualitative, although XRD and optical microscopy allowed the identification of most constituents. Some constituents were identified by comparison with published photos (Smart and Tovey, 1981; Welton, 1984).

7.4 FABRIC DESCRIPTION

7.4.1 Definitions of Terminology

Single clay platelets or mineral grains are referred to as individual particles or primary structural elements. These may combine through physico-chemical interaction to form structures referred to as microaggregates, roughly 2 to 10 μm in size, although they sometimes reach up to 40 μm.

Flocculation of microaggregates and individual clay particles form aggregates. They range in size from 20 to 40 μm and may be regular or irregular in shape, and can include silt and sand grains. Aggregates play a geometrically similar role in the fabric as silt and sand grains, but they are less competent in performance. They act as individual entities within the fabric.

The grouped association of aggregates and primary structural elements creates assemblages having defineable physical boundaries. They vary in type, extent, and geometry, and different types may be present at various levels in any one fabric. No one structural type can describe the arrangements observed in any one sample, and commonly, various assemblages combine in a complex microstructure.

Large clusters of aggregates, microaggregates, and silt and sand grains, bonded together to form clusters of several assemblages, form large assemblage types, defined by Beattie (1990) as macroassemblages. They are the largest structural units recognised in this investigation.

The extent, continuity, and proportion of various inter-assemblage arrangements result in the formation of discontinuous or continuous matrices. Huppert (1986) notes that where clay content is high in mudstones, grains are completely surrounded by a continuous clay matrix. Conversely, in siltstones and sandstones, domains occur where grains and inclusions are separated by clay and pores to form a discontinuous matrix. These matrix types represent broad end members only, with intermediaries to these being common in the fabrics.

The following section describes the fabric components, discussing each size in turn. The smallest primary structural elements are initially described, followed by progressively larger components; clay particles, microaggregates, grains, aggregates and matrix arrangements.

7.4.2 Primary Structural Elements

Primary structural elements, as defined in section 7.4.1, have been subdivided by Huppert (1986) according to their form and nature into the following groups of structural elements:

1] clay particles and microaggregates,
2] silt and sand grains,
3] microfossils and authigenic phases.

Huppert (1986, 1988) notes their common distinctive feature is stability in water in the absence of strong dispersing agents or external force. Disaggegation of the rock does not destroy these components.

7.4.2.1 Clay Particles

Individual clay particles, which are stable in mechanical and physico-chemical interaction, are extremely rare in the rocks of this study due to their strong tendency to coalesce and form microaggregates. Clay

particles are authigenic and occur either as pore filling material or, more commonly, as grain coatings.

7.4.2.2 Microaggregates

The dominant occurrence of clays in the samples is as microaggregates of coalesced clay particles. They occur in similar form to the elongated and isometric sheets described by Huppert (1986), and range in size from 1 to 40 μm.

Smectite is the dominant clay in all samples and is commonly in an open flocculated arrangement. It usually occurs as well developed, highly crenulated to flaky, authigenic coatings on detrital grains (plate 7.1A), webby pore lining (plate 7.1B), and pore bridges (plate 7.1C) with edge to face (EF) contacts. Smectite microaggregates range in size from 4 to 40 μm. Large sheets may develop where microaggregates with poorly defined contours grade into one another. Smectite may also occur as tightly packed face to face (FF) arrangements (plate 7.1D) representing the aggregated state of Van Olphen (1963).

Huppert (1986) observed smectitic microaggregates of an unusual morphology occurring as tightly packed spherical globules often associated with biogenic features. A very similar arrangement is observed in Tipau sandstone where smectite forms an onion skin arrangement with clay particles forming face to face (FF) contacts. The spheroids are approximately 10 μm in diameter (plate 7.1E).

Chlorite occurs as small authigenic (< 1 μm), euhedral, pseudohexagonal crystals. Individual platelets are orientated on edge with faces perpendicular to detrital grain surfaces (plate 7.1F). Kaolinite was rarely observed under SEM. It exists as small (~ 1 μm), regular blocks infilling pore space, or as grain coatings associated with feldspars. Filamentous illite is also rare but was observed closely associated with smectite in an open flocculated arrangement.

Identification of mixed layer clays under SEM is virtually impossible without adequate analytical facilities. A significant feature of most samples is the occurrence of an extremely fine (< 1 μm) clay carpet which covers most grains and is closely associated with flocculated smectite

A Large smectitic microaggregates covering grains. Feldspar 'bricks' infil interaggregate mesopores.

B Crenulated, webby smectite in open flocculated arrangement creating intramicroaggregate micropores.

C Smectite bridges connect a closely stacked FF smectite aggregate to feldspar grain, creating an elongated interaggregate micropore.

D Smectite clays in welded FF arrangement. Individual microaggregates are connected to others to form an open honeycomb structure.

E Spheroidal clay microaggregates having an onion skin appearance, with individual smectite clay plates arranged in FF arrangement.

F Large quartz grain with conchoidal fracturing, partly covered by chlorite. Authigenic chlorite is composed of small, euhedral, pseudohexagonal crystals orientated on edge, with faces perpendicular to the grain surface.

PLATE 7.1 SEM micrographs of smectitic microaggregates


000397 5.0 kV X1.10K 16.4µm

A

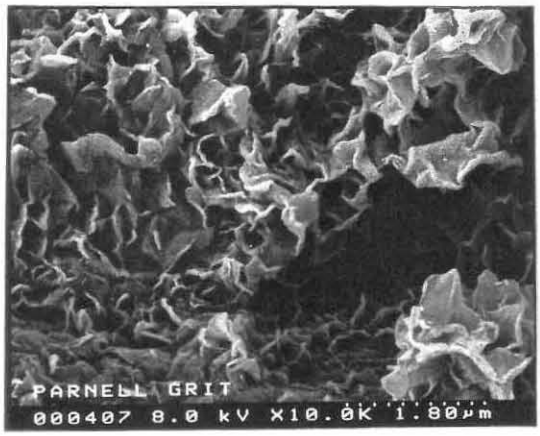
PARNELL GRIT
000407 8.0 kV X10.0K 1.80µm

B

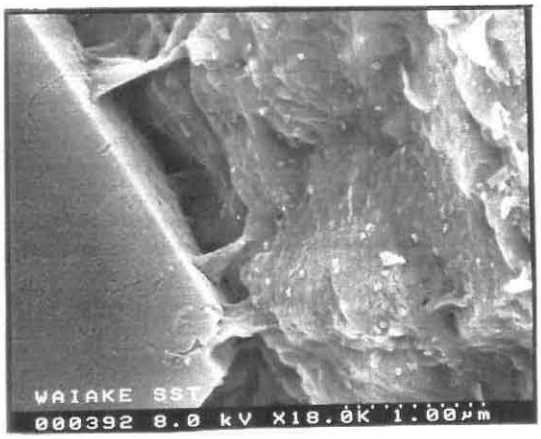
WAIAKE SST
000392 8.0 kV X18.0K 1.00µm

C

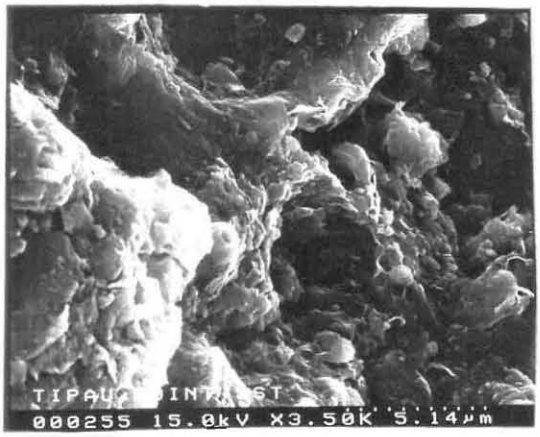
000255 15.0kV X3.50K 5.14µm

D


000259 15.0kV X900 20.0µm

E

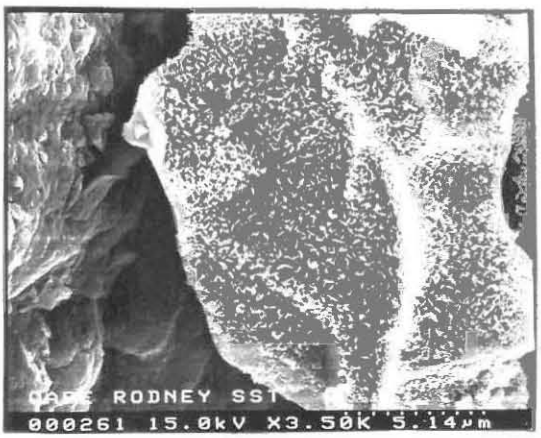
RODNEY SST
000261 15.0kV X3.50K 5.14µm

F

(plate 7.2A). This may, however, merely be a dessication feature produced during sample preparation.

7.4.2.3 Silt and Sand Grains

Individual silt and sand grains vary in size from less than 2 μm upto 200 μm. Detrital quartz is common, ranging from 5 to 200 μm and varying in shape from subrounded to subangular. Conchoidal fractures are evident on some grains (plate 7.1F). Feldspar is also very common and occurs as regular 'bricks' 10 μm long and infilling pores. Many feldspar crystals show dissolution fracturing along edges with associated development of authigenic kaolinite. Rutile is commonly observed in the volcaniclastic samples as long (10 μm) rods associated with feldspar grains and clays (plate 7.2C). Other minerals identified in chapter 6 occur as grains but have similar form in the fabric as quartz and feldspar grains.

Grains may be clean (plate 7.2D), partly coated with clay (plate 7.1F) or, more commonly, clay coated (plates 7.1A,7.2E). Feldspar grains are dominantly clean with clay occurring between grains and forming bridges. Huppert (1986) recognises that a clay coating radically affects the behaviour of a grain in physico-chemical interaction with other structural elements, which is now determined by the clay coating.

7.4.2.4 Microfossils and Authigenic Phases

Microfossils were not observed in the sandstones. Authigenic pyrite and quartz were observed in most samples. Pyrite forms framboids of crystallites, while quartz occurs as small (< 2 μm) rhombic crystals infilling pores or as quartz overgrowths (plate 7.2F). Authigenic phases were not easily identified under SEM and are seen as quantitatively insignificant.

7.5 AGGREGATES

Microaggregates may flocculate to produce aggregates. These are units of particle organisation having defineable physical boundaries and a specific mechanical function (Collins and McGown, 1974). They display a wide

A Fine clay 'carpet' totally covering grains is most likely a dessication feature.

B Bricks of feldspar infilling pore space. Smectitic microaggregates line the pore.

C Rutile rods closely associated with detrital feldspar and smectite clays. Note the large pore in the feldspar grain believed to have formed through dissolution. This effect was observed in thin section with the subsequent formation of zeolites.

D Dominantly tightly interlocking detrital quartz grains. Authigenic quartz infills a pore (top centre) and partly covers grain in lower left.

E Grain covered in clay which is observed to be peeling off the grain. Dominantly FF clay platelets now take on a more open arrangement.

F Clean detrital quartz grain with conchoidal fracture. Note development of authigenic, rhombic quartz crystals (druse) on the right.

PLATE 7.2 SEM micrographs of clay microaggregates and grains

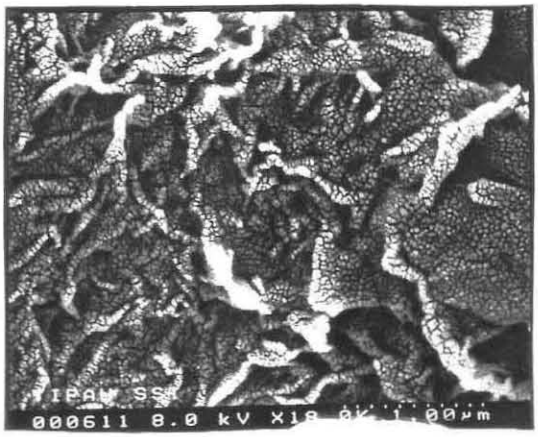
TIPAU SS
000611 8.0 kV X1

A

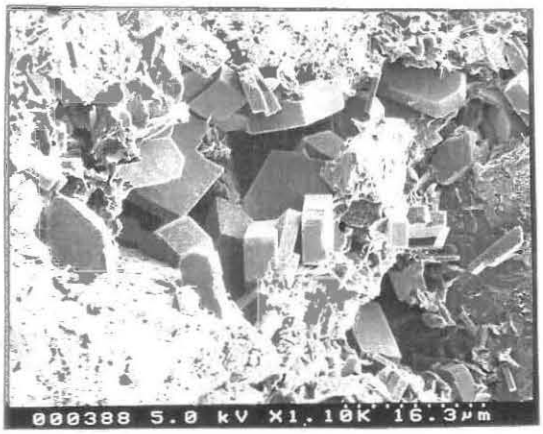
000388 5.0 kV X1.10K 16.3µm

B

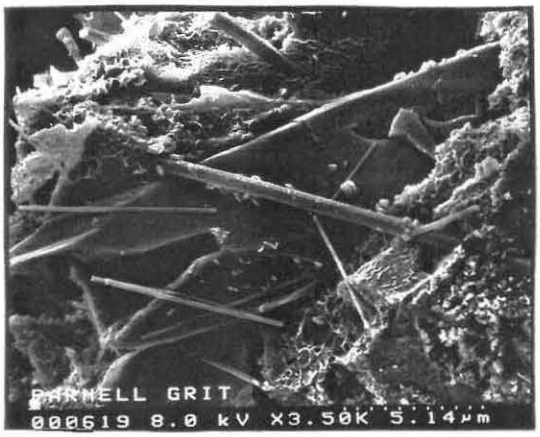
PARNELL GRIT
000619 8.0 kV X3.50K 5.14µm

C


CAPE RODNEY
000599 8.0 kV X254 70.8µm

D

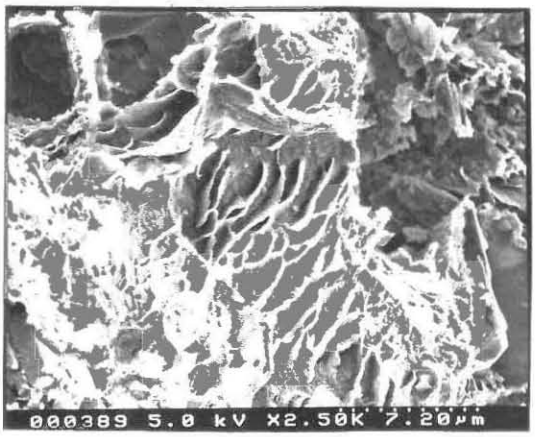
000389 5.0 kV X2.50K 7.20µm

E

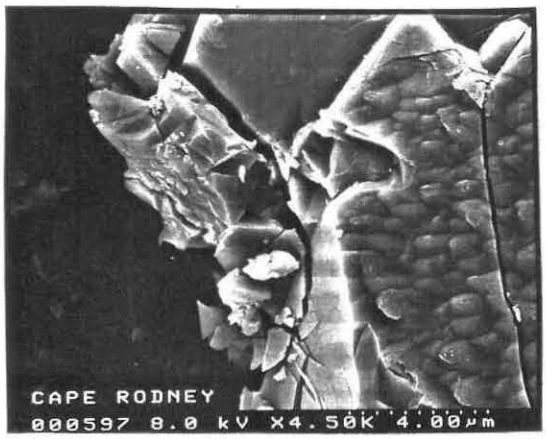
CAPE RODNEY
000597 8.0 kV X4.50K 4.00µm

F

range of shapes and sizes and are unstable in suspension and easily destroyed by external physical force.

Smectitic microaggregates form open, regular aggregates which may join with others to form elongated chains or bridges across pores (plate 7.3A). Irregular aggregates of crenulated smectite commonly line pores (plate 7.2B). Closely stacked FF smectitic microaggregates may coalesce to form regular aggregates which, in turn, are linked to other aggregates in a honeycomb structure (plate 7.1D). These are stronger than open aggregates, as they are characterised by a certain amount of inherent elasticity (Huppert, 1986), but water tends to separate them along basal planes.

Aggregates may include physically bound silt and sand grains. Regular spheroidal aggregates 40 μm in diameter and incorporating resorbed feldspar and FF arranged smectite microaggregates occur in Tipau sandstone (plates 7.3B,7.3C). Rock fragments having strong internal bonds form regular, clean (plate 7.3D) or clay coated aggregates (plate 7.3E).

Often aggregates cannot clearly be distinguished and occur as complex organisations of linked microaggregates (plate 7.3F) termed 'partly discernable particle systems' by Collins and McGown (1974).

7.5.1 Intra - aggregate arrangements

Aggregates have relatively open internal structures composed of webby smectite microaggregates, uniform regular bricks, and resorbed feldspar grains in random arrangements. Regular aggregates may be composed of resorbed feldspar remnants and tightly packed smectite in FF arrangements joined to other clay microaggregates by EF contacts to form an open honeycomb arrangement (plate 7.3C). More commonly, regular clay microaggregates are composed of flocculated, crenulated smectite connected to other microaggregates by clay connectors (plate 7.4A). A wide range of shapes and sizes in random orientation constitute the dominant internal aggregate arrangements.

A Smectite microaggregates connected to form an elongated bridge across an interaggregate mesopore.

B Very regular spheroidal aggregate surrounded by irregular aggregates combined to form macroassemblages.

C Higher magnification of B. Spheroid is composed of resorbed feldspar, and smectite in tight FF arrangement. Random orientation of components creates irregular intraaggregate micropores.

D Contact between two regular feldspar grains. Dissolution of feldspar may eventually lead to formation of authigenic kaolinite blocks or platelets.

E Two regular grains coated with clay (in FF arrangement) and separated by clay microaggregates. Regular feldspar bricks infill the interaggregate mesopore.

F Clay microaggregates and grains lacking any defineable physical boundary to form a partly discernable particle system (Collins and McGown, 1974).

PLATE 7.3 SEM micrographs of aggregates and their internal arrangements.

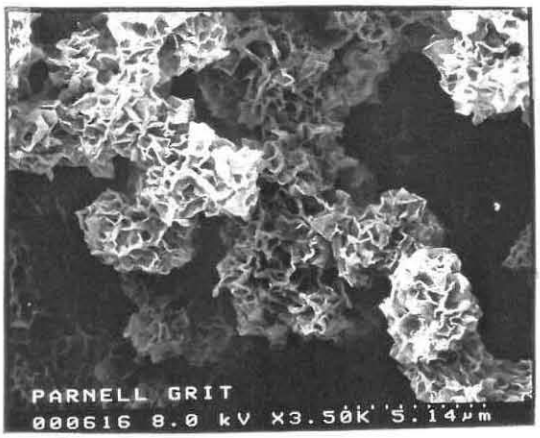
PARNELL GRIT
000616 8.0 kV X3.50K 5.14µm

A

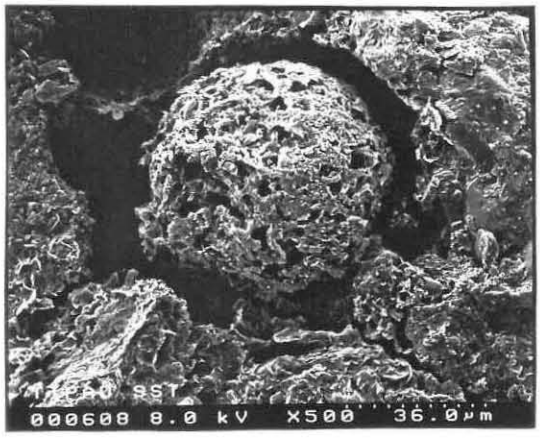
000608 8.0 kV X500 36.0µm

B

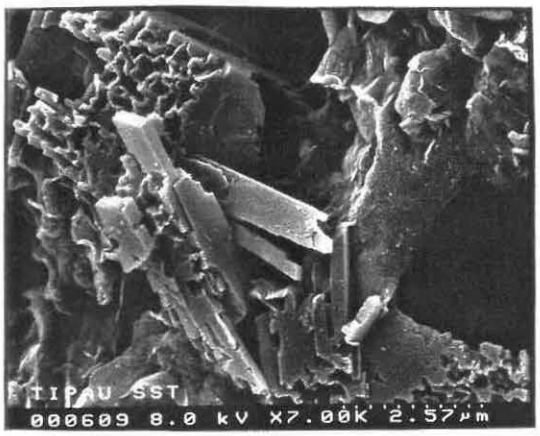
TIPAU SST
000609 8.0 kV X7.00K 2.57µm

C

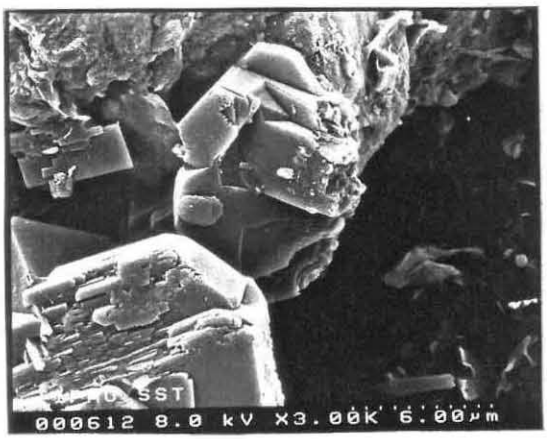
000612 8.0 kV X3.00K 6.00µm

D

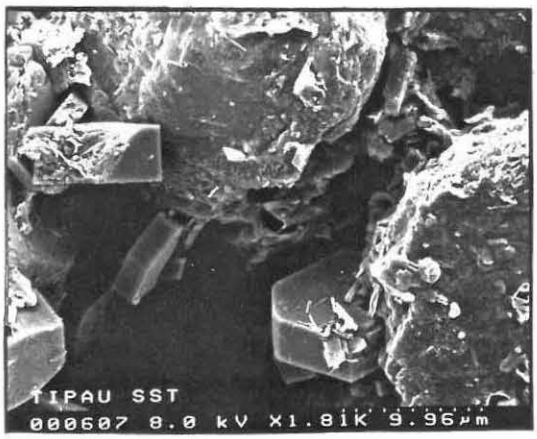
TIPAU SST
000607 8.0 kV X1.81K 9.96µm

E

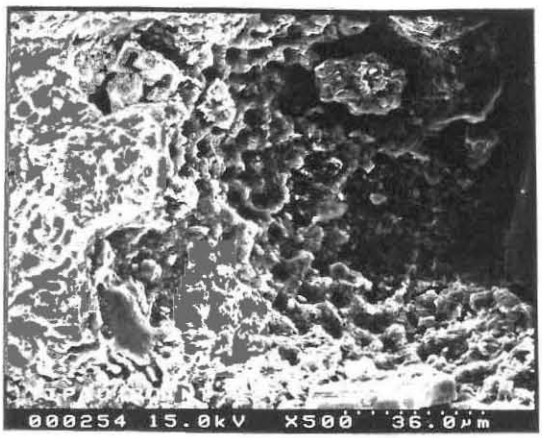
000254 15.0kV X500 36.0µm

F

7.6 MATRIX ARRANGEMENTS

7.6.1 Discontinuous Matrix

A discontinuous matrix is produced by structural assemblage types occurring as discrete domains. This matrix type is dominant in the rocks of this study. Assemblage types vary from macroassemblages where microaggregates, aggregates and grains are bonded together, to random domains of disorganised arrangements of microaggregates, with common intermediate varieties.

The observed fabrics are dominated by granular silt and sand size particles, often clay coated and arranged in a random fashion to form macroassemblages (plates 7.4B,7.4C,7.4D) separated by clay or macro pores (plate 7.4E). Clay microaggregates are arranged as grain coatings or as discrete aggregates having similar mechanical function in the fabric as the grains (plates 7.4F,7.5A).

Grains usually form regular aggregates in a loose arrangement akin to the 'rock wall' fabric described by Torresan and Schwab (1987). These aggregations form large assemblages (macroassemblages) connected together by point contacts or separated by large clay aggregates. Grains in the East Coast Bays samples are clay coated and loosely arranged with close grain to grain contacts separated by clay microaggregates (plates 7.4B,7.4C).

Parnell Grit samples are characterised by large grains (plate 7.5B), clay coated but in closer contact and with fewer clay microaggregates separating individual grains. In this sample, clay aggregates may be very large (> 90 μm) (plate 7.4F) and have similar status in the fabric as grains.

Cape Rodney sandstone is characterised by tightly interlocking, large, clean grains (plates 7.2D, 7.5C). Clay microaggregates occur as discrete aggregates (plate 7.5D) and are arranged in tightly stacked FF arrangements.

Clay aggregates may separate grains by bridges of small smectitic microaggregates arranged as elongated chains (plate 7.3A), occur as infilling between grains, or form clay connectors (plate 7.1C). Commonly,

A Intramicroaggregate micropores in flocculated smectite. Microaggregates are joined by clay bridges.

B Granular network of grains forming macroassemblages and creating inter-macroassemblage macropores.

C Large clay covered grains create a porous network. Grains may have coatings of detrital feldspar bricks (left grain).

D Rock wall arrangement of Torresan and Schwab (1987). Inter-macroassemblage macro and mesopores interconnect to form a porous network.

E Elongated inter-macroassemblage macropores separate two large assemblages in Parnell Grit.

F Large aggregate of clay. Cracks were produced through the process of air drying samples. Plate 7.1B is a magnified view of the intraaggregate flocculated clay arrangement. These large clay aggregates act as discrete entities in this fabric.

PLATE 7.4 SEM micrographs of assemblage arrangements and associated pore space.

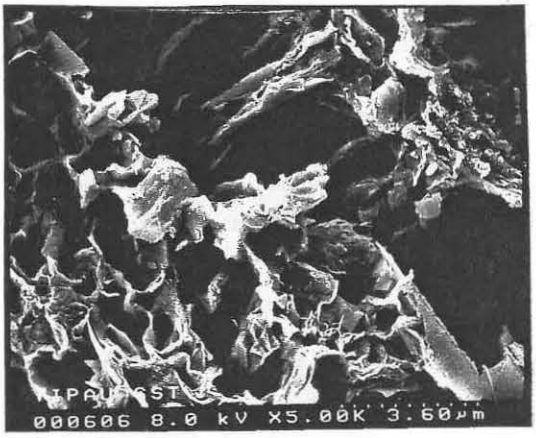
000606 8.0 kV X5.00K 3.60µm

A

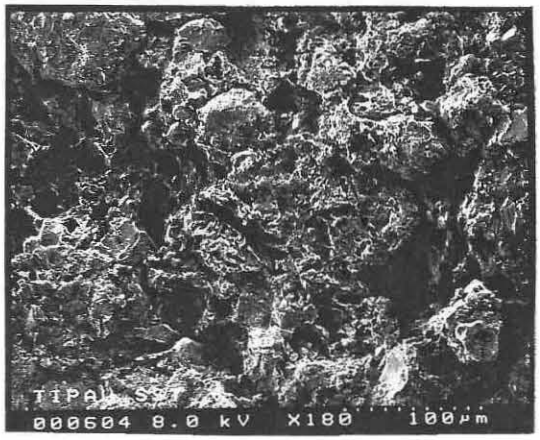
TIPAL SST
000604 8.0 kV X180 100µm

B

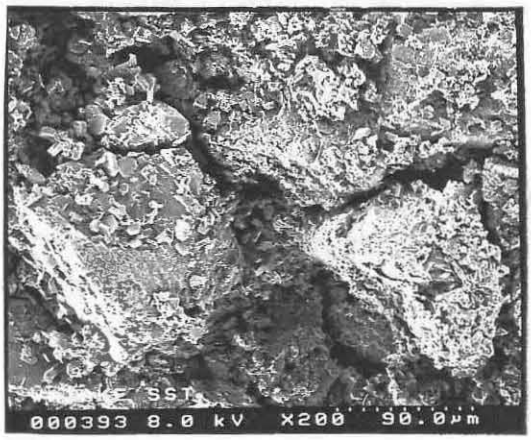
SST
000393 8.0 kV X200 90.0µm

C


ROTHESAY SST
000395 5.0 kV X110 164µm

D


PARNELL GRIT
000614 8.0 kV X60.0 300µm

E

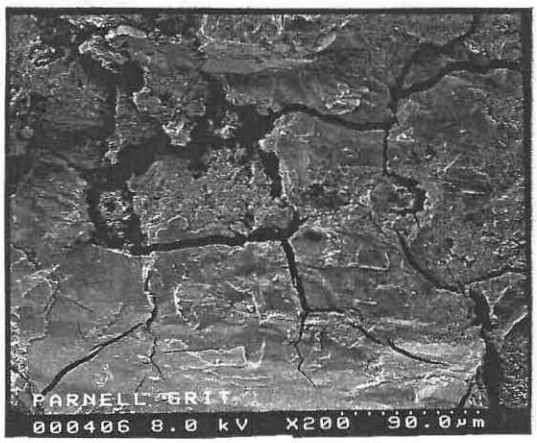
PARNELL GRIT
000406 8.0 kV X200 90.0µm

F

A Irregular inter-macroassemblage macropore. Note rutile rods protruding from the clay aggregate (bottom right).

B Tightly interlocking aggregates in Parnell Grit. This fabric occurs side by side with the view in plate 7.4F.

C Clean detrital quartz grain in tightly interlocking arrangement.

D Large detrital quartz grain in a sea of clay aggregates lacking defineable physical boundaries. This fabric arrangement resembles the turbostratic end member type described by Huppert (1986).

E Disorganised mass of microaggregates (random domain) filling pore space between detrital grains.

F Welded honeycomb network of smectitic microaggregates with tightly packed individual clay platelets in FF arrangements.

PLATE 7.5 SEM micrographs of microaggregate, aggregate, and grain arrangements.

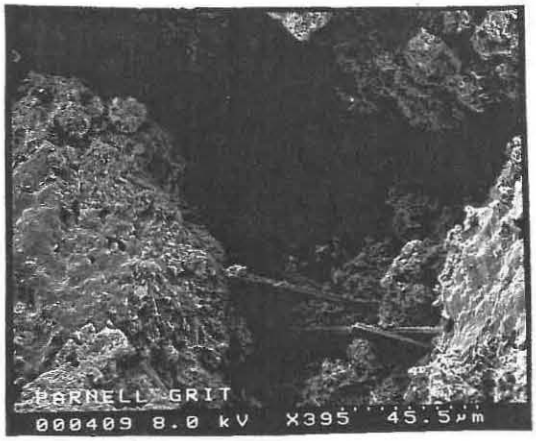
BARNELL GRIT
000409 8.0 kV X395 45.5µm

A


000405 8.0 kV X60.0 300µm

B

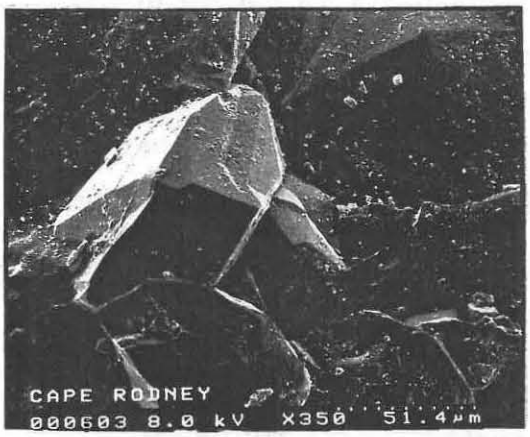
CAPE RODNEY
000603 8.0 kV X350 51.4µm

C

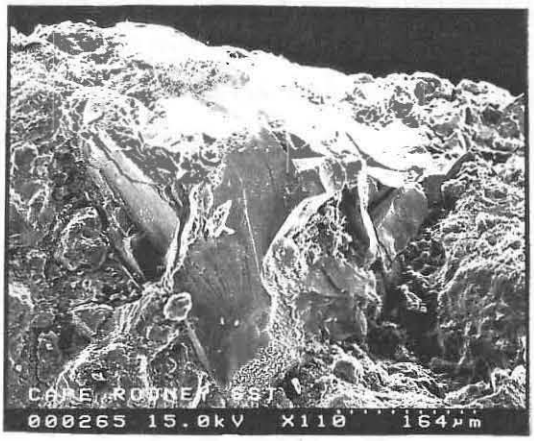
000265 15.0kV X110 164µm

D

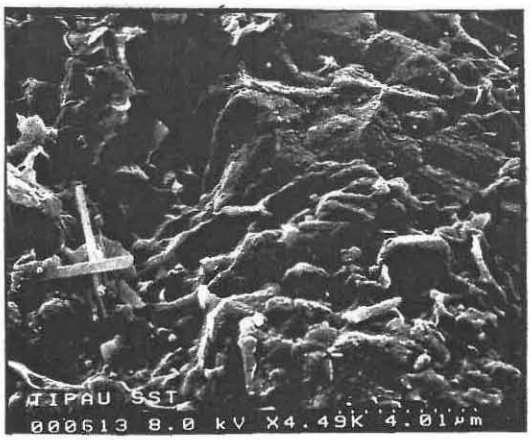
000613 8.0 kV X4.49K 4.01µm

E

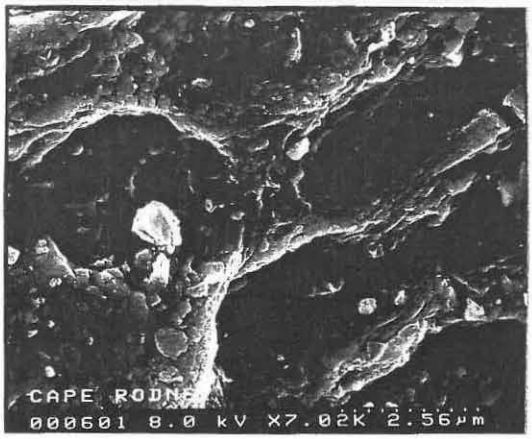
CAPE RODNEY
000601 8.0 kV X7.02K 2.56µm

F

TABLE 7.1 Classification of Pore Types
(after Huppert, 1986; Beattie, 1990)

Classification by boundary elements:

Interelemental Pores:	
Continuous matrix	intramatrix
	interparticle
	intermicroaggregate
	interaggregate/
	granular
Discontinuous matrix	intergranular
	interaggregate
	inter-macroassemblage
Intraelemental Pores:	
	intragranular
	intraaggregate
	intramicroaggregate
	pore of organic and/or diagenetic origin

Classification by Size:

ultrapores	< 0.1 μm
micropores	0.1 - 5 μm
mesopores	5 - 30 μm
macropores	> 30 μm

clay microaggregates are grain coatings, dominantly with open flocculated arrangements (plate 7.1A) several layers (several microns) thick (plate 7.2E).

The samples are more characterised by a discontinuous matrix dominated by clay coated detrital grains.

7.6.2 Continuous Matrix

Grains or detrital aggregates immersed within the matrix constitute a continuous matrix. Such an arrangement, which is characterised by a disorganised mass of microaggregates filling space between detrital grains and larger aggregates, though rare, is observed in some of the samples (plate 7.5E). Regular feldspar grains in a jumbled arrangement (plate 7.2B) may constitute matrix, but primarily matrix is dominated by flocculated smectite. In Tipau and CR sandstones, smectitic clays may occur in welded FF arrangements which are interconnected with other FF welded aggregates to form a welded honeycomb structure (plates 7.1D, 7.5F). These structures occur up to 20 μm in size, and although relatively uncommon, form side by side with open flocculated smectite.

7.7 PORE SPACE

Structural arrangements in microfabrics create pore space which varies in the rocks of this study from 10 to 32 %. The pore classification of Beattie (1990) modified from Huppert (1986) is adopted here. Pore types are classified according to their size, and relationship with surrounding structural units. Size classes are chosen to bear relationship to the status of pore water. Table 7.1 presents the classification of pore types.

The predominance of a discontinuous matrix in the samples, and the formation of large aggregates, results in a wide variety of pore sizes. All ECB samples are characterised by a range of interelemental pores from intergranular mesopores to inter-macroassemblage macropores. Interelemental pores tend to be irregular or elongated interaggregate and inter-macroassemblage pore types which increase from mesopores to macropores as grain sizes increase.

TABLE 7.2 Classification of Microfabric Types
(modified from Huppert, 1986)

Skeletal Microfabric

Has a discontinuous matrix and is essentially granular. Clay is either organised into regular or irregular aggregates which act as silt size entities in the fabric, or forms connector assemblages and coatings between and around grains. Pore space is dominated by isometric but irregular mesopores.

Matrix Microfabric

Has a continuous matrix in which grains are completely immersed, but intramatrix EF contact angles are predominantly large. The matrix microfabric stipulates EF contacts with predominantly large angles between microaggregates of the matrix. Pore space is dominated by isometric micropores.

Turbostratic Microfabric

Has a continuous matrix, but intramatrix EF contact angles are small with a significant number of FF contacts. Orientation is, however, not a necessary criterion for the turbostratic microfabric. Pore space is dominated by elongated micropores.

Inter-macroassemblage pores are dominantly elongated to irregular in Rothesay and Waiake sandstones ranging from less than 30 μm up to 100 μm (plate 7.4C). Tipau sandstone is characterised more by irregular inter-macroassemblage macropores (~ 50 μm). Parnell Grit has a variable fabric arrangement. Grains form tightly interlocking arrangements which reduce pore space, or else form loose granular arrangements where irregular, elongated inter-macroassemblage pores reach 200 μm in width and are greater than 300 μm in length. These may interconnect to form a porous network (plate 7.4E).

The tight interlocking fabric of CR sandstone reduces its porosity. Interelemental pores are commonly intergranular mesopores.

In all samples where a continuous matrix occurs pores are irregular intramatrix, interparticle or intermicroaggregate micropores (plates 7.1D, 7.4A, 7.5F).

Intraelemental pores range from intragranular macropores to intramicroaggregate micro and mesopores. Regular to irregular microaggregates dominated by smectitic clays result in intramicroaggregate micropores. Commonly, intraelemental pores are intraaggregate micro to mesopores which are elongated where microaggregates occur adjacent to sand grains (plate 7.1C). The random arrangement of components in most aggregates result in irregular intraaggregate micropores (plate 7.3C).

7.8 MICROFABRIC TYPES

Three types of microfabric have been defined by Huppert (1986) based on the continuity of matrix in samples. They represent end members used to define the complex array of fabric types which may occur in rock samples. These microfabric types are defined in table 7.2.

Cape Rodney Sandstone

Cape Rodney sandstone is not adequately described by any of the fabric types. Tightly interlocking grains dominate the sample and reduce porosity (plate 7.5C). In parts, smectite is arranged in welded FF honeycomb arrangements (plate 7.5F), and in others, sand grains are

immersed in a continuous matrix of clay microaggregates and silt grains (plate 7.5D). The sample displays a range of fabric types from skeletal to turbostratic and cannot be adequately described by any one type.

Parnell Grit

Parnell Grit is characterised as having a dominantly skeletal fabric. Areas of this sample are granular with interaggregate and inter-macroassemblage macropores (plates 7.4E,7.5A,7.5B). Large, irregular clay aggregates acting as discrete entities in the fabric occur alongside these granular arrangements (plates 7.4F). Few macropores exist, with pore space generally dominated by mesopores.

Tipau Sandstone

Tipau sandstone has a microfabric which is dominantly skeletal but which grades into areas which may be described as turbostratic. Smectitic clays are arranged as regular microaggregates (plate 7.3B) which act as silt sized entities in the fabric, or occur as webby, crenulated, pore lining or grain coatings. Aggregates of clay microaggregates and clay coated grains form weak assemblages in a discontinuous matrix. Pore spaces are limited to meso and micropores.

Welded FF arranged smectite clays are less common but do occur in association with flocculated microaggregates, and are more analagous of the turbostratic type matrix (plate 7.1D). This sample highlights the difficulty associated with defining any one fabric type exclusively to a sample.

Waiake Sandstone

Waiake sandstone is described as having a skeletal microfabric. Aggregates and clay coated grains are combined into assemblages which are clustered with neighbouring assemblages to form macroassemblages, in a dominantly discontinuous matrix (plate 7.4C). Aggregates have open internal structures which result in a porous network of inter-macroassemblage macropores. The aggregates are all of similar size which produces an even degree of openess throughout the fabric. They are connected to one another, and to other structural components, by point

contacts and behave essentially as individual units. The open internal structures of microaggregates, aggregates, and assemblages results in a large number of pore types and sizes ranging from micro to macropores.

Rothesay Sandstone

Rothesay sandstone has a very similar microfabric to that of Waiake sandstone, and is best described as skeletal. Clay coated grains and microaggregates of clay are loosely arranged into aggregates in a discontinuous matrix. The aggregates are clustered into macroassemblages (of similar size) which are connected through point contacts and so act as individual units in the overall fabric, and create an even degree of openess. Smectite clays are arranged as regular microaggregates which line pores, form bridges between grains, and act as silt sized entities. The open internal structure of all components results in pores occurring at all levels in the fabric, from micro to macropores.

This fabric is displayed in plate 7.4D, where it forms the rock wall arrangement of Torresan and Schwab (1987).

7.9 SUMMARY

Scanning Electron Microscopy was used to qualitatively characterise and classify the fabric of Waitemata sandstones.

Primary structural components were identified. Individual clay particles are extremely rare. Clay microaggregates dominate and are open, flocculated arrangements of smectite. They occur as discrete entities, as pore bridges or pore linings, or most commonly as grain coatings. Authigenic, euhedral, pseudohexagonal chlorite occurs as grain coatings. Common to most samples is an unusual clay 'carpet' completely covering grains and associated with smectitic microaggregates. Welded FF stacked smectite occurs as microaggregates but are limited in extent.

Individual silt and sand grains are dominantly subrounded to subangular quartz, regular 'bricks' of feldspar, and elongated rods of rutile. Contact between grains is common, especially between pore filling feldspar blocks. Authigenic pyrite and quartz were observed infilling pores and coating grains.

Assemblages having defineable physical boundaries were identified and particle arrangements discussed. Intraaggregate arrangements are composed of grain and clay microaggregates and have relatively open internal structures creating intraaggregate micro and mesopores. Matrix arrangements were divided into discontinuous and continuous matrices dependant on relative proportions of components. A discontinuous matrix dominates most samples where clay coated macroassemblages are separated by inter-macroassemblage macropores, elongated and interconnected in a porous network. A continuous matrix may occur in the same samples in limited proportion, where grains are arranged in a sea of clay. Clay may be arranged in tightly packed FF arrangements and interconnected to form a welded honeycomb arrangement.

The granular nature of the samples results in a dominance of interelemental, inter-macroassemblage macropores, lined by clay and interconnected. Intraelemental pores span a wide range down to intragranular micropores developed largely through dissolution of feldspar grains. Intramicroaggregate micro and mesopores are more common at this level.

The samples were classified according to microfabric types representing end members of complex fabric arrangements. East Coast Bays sandstones are dominated by skeletal microfabrics, but may grade into the turbostratic type. Parnell Grit is almost exclusively dominated by a skeletal microfabric where clay aggregates form discrete entities alongside granular aggregates. Cape Rodney sandstone is difficult to classify. A tight interlocking arrangement of clean grains reduces porosity and is not adequately described as skeletal. Conversely, welded honeycomb clay aggregates occur and may in part completely surround grains to form a turbostratic fabric.

These samples highlight the difficulty associated with defining any one fabric type to a rock sample. Waitemata sandstones may best be described as having skeletal fabrics grading, in some cases, to turbostratic microfabrics.

CHAPTER 8

GEOMECHANICAL BEHAVIOUR RELATED TO MINERALOGY AND MICROFABRIC

CHAPTER 8

GEOMECHANICAL BEHAVIOUR RELATED TO MINERALOGY AND MICROFABRIC

8.1 INTRODUCTION

The mineralogy and microfabric of the rocks of this study were characterised in chapters 6 and 7 respectively. In this chapter the geomechanical behaviour of the rocks is related to these two properties. Parameters used to describe geomechanical behaviour include strength (compressive and tensile), elasticity, and durability. These are related to mineralogy through simple linear regression against mean values of crystal proportions and sizes. A regression coefficient of r^2 equal to 0.5 is used as a cut-off point as described in chapter 5.

The relationship between geomechanical behaviour and microfabric is purely qualitative due to the morphological complexity of the samples. Each sample displays a range of fabric types. Thus, observed suites of structural arrangements constituting the microfabric of each sample are related to geomechanical behaviour.

8.2 GEOMECHANICAL BEHAVIOUR AND MINERALOGY

Importantly, no correlations were found between any strength parameter and any mineralogical property. Linear regression produced r^2 values of less than 0.3 in all cases. These results are very interesting as they support previous findings in chapter 5 that strength and durability are not related to quantity, size (this includes the gravel component in Parnell Grit), or type of minerals present. Rather, it is the arrangement of individual components in the rock fabric which directly influence geomechanical behaviour.

Similarly, no correlations were found to exist between clay abundances and geomechanical behaviour. This is intuitively reasonable as the dominant clay (smectite) occurs in similar quantity in all samples. It is the arrangement of clays into flocculated or FF stacked microaggregates and aggregates, and their association and interaction with other

structural elements in the fabric, which directly control the strength and durability of the rocks.

8.3 GEOMECHANICAL BEHAVIOUR AND MICROFABRIC

The samples exhibit microfabrics characteristic of the skeletal and turbostratic end member types proposed by Huppert (1986). Observed suites of structural arrangements are qualitatively related to measured geomechanical behaviour in the following section.

8.3.1 Strength

Cape Rodney Sandstone

Cape Rodney sandstone is the strongest sample in this investigation in both compression and tension. It is characterised by a predominantly discontinuous matrix and observed fabric arrangements vary from skeletal to turbostratic. The microfabric is dominantly composed of tightly interlocking clean quartz grains which results in low porosity. Pores are mainly restricted to interelemental interaggregate meso or micropores.

Stacked FF welded honeycomb clay aggregates occur in limited quantity and extent in this sample. Huppert (1986) notes such aggregates are less competent in performance compared with silt and sand grains as internal cohesion is determined by contacts between their component microaggregates. The welded FF arrangement produces a certain amount of inherent elasticity and allows the aggregates to withstand external physical forces better than open flocculated arrangements. Water may separate these layers along basal planes through the process of wetting and drying.

Clay aggregates are limited in quantity and extent in CR sandstone. It is the interlocking quartz grains (with large surface contact areas and lack of weak grain connectors), and low porosity (with a dominance of intergranular mesopores over larger pore spaces) which enable this rock to withstand high compressive and tensile stresses.

The fabric arrangement is also related to the deformability of the rock. Initial deformation is a result of bending of FF stacked smectitic aggregates and closure of pore space. Brittle failure occurs when contacts between interlocking quartz grains are broken.

Parnell Grit

Parnell Grit is much weaker than CR sandstone, but slightly stronger than ECB sandstones in both compression and tension. The fabric is predominantly skeletal and characterised by large smectitic aggregates which act as discrete entities in the fabric. Aggregates have open, flocculated internal structures and are connected to surrounding grains by clay bridges and buttresses. The open structure of these aggregates makes them unstable in suspension and they are easily destroyed through external forces. These aggregates, and associated connector assemblages, assume decisive roles as weak links in stress transmission (Huppert, 1986).

Parts of the fabric are characterised by close grain to grain contacts between clean silt and sand grains. These impart a certain amount of added strength to the rock. Grains and clay aggregates are combined to form macroassemblages with elongated and irregular inter-macroassemblage macropores. Though these are large, they are few in number. Pore spaces are mainly confined to intramicroaggregate mesopores and interaggregate meso and macropores. It is with these macropores that the direct effect of water infiltration and saturation occurs, with associated loss in cohesion and bonding of smectitic microaggregates, and an associated strength reduction.

Parnell Grit is highly deformable. This is directly related to macropores and mesopores at various levels in the fabric. As compressive strengths are applied, pore spaces close prior to collapse of point grain contacts and other clay connectors. Slightly greater stresses are required to produce failure (in Parnell Grit) than those required for ECB sandstones. This may be due to the few clean grain to grain contacts arranged in the Parnell Grit's fabric. The rock becomes elastically stiffer for a very short period, as compressive stresses are applied, prior to failure.

Tipau Sandstone

Tipau sandstone is the strongest ECB sandstone in both compression and tension. It is characterised by a predominantly discontinuous matrix and is described as having a skeletal microfabric which grades into the turbostratic type end member. Macroassemblages are limited in number in the fabric.

More commonly, aggregates occur with open internal structures, which creates an abundance of intraaggregate and intramicroaggregate micropores. The dominance of microaggregates, aggregates of clay, and clay coated grains, with associated buttresses and connector assemblages, creates weak links in stress transmission through the sample. All grains in this sandstone are clay coated, except for regular feldspar bricks which infill pores in a loosely packed state. These feldspar grains are, however, limited in extent, and proportionally insignificant in the overall fabric. Clay coatings on grains affect their behaviour in physico-chemical interaction with other structural features, which is now controlled by its clay skin (Huppert, 1986) - flocculated smectite in this case.

Importantly, welded honeycomb structures were observed in this fabric. These FF welded arrangements are more competent than open flocculated arrangements and are almost certainly responsible for this sample's greater strength compared with those of Waiake and Rothesay sandstones. The only other sample with similar FF welded aggregates is CR sandstone.

The highly deformable nature of this sandstone can be related to pore closure as stresses are applied. Pore spaces are restricted to meso and micropores. Once these have closed, in response to external forces, slight increases in stress result in rapid breakage of weak clay connectors. The FF welded aggregates produce a certain amount of inherent elasticity and allow the rock to withstand slightly greater physical forces (than Waiake and Rothesay sandstones) prior to failure. This agrees with previous observations made in chapter 4.

Waiake Sandstone

Waiake sandstone is a very weak rock with high porosity. It is highly deformable and its fabric is described as skeletal. The fabric is dominated by macroassemblages of aggregates, microaggregates, and clay coated silt and sand grains, loosely arranged, and having open internal structures, in a dominantly discontinuous matrix. Aggregates are connected to others at point contacts and act as individual units. Pore spaces are common at all levels in the fabric and range from macropores to micropores. Open, flocculated, smectitic microaggregates create an abundance of intramicroaggregate micropores.

All grains are clay coated with no direct grain to grain contacts. Although feldspar bricks are clean and make contact, they are loosely arranged and do not impart any significant strength to the rock. The clay coatings on grains radically affect their behaviour, as it is now the clay coatings which control their interaction with other fabric features. Microaggregates of smectitic clays form connectors between grains and aggregates, and these become weak links for stress transmission. Their open internal structures make them unstable in suspension and they are easily destroyed through external physical forces.

Thus, it is the predominance of weak clay connectors, the large number of clay coated grains and lack of clean grains, and the dominance of aggregates having open internal structures, arranged in a discontinuous matrix, which accounts for this sandstone's low strength.

Macroassemblages are common and result in a porous network of macropores. The rock's high deformability is related to rapid closure of these large pores. There are no clean interlocking grains or welded honeycomb aggregates in the fabric and so the sample cannot withstand even small physical forces. Saturating the sandstone flocculates clays into weak, open, crenulated arrangements. This results in the material having saturated compressive and tensile strengths very much lower than dry strengths.

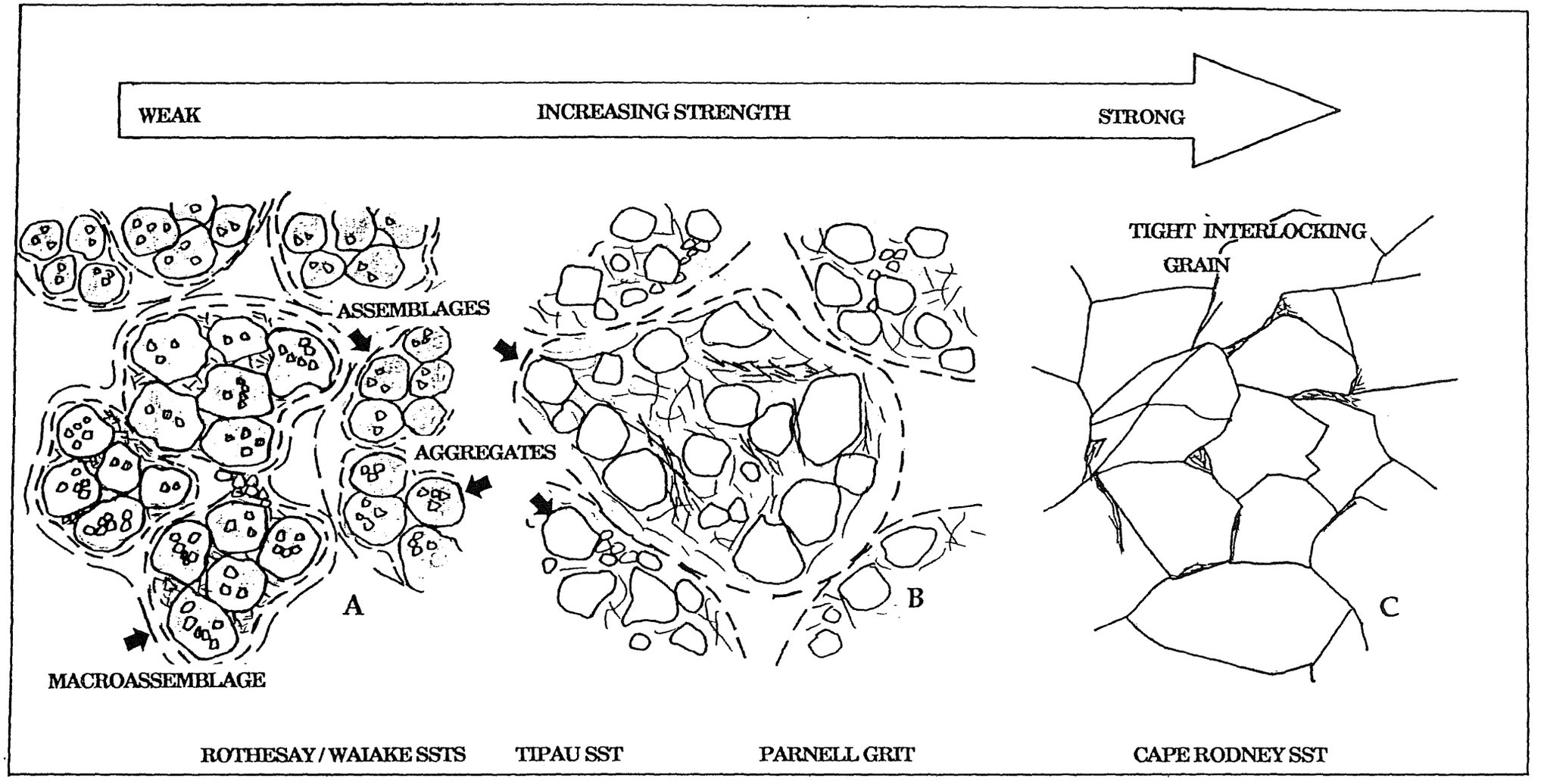

FIGURE 8.1 Fabric arrangements related to strength. Open fabrics (A) are characteristic of low strength sandstones. Tightly interlocking grains (C) are characteristic of the strong CR sandstone. (B) is an intermediary, where assemblages are the largest structures in the fabric.

Rothesay Sandstone

Rothesay sandstone is the weakest sample in this study. It has a discontinuous matrix and is defined as having a skeletal microfabric similar to that of Waiake sandstone. It is characterised by macroassemblages, aggregates, and microaggregates with open internal structures. All silt and sand grains are clay coated and no direct grain to grain contacts occur. The loose arrangement of these clay coated grains results in low strength as bond strengths within open flocculated clays (with high EF contact angles) are weak. Clay microaggregates line pores and form bridges connecting grains and aggregates.

The rock is the most porous of the samples and this is directly observed in the microfabric, where a well developed porous network separates macroassemblages. Pore spaces are dominant at all levels in the fabric, but it is the greater number of pores and dominance of meso and macropores (over micropores) that account for its greater deformability compared with other samples. As stresses are initially applied, pore closure is rapid. Slight increases in stress cause breakage of weak clay connectors, resulting in the low strength of the sandstone.

8.3.1.1 Discussion

Huppert (1986,1988) observed that rocks characterised by a continuous matrix tended to have higher compressive strengths than those with a discontinuous matrix. All rocks of this study have predominantly discontinuous matrices, but compressive strengths vary greatly between Cape Rodney and ECB sandstones. This means that it is the structural arrangements occurring within these discontinuous matrices which determine the strength.

There is a definite trend between strength and observed suites of structural arrangements in the rock fabrics (figure 8.1 and table 8.1). The strongest CR sandstone has a tightly interlocking network of grains with large contact surface areas and few meso and macropores. Welded FF arrangements of clay aggregates occur in this sample, which is the strongest clay aggregate arrangement observed in the samples. The

TABLE 8.1 Fabric features characteristic of ECB and CR sandstones. Similar trends exist for durabilities, but welded FF aggregates in Tipau sandstone do not enhance durability, hence it's similar slake index to Rothesay sandstone.

LOW STRENGTH → HIGH STRENGTH

	ROTHESAY SST	WAIAKE SST	TIPAU SST	PARNELL GRIT	CAPE RODNEY SST
MATRIX	DISCONTINUOUS	DISCONTINUOUS	DOMINANTLY DISCONTINUOUS	DISCONTINUOUS	DISCONTINUOUS/ CONTINUOUS
FABRIC TYPE	SKELETAL	SKELETAL	SKELETAL/TURBOSTRATIC	SKELETAL/TURBOSTRATIC	
CLAY MICROAGGREGATES	OPEN FLOCCULATED	OPEN FLOCCULATED →	OPEN FLOCCULATED/ WELDED FF HONEYCOMB	OPEN FLOCCULATED →	WELDED FF
GRAIN CONTACTS	NONE	NONE → MANY CLAY CONNECTORS AND BRIDGES	NONE → FEW CONNECTORS	FEW → RARE CONNECTORS LARGE CLAY AGGREGATES ACT AS DISCRETE ENTITIES	TIGHT INTERLOCKING
GRAINS	CLAY COATED	CLAY COATED	CLAY COATED →	CLAY COATED/CLEAN →	CLEAN
PORES	DOMINANT AT ALL LEVELS. LARGE PROPORTION OF MACROPORES →		PORES DOMINANT AT ALL LEVELS BUT FEWER MACROPORES →		RESTRICTED TO MESO AND MICROPORES

limited extent of the clay means it is insignificant in reducing rock strength.

Parnell Grit's fabric represents an intermediate between the strong CR sandstone and those of the ECB sandstones. Strength is lost as grain to grain contacts decrease, and clay coatings, connectors, and aggregates increase. Parnell Grit is characterised by fewer grain to grain contacts than found in CR sandstone, but these are still more than were observed in ECB sandstones.

Progressively weaker sandstones are dominated by macroassemblages of clay coated grains and open flocculated smectitic aggregates connected by point contacts. Clay microaggregates connect grains to form bridges or coat sand and silt grains; it is these connectors and clay coatings that radically reduce sandstone strength. The higher proportion of continuous matrix (where honeycomb structures of smectitic aggregates in welded FF stacks are more competent than flocculated arrangements) in the Tipau sandstone, is reflected in its greater strength compared with Waiake and Rothesay sandstones. Parnell Grit is stronger still, and composed of a number of clean grain to grain contacts which are unobserved in ECB samples.

As rock strength decreases, inter-macroassemblage macropores become more dominant in the fabrics. Weak Rothesay and Waiake samples have porous networks of interlocking inter-macroassemblage macropores which allow rapid infiltration of water, and flocculation of clays. These clays coat grains and significantly reduce the rock's ability to transmit stress. Once the rocks are saturated, failure is rapid, and indicated by a marked decrease in both compressive and tensile strengths of saturated cores. Pore space at all levels of the fabric increases within the weaker samples.

The distribution and size of pores is also important in controlling the sample's strength. The weaker Rothesay and Waiake sandstones are dominated by pores at all levels in the fabric, but are the only samples which have interconnecting porous networks of inter-macroassemblage macropores. These quickly fill with water upon saturation, resulting in a loss of strength. In Tipau sandstone, macropores are rare. Meso and

micropores occur in, and between, aggregates and microaggregates. Similarly, in Parnell Grit, macropores are limited in number and it is the dominance of intra-aggregate mesopores which affect the sample's strength. Cape Rodney sandstone has no macropores, few mesopores, with pores limited to micropores.

These results indicate quite clearly that it may not necessarily be total porosity which is important in controlling strength, but rather the distribution and size of pores. This implies that it is not the clay proportion which controls the rock's loss of strength on saturation, but the ability of water to reach the clays (and therefore the fabric). The interconnecting macropores in Waiake and Rothesay sandstones allow for easy access of water to flocculate the clay fabrics into weaker states, whereas in CR sandstone, the lack of macro and mesopores severly hinders water infiltration. Parnell Grit and Tipau sandstone are intermediates between these, characterised by mesopores and very few macropores (Parnell Grit) which allow moderately easy access to water.

8.3.2 Durability

The observed trends between strength and fabric features are very similar for durability. This is not unexpected as strength was shown in chapter 5 to be closely related to slake durability. Huppert (1986) notes that rocks with a continuous matrix are more durable than those with a discontinuous matrix. Durability decreases in fabrics dominated by clay aggregates and connectors. Variable durabilities in the sandstones of this study are a direct result of structural arrangements within the predominantly discontinuous matrices.

Cape Rodney Sandstone

Interlocking grain to grain contacts with large surface contact areas in CR sandstone result in a durable rock. Immersion in water has little effect on the sample, and it is solely mechanical abrasion which produces a minimal loss of material in the slaking process.

Parnell Grit

Parnell Grit is less durable than CR sandstone but far more durable than ECB sandstones. Immersion in water has the effect of flocculating large smectitic microaggregates and aggregates. Upon agitation, the clay matrix is easily broken down as clay bonds are greatly reduced. More competent grains are loosened but remain in the slaking drums and are not included as 'lost' material. The large clay aggregates reduce the sample's durability, but grain to grain contacts between clean grains provide a degree of resistance to breakdown.

Tipau Sandstone

Tipau sandstone has the lowest durability of all the samples. This indicates that welded FF stacked smectitic aggregates, which are associated with this sample's increased strength over other ECB sandstones, are split along basal planes upon immersion in water. The clay expands and flocculates, strength and cohesion are reduced, and mechanical agitation causes aggregates to break down. Lack of strong grain contacts, the abundance of clay coated grains, clay connectors, and aggregates with associated pore spaces, account for this sample's low durability.

Waiake Sandstone

Waiake sandstone has a low durability, and this is attributed to the dominance of pores at all levels in the fabric. Also, upon immersion in water, clays (clay connectors and grain coatings) expand greatly, which reduces the effects of cohesion. Areas of bonding between fabric elements are greatly reduced in samples having a discontinuous matrix, especially where aggregates act as individual units joined through weak point contacts. This sample's slightly greater durability than that of Tipau sandstone may be due to weak connector assemblages, which are not laterally confined by the matrix, being restored once the sample is removed from the water. This was noted by Huppert (1986).

Rothesay Sandstone

Rothesay sandstone has a low durability comparable to that of Waiake sandstone. Its similar overall fabric and structural arrangement of components within the dominantly discontinuous matrix, result in their similarly low slake durabilities. This is attributed to the effect of weak connector assemblages, clay coated grains, and dominance of pores at all levels in the fabric.

8.3.2.1 Discussion

The durability of the rocks of this study is closely related to the fabric (in terms of pores and aggregates) and not simply to clay content and mineralogy (which are similar for all samples). Upon immersion in water, clay aggregates expand and flocculate into weaker states, reducing strength and cohesion, and resulting in low durabilities. Pore distributions are also important, with less durable samples characterised by having networks of macropores through to micropores. Where clay aggregates act as individual units joined by weak point contacts (and separated by meso and macropores), areas of bonding are reduced. As found with strength, the increasing abundance of clay coated grains, clay connectors, aggregates, and pore spaces, are associated with samples having very low durabilities.

8.4 SUMMARY

The geomechanical behaviour of the rocks of this study is not related to mineralogy. Mineral type, abundance, and size have no influence on the strength, deformation, or durability of the samples studied. Similarly, clay type and abundance does not appear to be related to geomechanical behaviour. This last statement may be too generalised a conclusion considering the similar clay proportions in each sample.

Sample strength increases as the proportion of clean detrital grains with large surface contact areas increases. Samples having a proportion of continuous matrix in the fabric, characterised by welded FF stacked clay aggregates in a honey comb arrangement, impart a greater resistance to

failure than do open flocculated arrangements. As the proportions of clay microaggregates and aggregates, clay coated grains, clay bridges and connectors, and pore space (especially macropores) increase, the strength and durability of the materials decrease.

Durability is not simply related to clay content and mineralogy, but has been shown to be influenced by the fabric in terms of pores and aggregates. The least durable sandstones have fabrics dominated by pores at all levels, with a predominance of macropores. When samples are immersed in water, large clay aggregates flocculate into weaker states (as bond strengths are reduced), with an associated reduction in cohesion. Mechanical agitation easily breaks down these weakened aggregates. More durable samples have fewer large clay aggregates, more clean grain to grain contacts, and pores are restricted to micropores with rare meso and macropores.

Huppert's (1986, 1988) study of rock fabrics related strength to fabrics composed of continuous and discontinuous matrices. As all rocks of this study have predominantly discontinuous matrices, rock fabrics at a more detailed scale were shown to be responsible for changes in strength and durability. The structural arrangement of individual components within the fabric play a significant role in controlling the rocks geomechanical behaviour.

CHAPTER 9

CONCLUSIONS

CHAPTER 9

CONCLUSIONS

9.1 INTRODUCTION

The primary aim of this study was to determine the means by which the petrography of a selection of Waitemata Group rocks influences their geomechanical behaviour. This investigation was prompted due to the poor understanding of the geomechanics of weak rocks in general, and the controls on their strength in particular.

Standardised strength and elasticity laboratory tests were carried out on cores drilled from intact blocks of rock; bulk rock properties (density, porosity, void ratio, particle size, and durability) and petrological properties (mineralogy, texture, and fabric) were similarly determined from material from the same intact block samples. Simple linear regression between two variables was used to relate strength to bulk rock properties, field jointing characteristics, and petrology. Microfabric was determined from SEM investigations and qualitatively related to strength, elasticity, and durability.

This chapter summarises the main findings established from the investigation.

9.2 LITHOLOGY

The Waitemata Group rocks are a large body of flysch and associated rocks of Upper Oligocene to Lower Miocene age. The study rocks are members of the East Coast Bays Formation and the Cape Rodney Formations which, in turn, are members of the central Warkworth Subgroup. They form near-horizontal beds in the field, with regular vertical joints through individual units.

9.3 BULK ROCK PROPERTIES

9.3.1 Bulk Density and Porosity

The rocks of this study have low dry bulk densities ranging from 1742 to 2313 $kg.m^{-3}$. Saturated bulk densities are higher than dry densities for all samples and range from 2061 to 2408 $kg.m^{-3}$.

The rocks span a range of porosities from 9.6 to 31.9 %. Cape Rodney sandstone is the least porous rock while the ECB sandstones are the most porous. Porosity is directly related to bulk density, with the more porous rocks having the lowest bulk densities.

9.3.2 Grain Density and Void Ratio

Grain densities are similar for all samples, ranging from 2380 to 2565 $kg.m^{-3}$. This indicates that the samples have similar mineral constituents. Grain density values are in keeping with those of felsic composition, dominantly quartz, feldspar, and volcanic glass.

Void ratios range from 0.11 to 0.47, which are high for sandstones. The values are similar to those of granular soils or porous sedimentary rocks. The high void ratios suggest a wide spacing of grains in the material. By definition, void ratios are closely related to porosity.

9.3.3 Particle Size

Each sandstone is dominated by sand size grains, ranging from 50 to 80 %. Parnell Grit is dominated by 48% gravel size material. Percentage of < 2 μm material is low in all samples and ranges from 6 to 10 %. Tipau sandstone has a large proportion of silt and is classified as a sandy silt. Parnell Grit is a silty sandy conglomerate. All other samples classify as silty sands, after Folk *et al.* (1970).

9.4 GEOMECHANICAL PROPERTIES

9.4.1 Strength

Compressive Strength

Compressive strengths span an order of magnitude ranging from 7.2 to 79 MPa (oven dry) and 1.9 to 62 MPa (saturated). Cape Rodney sandstone classifies as a moderately strong rock while Parnell Grit is classified as a weak rock. East Coast Bays sandstones range from very weak to extremely weak rocks. All samples dominantly fail in compression through the cataclasis mode of failure described by Hawkes and Mellor (1970).

Cape Rodney sandstone is the only sample with a compressive strength comparable to previously published data for sandstones. East Coast Bays samples have strength values more characteristic of weak shales or coal.

Tensile Strength

The Indirect Brazilian test was used to determine tensile strengths. Results span an order of magnitude ranging from 1.1 to 10 MPa (oven dry) and 0.9 to 7.1 MPa (saturated). The ECB sandstones are the weakest rocks in both compression and tension. Tensile strengths undergo upto 60 % reduction upon saturation. Oven dry tensile strengths are, on average, 85 % lower than dry compressive strengths. This is remarkably consistent for all samples.

Tensile strengths for sandstones in general range from 1 to 25 MPa (Attewell and Farmer, 1976; Jumikis, 1983). All samples in this study have tensile strengths less than 10 MPa. They fall within the lower strength range of sandstones and are more characteristic of shales, limestones, or coal.

9.4.2 Dynamic Youngs Modulus

Measurement of dynamic Youngs Modulus at initial (E_i) and peak (E_p) stresses was attempted through the measurement of seismic waves through rock cores, using the laboratory ultrasonic pulse method.

The study rocks are all highly deformable. The E_i values range from 0.08 to 0.24 GPa while E_p values range from 1.2 to 6.4 GPa. All samples except CR sandstone have values less than 2 GPa and have deformation characteristics more akin to those of sands.

Initial deformation in all rocks is due to pore and microcrack closure. This is rapid in CR sandstone which is followed by recoverable elastic deformation (strain softening) as the rock compresses. At high stresses, sudden collapse of grain contacts results in rapid macrocrack development and brittle failure. In ECB sandstones, pore and crack closure is rapid and occurs at very low stresses. Youngs Modulus increases as loads are applied and there is a decreased strain with every increment of load, representing a non-elastic (strain hardening) response. Microcrack development and propagation rapidly follows with a small increase in stress. Parnell Grit is capable of resisting slightly higher compressive stresses than ECB sandstones prior to failure.

Cape Rodney sandstone and Parnell Grit deform rapidly in the saturated state due to the mechanism of stress corrosion. Wave attenuation was too great in ECB sandstones to allow the measurement of Youngs Modulus in the saturated state.

9.4.3 Hardness

Dynamic rebound hardness 'R' was measured using the L-Type Schmidt Hammer *in situ* and on intact blocks of rock. Shore hardness was determined on rock cores. *In situ* rebound 'R' values range from 17.5 to 26.9, compared with 'R' values on intact blocks which range from 13.6 to 34.8. Shore Hardness values range from 11.2 to 45.2. The errors associated with the Schmidt Hammer results are due to the variability of individual

sandstone units, while lowering of values is due to the effect of discontinuities and microcracks.

There is a much greater range in R_{block} values than for *in situ* readings, and also, there are smaller errors associated with R values recorded on intact block samples. This suggests that field conditions reduce hardness variability between sites, but increase variability within sites. Intact blocks were assumed free of cracks as cores were drilled from the same blocks and displayed no weakening through the presence of cracks.

Shore hardness values follow similar trends to those recorded with the Schmidt Hammer. Weaker ECB sandstones have lower hardness values compared with the more dense CR sandstone, which, in all cases, has the highest rebound value. Porosity of the samples is believed to directly influence hardness. More porous rocks tend to absorb the hammer impact while the least porous, more dense, CR sandstone results in a greater rebound value.

9.4.4 Durability

The samples span a range of durabilities from very high for CR sandstone to low durabilities for ECB sandstones. Loss of material after two slaking cycles is minimal from CR sandstone (2 %) but greater in Parnell Grit (17 %). Much more material is lost from the weaker ECB sandstones, ranging from 50 to 59 %.

Mechanical abrasion is solely responsible for loss of material from CR sandstone. Simple wetting and drying is sufficient to almost totally disintegrate Waiake sandstone. Low durabilities for Parnell Grit, Rothesay sandstone, and Tipau sandstone are due to a combination of wetting and drying, and mechanical abrasion. Physical plucking of grains from the clay matrix was directly observed in Parnell Grit.

9.5 PETROLOGICAL PROPERTIES

9.5.1 Mineralogy

Mineralogical composition and abundance were determined from XRD and optical microscopy. Clay mineral types and abundances were determined from XRD, optical microscopy, and SEM.

The dominant constituents in all samples are volcanic and detrital rock fragments. Andesitic and dacitic volcanic rock fragments are dominant over detrital rock fragments in CR sandstone and Parnell Grit. Detrital rock fragments occur in equal proportion with volcanic fragments in ECB sandstones.

Quartz is abundant in all samples. Calcic plagioclase is most abundant in Parnell Grit and occurs in lesser amounts in other samples. Cape Rodney sandstone is characterised by a calcite cement, while all other samples have argillaceous matrices. Authigenic and clay minerals were hard to distinguish in thin section.

Clay minerals make up less than 10 % of the sandstone mineralogy. The dominant clay mineral is smectite and was identified as strongly swelling montmorillonite. Illite and kaolinite are much less abundant and are restricted to authigenic grain coatings. Smectite-chlorite occurs in CR sandstone and is restricted to this sample. Mixed layer clays make up the remainder of the < 2 μm size fraction but could not clearly be identified due to their diffuse and broad XRD patterns.

9.5.2 Microfabric

Microfabric was qualitatively characterised and classified using scanning electron microscopy.

The rocks exhibit a range of structural arrangements which resemble the microfabric end member types proposed by Huppert (1986). All samples have dominantly skeletal fabrics with discontinuous matrices. Cape Rodney and Tipau sandstones have portions of continuous matrix where

clay aggregates are arranged in honeycomb structures, with individual clay platelets in FF welded stacks.

Clay microaggregates are primarily smectite in open flocculated arrangement. They occur as pore bridges or linings, or as discrete entities (in Parnell Grit). The fabrics of ECB sandstones are characterised by macroassemblages composed of smectitic aggregates and clay coated silt and sand grains. Consequently, pore spaces are large inter-macroassemblage macropores. Parnell Grit has some clean grains in direct contact with one another, while CR sandstone is almost totally composed of tightly interlocking quartz grains which restrict pore space to intergranular and intramicroaggregate micropores.

9.6 GEOMECHANICAL BEHAVIOUR AND BULK ROCK PROPERTIES

Both compressive and tensile strengths are closely related to bulk rock properties. Good correlations exist between strength and dry bulk density, porosity, and void ratio. The results suggest that both compressive and tensile strengths are controlled by the closeness of packing of grains and the resulting pore space. The lack of any relationship between grain density and strength suggest that mineral type has an insignificant effect on geomechanical behaviour. Similarly, no relationship was found to exist between strength and particle size.

The good correlation between strength and durability reflects the influence of compressive and tensile breakage and plucking of grains in the mechanical slaking process. The softening factor for compressive stresses is very closely related to durability, indicative of the effect that saturation has on disintegrating samples.

Importantly, no correlations were found between *in situ* Schmidt Hammer rebound values and strength. Conversely, relationships between strength and 'R' values on intact blocks are good. This reflects a higher degree of experimental control, as strength parameters were determined from cores drilled directly from the blocks tested with the Schmidt Hammer. The results suggest that the Schmidt Hammer is not a good field indicator of sandstone strength. The strong relationship between

strength and Shore Hardness again reflects the higher degree of control in the test method.

No relationships were found between Dynamic Youngs Modulus at initial and peak stresses, and strength. Similarly, compressive and tensile strengths are not related to any field properties.

9.6.1 Dynamic Youngs Modulus and Field Properties

Dynamic Youngs Modulus at both initial and peak stresses are related to Schmidt Hammer rebound values. This is important, and intuitively reasonable, as the Schmidt Hammer is measuring the distance of rebound of a mass impacting on a surface. The amount of deformation the rock undergoes is directly related to this elastic rebound. It is suggested that the Schmidt Hammer can more accurately be used as a field indicator of rock elasticity than as a predictor of rock strength.

9.6.2 Dynamic Youngs Modulus and Jointing

There is a significant correlation between Dynamic Youngs Modulus at peak stress and jointing. The relationship is an inverse one, with the highly deformable ECB sandstones characterised by wide joint spacing and the least deformable CR sandstone characterised by close cross joints. In all cases, the joints are extension or tension joints. The ECB sandstones are capable of storing applied stress through plastic deformation, resulting in fewer and more widely spaced joints. Conversely, the less deformable CR sandstone releases stress through brittle fracture, resulting in more closely spaced joints.

The homogeneous, regular joint pattern of ECB sandstones is probably a result of their having been subjected to a simple, uniform stress history such as gradual loading through burial associated with tectonic quiescence. The regular jointing in Parnell Grit reflects a similar stress history and loading environment to that of the neighbouring flysch deposits. The geometrically more complex jointing in CR sandstone reflects a more variable stress history, associated with brittle fracture of the unit when loaded.

9.7 GEOMECHANICAL BEHAVIOUR AND PETROLOGY

Importantly, no relationships were found between any strength parameter and any mineralogical property. This supports the conclusion that strength (and durability) are not related to mineral quantity, size, or type, but rather it is the arrangement of individual components in the rock fabric which influence geomechanical behaviour.

9.7.1 Geomechanical Behaviour and Microfabric

There is a definite relationship between strength and observed suites of structural arrangements within the rock fabrics. The stronger CR sandstone has a tightly interlocking network of clean quartz grains with large areas of contact between grain boundaries. A continuous matrix occurs to a limited extent in the rock; it is characterised by the relatively competent welded honeycomb arrangement of clay aggregates.

Progressively weaker sandstones have more clay coated grains, and clay microaggregates and aggregates have a more open flocculated arrangement. These aggregates become prominant in the weaker rocks, as grain connectors, bridges, and grain coatings. These assume decisive roles as weak links for stress transmission.

Extremely weak ECB sandstones are characterised by a dominance of macroassemblages resulting in an interconnected porous network of inter-macroassemblage macropores. Stronger sandstones are characterised by a limited quantity of mesopores and an absence of macropores.

Fabric arrangements support earlier conclusions about sandstone deformation. The weaker rocks are highly deformable, and this is related to pore closure as stresses are applied. Further slight increases in stress result in breakage of weak clay connectors, resulting in low strength. In the less deformable CR sandstone, initial deformation is a result of bending of honeycomb clay aggregates and closure of existing pore space. The interlocking grain network can resist greater stresses prior to breakage of grain contacts and brittle failure. A small portion of clean

grain to grain contacts in Parnell Grit results in its slightly greater strength compared with those of ECB sandstones.

The observed trends between strength and fabric features are very similar for durability. Variable durabilities in the sandstones are a direct result of structural arrangements within the predominantly discontinuous matrices. The Tipau sandstone, with its portions of welded FF stacked clay platelets in the fabric, is less durable than the other ECB sandstones, which are characterised by flocculated clay microaggregates. This means that the FF stacked aggregates are split along basal planes upon immersion in water. Weak connector assemblages, which are not laterally confined by the matrix in Waiake and Rothesay sandstones, provides their slightly greater durabilities over that of Tipau sandstone.

Interlocking grain to grain contacts increase in Parnell Grit and more so in CR sandstone, resulting in their increased durabilities over the ECB sandstones.

9.8 SUMMARY

The investigation provides a better understanding of the properties of the sample rocks in general. The geomechanical behaviour of Waitemata Group rocks have been characterised and described. Petrological properties have similarly been identified and discussed.

It has been shown that the geomechanical behaviour of the sandstones is closely related to bulk rock properties, durability, and hardness. However, the Schmidt Hammer was found to be an unreliable indicator of rock strength *in situ* and implies that for these rocks at least, it should not be used for predicting rock strength in the field. Dynamic Youngs Modulus is related to Schmidt hardness, suggesting the instrument provides a better indication of rock elasticity, rather than strength.

Importantly, it has been shown that mineral type, abundance, and size have no influence on the geomechanical behaviour of the samples studied, but rather the rock fabric plays a determinative role. The study rock's strength, deformability, and durability are directly controlled by the complex array of structural arrangements, and by the distribution and

size of pores, which constitute the rock fabric, The strong, durable samples have many clean grain to grain contacts, few large clay aggregates, and pores are restricted to micro and rare mesopores. Progressively weaker, less durable, and more highly deformable samples, are characterised by an increase in clay aggregates, clay coated grains, clay connectors, and pore space, with fewer clean grain contacts. As interconnecting macropores become dominant in the fabric of weaker samples, water is able to quickly reach the clay aggregates and flocculate them into weaker states with reduced cohesion, resulting in low durabilities.

9.8.1 Future Research

This investigation has supported previous findings that microfabric is the crucial factor in determining rock strength and durability. In particular, it is the association of the clay minerals that influence geomechanical behaviour, and in rocks with a similar proportion of clay-size (< 2 μm) components, the proportion, size, and sorting of the larger clasts are relatively unimportant (within the bounds examined). Future research into the level (in terms of proportion) at which the clay minerals begin to exert this dominant influence would be of considerable value, as this will define the point at which a material classified as a sandstone takes on the behaviours characteristic of 'soft' rocks. In engineering terms, the recognition of a soft rock response is essential for appropriate design and treatment.

The current research has also raised serious questions regarding the applicability of using the Schmidt Hammer as a field index of rock strength - a common test which is often used in engineering and geomorphological studies. The hammer has been shown to be insensitive to variations in strength, and to have a high variability in measurements recorded at one site. Conversely however, it has been shown to be of some value as an indicator of the elastic properties of the rocks. Further research into the Schmidt Hammer response over a wider range of rock strength and elasticity is required to better define the appropriate uses of this equipment.

Field jointing characteristics (spacing) were related to geomechanical behaviour. Further work needs to be done in quantifying joint spacing and continuity at various sites so that more accurate models for joint development may be devised.

Finally, this study has provided a database of geomechanical and petrographical information for a variety of Waitemata Group rocks outcropping mainly along the East Coast Bays coastline. This information may lay the groundwork for possible future investigations into cliff stability and shoreline retreat along this stretch of coast.

REFERENCES

REFERENCES

Anon., 1983: *PUNDIT Manual for use with the portable ultrasonic non-destructive digital indicating tester, mark iv.* C.N.S. Electronics Ltd.

Alldred, H.B., 1980: *Sedimentology and structure of the Waitemata Group Wenderholm - Orewa Sections, North Auckland.* Unpublished B.Sc. (Hons) Thesis. University of Auckland.

Attewell, P.B., and Farmer, I.W., 1976: *Principles of Engineering Geology.* Chapman and Hall. London.

Ballance, P.F., 1974: An inter-arc flysch basin in northern New Zealand: Waitemata Group (Upper Oligocene to Lower Miocene). *The Journal of Geology. Vol. 82, no. 4, pp. 439 - 472.*

Ballance, P.F., 1976: Stratigraphy and Bibliography of the Waitemata Group of Auckland, New Zealand. *New Zealand Journal of Geology and Geophysics. Vol. 19, no. 6, pp. 897 - 932.*

Ballance, P.F., 1976: Evolution of the Upper Cenozoic Magmatic Arc and Plate Boundary in Northern New Zealand. *Earth and Planetary Science Letters. Vol. 28, pp. 356 - 370.*

Ballance, P.F., 1979: The Geological History and Physiography of the Auckland District IN Brook, R.J., 1979: *The Natural History of Auckland: An Introduction.* Auckland War Memorial Museum Handbook.

Ballance, P.F., and Williams, P.W., 1982: The Geomorphology of Auckland and Northland IN Soons, J.M., and Selby, M.J., (EDS): *Landforms of New Zealand.* Longman Paul Ltd. Auckland.

Bandis, S.C., 1990: Mechanical properties of rock joints IN Barton, N., and Stephansson, O., 1990: *Rock Joints.* A.A. Balkema. Rotterdam.

Bannock, S. M., 1991: *Geological, geomechanical and pavement properties of basecourse aggregates in the Otorohanga County.* Unpublished M.Sc Thesis. University of Waikato.

Barden, L., McGown, A., Collins, K., 1973: The collapse mechanism in partly saturated soil. *Engineering Geology. Vol. 7, no. 1, pp. 49 - 60.*

Barton, N., Stephansson, O., 1990: *Rock Joints. Proceedings of the International Symposium on Rock Joints.* Loen, Norway. June, 1990. A.A. Balkema, Rotterdam.

Beattie, A.G., 1990: *Petrological Controls on the Geomechanical Behaviour of Coal Measure Soft Rocks, Waikato, New Zealand.* Unpublished M.Sc. Thesis. University of Waikato.

Beavis, F.C., 1985: *Engineering Geology.* Blackwell. Melbourne.

Bell, F.G., 1978: The physical and mechanical properties of the Fell Sandstones, Northumberland, England. *Engineering Geology. Vol. 12, no. 1, pp. 177 - 287.*

Beutelspacher, H., van der Marel, H.W., 1968: *Atlas of Electron Microscopy of Clay Minerals and their Admixtures.* Elsevier. New York.

Bieniawski, Z.T., 1988: The Rock Mass Rating (RMR) System (Geomechanics Classification) in Engineering Practice IN Kirkaldie, L., (ED), 1988: *Rock Classification Systems for Engineering Purposes.* ASTM. STP 984. Philadelphia.

Bohor, B.F., and Hughes, R.E., 1971: Scanning Electron Microscopy of clays and clay minerals. *Clays and Clay Minerals, Vol. 19, no. 1, pp. 49 - 54.*

Borst, R.E., and Kellor, W.D., 1969: *Scanning Electron Micrographs of API Reference Clay Minerals and other Selected Samples. Proc. Int. Clay Conference.* Tokyo, Vol. 1, pp. 871 - 901.

Bouma, A.H., 1962: *Sedimentology of some flysch deposits. A graphic approach to facies interpretation.* Elsevier Publishing Company.

Brenchley, P.J., 1969: Origin of Matrix in Ordovician Greywackes, Berwyn Hills, North Wales. *Journal of Sedimentary Petrology. Vol. 39, no. 4, pp. 1297 - 1301.*

Brindley, G.W., and Brown, G., (EDS), 1980: *Crystal Structures of Clay Minerals and their X - Ray Identification.* Mineralogical Society. London.

Brown, E.T., (ED), 1981: *Rock Characterisation Testing and Monitoring. ISRM Suggested Methods. International Society for Rock Mechanics.* Pergamon Press.

Carmichael, R.S., (ED), 1984: *Handbook of the Physical Properties of Rocks.* Vol 3. CRC Press Inc. Boca Raton. Florida.

Caruso, L., Simmons, G., Wilkens, R.H., 1985: The physical properties of a set of sandstones - Part I. The Samples. *Int. J. Rock Mech. Min. Sci. and Geomech. Abstr. Vol. 22, No. 6, pp. 381 - 392.*

Codling, A.P., 1970: *Waitemata Rocks of Hobson Bay - Mission Bay area, Auckland.* Unpublished B.Sc. (Hons) Thesis. University of Auckland.

Collins, K., and McGown, A., 1974: The form and function of microfabric features in a variety of natural soils. *Geotechnique. Vol. 24, No. 2, pp 223 - 254.*

Daily, W.D., and Lin, W., 1985: Laboratory-determined transport properties of Berea Sandstone. *Geophysics. Vol. 50, No. 5, pp. 775 - 784.*

Day, M.J., Goudie, A.S., 1977: *Field assessment of rock hardness using the Schmidt Test Hammer. British Geomorphological Research Group.* Technical Bulletin 18: 19 - 29.

Deere, D.U., and Miller, R.P., 1966: *Engineering Classification and Index Properties for Intact Rock.* Air Force Weapons Laboratory. Technical Report No. AFWL - TR - 65 - 116.

Derski, W., Izbicki, R., Kisiel, I., Mroz, Z., 1989: *Rock and soil mechanics. Developments in Geotechnical Engineering. Vol. 48.* Elsevier Amsterdam.

Dobereiner, L., and de Freitas, M.H., 1986: Geotechnical properties of weak sandstones. *Geotechnique. Vol. 36, No. 1, pp. 79 - 94.*

Dyke, C.G., and Dobereiner, L., 1991: Evaluating the strength and deformability of sandstones. *The Quarterly Journal of Engineering Geology. Vol. 24, no. 1, pp. 123 - 134.*

Farmer, I.W., 1983: *Engineering Behaviour of Rocks.* Second Edition. Chapman and Hall. London.

Folk, R.L., 1968: *Petrology of Sedimentary Rocks.* Hemphills Austin. Texas.

Folk, R.L., Andrews, P.B., Lewis, D.W., 1970: Detrital sedimentary rock classification and nomenclature for use in New Zealand. *New Zealand Journal of Geology and Geophysics. Vol. 13, no. 4, pp. 937 - 968.*

Gabrielson, R. H., 1990: Characteristics of joints and faults IN Barton, N., and Stephansson, O., (EDS) 1990: *Rock Joints.* A.A. Balkema. Rotterdam.

Geelen, J.N., 1973: *The Stratigraphy of the Waitemata Group along the North Manukau Coastline.* Unpublished M.Sc. Thesis. University of Auckland.

Geological Society Engineering Group Working Party, 1977: Working Party Report: The Description of rock masses for engineering

purposes. *Quarterly Journal of Engineering Geology. No. 10, pp. 355 - 388.*

Geological Society Engineering Group Working Party, 1988: Engineering Geophysics: Report by the Geological Society Engineering Group Working Party. *Quarterly Journal of Engineering Geology. No. 21, pp. 207 - 271.*

Gillot, J.E., 1975: Relationships between origin and microstructure of rocks and soils to engineering behaviour. *Bull. of the Int. Assoc. of Eng. Geol. No. 11, pp.77 - 82.*

Gillot, J.E., 1986: Some clay related problems in Engineering Geology. *Clay Minerals, Vol. 21, no. 3, pp. 261 - 278.*

Glading, A.V., 1987: *Aspects of the Engineering and Quaternary Geology., Whitford - Brookby - Beachlands, Auckland.* Unpublished M.Sc. Thesis. University of Auckland.

Gokhale, K.V.G.K., and Rao, D.M., 1981: *Experiments in Engineering Geology.* Tata McGraw - Hill Publishing Company Ltd. New Delhi.

Goodman, R.E., 1980: *Introduction to Rock Mechanics.* John Wiley and Sons. New York.

Grabowska-Olszewska, B., 1975: SEM analysis of microstructures of loess deposits. *Bull. of the Int. Assoc. of Eng. Geol. No. 11, pp. 45 - 48.*

Gregory, M.R., 1966: *Rocks of the Waitemata Group, Whangaparoa Peninsula, Northland.* Unpublished M.Sc. Thesis. University of Auckland.

Hawkes, I., and Mellor, M., 1970: Uniaxial Testing in Rock Mechanics Laboratories. *Engineering Geology. Vol. 4, no. 3, pp. 177 - 287.*

Hobbs, B.E., Winthrop, D.M., Williams, P.F., 1976: *An Outline of Structural Geology.* John Wiley and Sons. New York.

Hume, T.M., and Nelson, C.S., 1982: *X - Ray diffraction analytical procedures and some mineralogical characteristics for South Auckland Region sediments and sedimentary rocks, with special reference to their clay fraction.* Occassional Report No. 10. Dept. of Earth Sciences, University of Waikato.

Huppert, F., 1986: *Petrology of Soft Tertiary Sedimentary Rocks and its Relationship to Geomechanical Behaviour, Central North Island, New Zealand.* Unpublished Ph.D. Thesis. University of Auckland.

Huppert, F., 1988: Influence of microfabric on geomechanical behaviour of Tertiary fine-grained sedimentary rocks from Central North Island, New Zealand. *Bulletin of the International Association of Engineering Geology. No. 38, pp. 83 - 93.*

Hutchison, C.S., 1974: *Laboratory Handbook of Petrographic Techniques.* John Wiley and Sons. New York.

Irfan, T.Y., Dearman, W.R., 1978: Engineering Classification and Index Properties of a Weathered Granite. *Bulletin of the International Association of Engineering Geology. Vol. 17, pp. 79 - 90.*

Johnston, D.H., Toksov, M.N., 1980: Ultrasonic P and S Wave Attenuation in dry and saturated rocks under pressure. *Journal of Geophysical Research. Vol. 85, no. B2, pp. 925 - 936.*

Jones, M.E., Preston, R.M.F., (EDS), 1987: *Deformation of Sediments and Sedimentary Rocks.* Geological Society Special Publication No. 29. Blackwell Scientific Publications. Oxford. London.

Jumikis, A.R., 1983: *Rock Mechanics.* Second Edition. Trans Tech Publications. Gulf Publishing Company. Houston.

King, M.S., 1983: Static and dynamic elastic properties of rocks from the Canadian Shield. *Int. Jour. of Rock Mech. and Min. Sci. and Geomech. Abstracts. Vol. 20, no. 5, pp. 237 - 241.*

King, M.S., 1984: Elastic wave velocities in quartz monzonite at different levels of water saturation. *Int. Jour. of Rock Mech. and Min. Sci. and Geomech. Abstracts. Vol. 21, no. 1, pp. 35 - 38.*

Kirkaldie, L., Williamson, D.A., Patterson, P.V., 1988: Rock Material Field Classification Procedure IN Kirkaldie, L., (ED), 1988: *Rock Classification Systems for Engineering Purposes.* ASTM. STP 984. Philadelphia.

Kowallis, B.J., Jones, L.E.A., Wang, H.F., 1984: Velocity-Porosity-Clay content Systematics of poorly consolidated Sandstones. *Journal of Geophysical Research. Vol. 89, no. B12, pp. 10355 - 10364.*

Lama, R.D., and Vutukuri, V.S., 1978: *Handbook on Mechanical Properties of Rocks. Testing Techniques and Results, Volume II.* Trans Tech Publications. Switzerland.

Lama, R.D., and Vutukuri, V.S., 1978: *Handbook on Mechanical Properties of Rocks. Testing Techniques and Results, Volume IV.* Trans Tech Publications. Switzerland.

Lewis, D.W., 1984: *Practical Sedimentology.* Hutchinson Ross Publishing.

Lowe, D.J., and Nelson, C.S., 1983: *Guide to the Nature and Methods of Analysis of the Clay Fraction of Tephras from the South Auckland Region, New Zealand.* Occassional Report No. 11, Dept. of Earth Sciences. University of Waikato.

Manning, P.A., 1983: *Engineering geology of a section along the Northern Coast of the Manukau Harbour, Auckland.* Unpublished M.Sc. Thesis. University of Auckland.

Matula, M., 1981: Rock and soil descriptions and classification for engineering geological mapping. Report by the IAEG

Commission on Engineering Geological Mapping. *Bulletin of the International Association of Engineering Geology. No. 24, pp. 235 - 274.*

Mellor, M., and Hawkes, I., 1971: Measurement of Tensile Strength by Diametral Compression of Discs and Annuli. *Engineering Geology. Vol. 5, no. 3, pp. 173 - 227.*

Moon, V.G., 1989: *Relationships between Geomechanics and Petrography of Ignimbrite.* Unpublished Ph.D Thesis. University of Waikato.

Nelson, C.S., Cochrane, R.H., 1970: *A rapid X-Ray method for the qualitative determination of selected minerals in fine grained and altered rocks.* TANE 16: 152 - 162.

New Zealand Geomechanics Society, 1988: *Guidelines for the field description of soils and rocks in engineering use.* New Zealand Geomechanics Society, Institute of Professional Engineers, Wellington, New Zealand.

New Zealand Geological Survey., 1972: *Geological Map of New Zealand, 1 : 100000. North Island (First Edition).* Department of Scientific and Industrial Research, Wellington, New Zealand.

O'Connell, R.J., and Budiansky, B., 1974: Seismic velocities in dry and saturated cracked solids. *Journal of Geophysical Research. Vol. 79, no. 35, pp. 5412 - 5426.*

O'Connell, R.J., and Budiansky, B., 1977: Viscoelastic properties of fluid-saturated cracked solids. *Journal of Geophysical Research. Vol. 82, no. 36, pp. 5719 - 5736.*

Osipov, V.I., 1975: Structural bonds and the properties of clays. *Bull. of the Int. Assoc. of Eng. Geol. No. 12, pp. 13 - 20.*

Osipov, V.I., and Sokolov, V.N., 1978: A study of the nature of the strength and deformation properties of clay soils with the help of the

scanning electron microscope. *Bulletin of the International Association of Engineering Geology. No. 17, pp. 91 - 94.*

Pandit, B.I., and King, M.S., 1979: The variation of elastic wave velocities and quality factor Q of a sandstone with moisture content. *Canadian Journal of Earth Sciences. Vol. 16, no. 12, pp. 2187 - 2195.*

Pettijohn, F.J., 1975: *Sedimentary Rocks.* Third Edition. Harper and Row Publishers. New York.

Price, N.J., 1966: *Fault and joint development in brittle and semi-brittle rock.* Pergamon Press. Oxford.

Poole, R.W., Farmer, I.W., 1980: Consistency and Repeatability of Schmidt Hammer rebound data during field testing. *Int. Jour. of Rock Mech. and Min. Sci. and Geomech. Abstracts. Vol. 17, no. 3, pp. 167 - 172.*

Read, S.A.L., Miller, P.J., White, T., Riddolls, B.W., 1981: *Geomechanical properties of New Zealand soft sedimentary rocks. Proceedings of the International Symposium on Weak Rock, Tokyo.*

Samalivkova, M., 1985: Characteristics of discontinuities and their influence on the mechanical behaviour of the rock mass. *Bull. of the Int. Assoc. of Eng. Geol. No. 31, pp. 111 - 122.*

Sayers, C.M., Van Munster, J.G., King, M.S., 1990: Stress - induced Ultrasonic Anisotropy in Berea Sandstone. *Int. Jour. of Rock Mech. and Min. Sci. and Geomech. Abstracts. Vol. 27, no. 5, pp. 429 - 436.*

Schofield, J.C., 1967: *Sheet 3 Auckland Geological Map of New Zealand, 1:250000.* Department of Scientific and Industrial Research, Wellington, New Zealand.

Scholle, P.A., 1979: *A Color Illustrated Guide to Constituents, Textures, Cements, and Porosities of Sandstones and Associated Rocks.* The American Association of Petroleum Geologists. Memoir 28.

Searle, E.J., 1981: *City of Volcanoes.* A Geology of Auckland. Longman Paul Ltd.

Selby, M.J., 1982: *Hillslope Materials and Processes.* Oxford University Press. Oxford.

Selby, M. J., 1985: *Earths Changing Surface.* Clarendon. Oxford

Shakes, B.G., 1983: *The Engineering Geology of the Kaukapakapa Area.* Unpublished M.Sc. Thesis. University of Auckland.

Sheory, P.R., Barat, D., Das, M.N., Mukherjee, K.P., Singh, B., 1984: Schmidt Hammer rebound data for estimation of large scale *in situ* coal strength. *Int. Jour. of Rock Mech. and Min. Sci. and Geomech. Abstracts. Vol. 21, no. 1, pp. 39 - 42.*

Shelton, J.W., 1964: Authigenic Kaolinite in Sandstone. *Journal of Sedimentary Petrology. Vol. 34, no. 1, pp. 102 - 111.*

Simpson, K.A., 1988: *Rock properties and slope processes of the Waitemata Group soft rock along sections of the East Coast of Auckland, New Zealand.* Unpublished M.Sc. Thesis. University of Auckland.

Smart, P., and Tovey, N.K., 1981: *Electron Microscopy of soils and sediments, examples.* Clarendon Press. Oxford.

Swolfs, H.S., Brechtel, C.E., Brace, W.F., Pratt, H.R., 1981: Field Mechanical Properties of a jointed Sandstone IN Carter, W.L., Friedman, M., Logan, J.M., Stearns, D.W., (EDS) 1981: *Mechanical Behaviour of Crustal Rocks. The Handin Volume. Geophysical Monograph 24.*

Torresan, M.E., and Schawb, W.C., 1987: Fabric and its relation to sedimentologic and physical properties of near-surface sediment, Shelikof Strait and Alsek Prodelta, Alaska. *Journal of Sedimentary Petrology, Vol. 57, no. 3, pp. 408 - 418.*

Vickers, B., 1983: *Laboratory work in Soil Mechanics.* Second Edition. Fletcher and Son Ltd. Norwich.

Vutukuri, V.S., Lama, R.D., Salvja, S.S., 1974: *Handbook on Mechanical Properties of Rocks. Testing Techniques and Results. Volume I.* Trans Tech Publications. Switzerland.

Waldvogel, Y., and Selby, M.J., 1980: *Geomechanics Manual No. 2: Geotechnical Mapping and Rock Mass Strength Classification.* Unpublished Internal Report of the Department of Earth Sciences, University of Waikato.

Weigel, V.H., 1976: *Some aspects of the Waitemata Group of Southwest Auckland.* Unpublished M.Sc. Thesis. University of Auckland.

Welton, J., 1984: *SEM Petrology Atlas.* The American Association of Petroleum Geologists. U.S.A.

Wilkens, R.H., Simmons, G., Wissler, T.M., Caruso, L., 1986: The physical properties of a set of sandstones - Part III. The effects of fine-grained, pore-filling material on compressional wave velocity. *Int. J. Rock Mech. Sci. and Geomech. Abstr. Vol. 23, No. 4, pp. 313 - 325.*

Williams, H., Turner, F.J., Gilbert, C.M., 1982: *Petrography. An Introduction to the study of rocks in thin sections.* Second Edition. W.H. Freeman and Company. San Francisco.

Williamson, D.A., and Kuhn, C.R., 1988: The Unified Rock Classification System IN Kirkaldie, L., (ED), 1988: *Rock Classification Systems for Engineering Purposes.* ASTM. STP 984. Philadelphia.

Wilson, G., 1982: *Introduction to small - scale geological structures.* George Allen and Unwin. Boston.

Wilson, M.D., and Pittman, E.D., 1977: Authigenic clays in sandstones: Recognition and influence on reservoir properties and paleoenvironmental analysis. *Journal of Sedimentary Petrology. Vol. 47, no. 1, pp. 3 - 31.*

Wilson, M.J., (ED), 1987: *A Handbook of Determinative Methods in Clay Mineralogy.* Chapman and Hall. New York.

Winkler, K.W., 1983: Frequency dependant ultrasonic properties of high porosity sandstones. *Journal of Geophysical Research. Vol. 88, no. B11, pp. 9493 - 9499.*

Winkler, K.W., 1985: Dispersion analysis of Velocity and Attenuation in Berea Sandstone. *Journal of Geophysical Research. Vol. 90, no. B8, pp. 6793 - 6800.*

Yang, H.J.P., and King, M.S., 1986: A study of elastic wave velocities in dry and water saturated, regularly jointed rock masses. *Int. Jour. of Rock Mech. and Min. Sci. and Geomech. Abstracts. Vol. 23, no. 3, pp. 277 - 280.*